

TURKISH JOURNAL OF SCIENCE AND TECHNOLOGY (TJST)

Year: 2018 Vol: 13 Number: 2

Address:

Fırat Universitesi
Fen Bilimleri Enstitüsü
23119, Elazig - TURKEY

Tel: 0 424 212 27 07

Fax: 0 424 236 99 55

e-mail: fenbilimdergi@firat.edu.tr

New ISSN

Online: 1308-9099

Printed: 1308-9080

Old ISSN

Online: 1306 – 8555

Printed: 1306 – 8547

Refereed journal. Published twice a year

<http://web.firat.edu.tr/fenbilimleri/Dergiler/TJST/index.html>

TURKISH JOURNAL OF SCIENCE & TECHNOLOGY (TJST)

Published by Firat University

Owner

Prof. Dr. Kutbeddin DEMİRDAĞ

Rector of the Firat University

Editor

Assoc.Prof. Dr. Erkan TANYILDIZI

Firat University, Technology Faculty
Department of Software Engineering

Responsible Director

Prof. Dr. Soner ÖZGEN

Director of the Graduate School of Natural and
Applied Sciences of Firat University

Editor

Assis. Prof. Dr. Sencer ÜNAL

Firat University, Engineering Faculty
Department of Electrical-Electronics Engineering

Editorial Board

Prof. Dr. Soner ÖZGEN

Assoc.Prof. Dr. Erkan TANYILDIZI

Assis. Prof. Dr. Sencer ÜNAL

ADVISORY BOARD

Eyüp BAĞCI

Firat University, Department of Biology,
Elazig-Turkey

Eres SOYLEMEZ

Middle East Technical University,
Department of Engineering Science,
Ankara-Turkey

Coskun BAYRAK

UALR Donaghey Collage of Eng. and
Information Tech.Dept. of Computer
Science, Little Rock, AR, USA

Hikmet GECKIL

Inonu University, Department of Biology,
Malatya-Turkey

Metin CALTA

Firat University, Fisheries Faculty, Elazig-
Turkey

Ertan GOKALP

Karadeniz Technical University,
Department of Geodesy and Photogrametry
Engineering, Trabzon-Turkey

Abdulkadir ŞENGÜR

Firat University, Department of Electronics
and Computer Education, Elazig-Turkey

M. Polat SAKA

Middle East Technical University,
Department of Engineering Science,
Ankara-Turkey

Ali DEMİR

Istanbul Technical University, Department
of Textile Engineering, İstanbul-Turkey

Hasan EFEOGLU

Ataturk University, Department of
Electrical-Electronics Engineering,
Erzurum-Turkey

Yanhui GUO

St. Thomas University, School of Science
and Technology, Miami, FL, USA

İbrahim TURKMEN

Balıkesir University, Department of
Geology Engineering, Balıkesir-Turkey

Deniz UNER

Middle East Technical University,
Department of Chemical Engineering,
Ankara-Turkey

Orhan ERMAN

Firat University, Department of Biology,
Elazig-Turkey

Rusen GECIT

Middle East Technical University,
Department of Engineering Science,
Ankara-Turkey

Siqing XIA

Tongji Univ, State Key Lab Pollut Control
& Resource Reuse, Coll Environm Sci &
Engn, Shanghai 200092, R China

Zihni DEMİRBAG

Karadeniz Technical University,
Department of Biology, Trabzon-Turkey

Hanefi GULDEMİR

Firat University, Department of Electronics
and Computer Education, Elazig-Turkey

Nilgun GULEC

Middle East Technical University,
Department of Geology Engineering,
Ankara-Turkey

Erdogan GUNEL

West Virginia University, Department of
Statistics, Morgantown, USA

Sedigheh GHOFrani

Islamic Azad University, Electrical
Engineering Department, Tehran South
Branch, Iran

Wang XIBAO

Tianjin University, The School of Materials
Science and Engineering, China

Brain WOERNER

West Virginia University, Department of
Computer Sciences & Electrical
Engineering, Morgantown, WV, USA

İbrahim TURKMEN

Balıkesir University, Department of
Geology Engineering, Balıkesir-Turkey

A. Kadri CETIN

Firat University, Department of Biology,
Elazig-Turkey

Muhsin Tunay GENÇOĞLU

Firat University, Engineering Faculty,
Department of Electrical-Electronics
Engineering, Elazig-Turkey

Metin BALCI

Middle East Technical University,
Department of Chemistry, Ankara-Turkey

Tuncay OREN

Ottawa Univ, Fac Eng, Inform Technol.
McLeod Inst Sim.t Sci, Ottawa, ON KIN
6N5 Canada

Halil ONDER

Middle East Technical University,
Department of Civil Engineering, Ankara-
Turkey

Nazmi POLAT

Ondokuz Mayıs University, Department of
Biology, Samsun-Turkey

Mustafa DORUCU

Firat University, Fisheries Faculty, Elazig-
Turkey

Binod Chandra TRIPATHY

Mathematical Sciences Division, Institute of
Advanced Study Science and Technology
Paschim Boragaon; Guwahati, India

Erkan TANYILDIZI

Firat University, Department of Software
Engineering, Elazig-Turkey

Farid EL-TANTAWY

Suez Canal University, Faculty of
Science, Department of Physics, Ismailia,
Egypt

Saleem HASHMI

International College of Technology,
Dublin, Ireland

Sakir ERDOĞDU

Karadeniz Technical University,
Department of Civil Engineering, Trabzon-
Turkey

Eoin CASEY

University College Dublin, Chemical and
Bioprocess Engineering, Dublin, Ireland

Serdar SALMAN

Marmara University, Department of Metal
Education, İstanbul-Turkey

Sencer ÜNAL

Firat University, Engineering Faculty,
Department of Electrical-Electronics
Engineering, Elazig-Turkey

İÇİNDEKİLER / CONTENTS

1. The Effects of The Perforation Shapes, Sizes, Numbers and Inclination Angles on The Thermal Performance of A Perforated Pin Fin <i>Perforeli Kanatlarda Şekil, Boyut Ve Eğim Açısının Isıl Performansa Etkisi</i> Hisham H. Jasim, Mehmet Sait Söylemez	1-13
2. Calculation of Optimum Insulation Thickness and Energy Savings for Different Climatic Regions of Turkey <i>Türkiye'nin Farklı İklim Bölgeleri İçin Enerji Tasarrufu ve Optimum Yalıtım Kalınlığının Hesaplanması</i> Ebru Kavak AKPINAR, İbrahim Halil DEMİR	15-22
3. Some Population Parameters of Mirror Carp (<i>Cyprinus carpio</i> L., 1758) Living in Keban Dam Lake, Elazığ, TURKEY <i>Keban Baraj Gölünde Yaşayan Aynalı Sazan (<i>Cyprinus carpio</i> L., 1758)'de Bazı Büyüme Parametreleri</i> Metin ÇALTA, Mustafa DÜŞÜKCAN, Burcu SAYIN	23-28
4. Occupational Health Risk Analysis and Assessment in Cement Production Processes <i>Çimento Üretim Proseslerinde İş Sağlığı Risk Analizi ve Değerlendirmesi</i> Vedat KARAHAN, Cevdet AKOSMAN	29-37
5. Investigation of Diffusion and Adsorption of Acetone in Building Materials by Dynamic Method <i>Asetonun Yapı Malzemelerindeki Difüzyon ve Adsorpsiyonunun Dinamik Metotla İncelenmesi</i> Şakir Yılmaz, Cevdet AKOSMAN	39-46
6. <i>Pseudomonas aeruginosa</i> Expressing <i>Vitreoscilla</i> Hemoglobin Shows Increased Production of L-Lysine α-Oxidase: an Enzyme used in Cancer Therapy <i>Vitreoscilla Hemoglobini İçeren <i>Pseudomonas aeruginosa</i>'da Kanser Tedavisinde Kullanılan Bir Enzim Olan L-Lisin α-Oksidaz Üretimi Arttırılması</i> Hüseyin Kahraman	47-52
7. Data Mining Techniques Based Students Achievements Analysis <i>Veri Madenciliği Teknikleri ile Öğrencilerin Başarımların Analizi</i> Dönüş Şengür, Songül Karabatak	53-59
8. Prediction Of The Action Identification Levels Of Teachers Based On Organizational Commitment And Job Satisfaction By Using K-Nearest Neighbors Method <i>Öğretmenlerin Örgütsel Bağlılık Ve İş Doyumuna Dayalı Eylem Kimlikleme Düzeylerinin K-En Yakın Komşular Yöntemi Kullanılarak Tahmin Edilmesi</i> Dönüş Şengür, Muhammed Turhan	61-68
9. Length-Weight Relationship of Common Carp (<i>Cyprinus carpio</i> L., 1758) from Taqtaq Region of Little Zab River, Northern Iraq <i>Kuzey Irak'taki Küçük Zap Suyunun Tagtag Bölgesinden Elde Edilen Sazan Balığı (<i>Cyprinus carpio</i> L., 1758) Boy-Ağırlık İlişkisi</i> Rzgar Farooq RASHID, Metin ÇALTA, Asiye BAŞUSTA	69-72

The Effects of The Perforation Shapes, Sizes, Numbers and Inclination Angles on The Thermal Performance of A Perforated Pin Fin

Hisham H. Jasim^{1,2} and Mehmet Sait Söylemez¹

¹ Department of Mechanical Engineering, University of Gaziantep, 27310 Gaziantep, Turkey

² University of Baghdad, Baghdad, Iraq

ha19211@mail2.gantep.edu.tr, enghisham78@yahoo.com

(Geliş/Received: 03.04.2017; Kabul/Accepted: 22.04.2018)

Abstract

Many of the proposed methods introduced the perforated fin with the straight direction to improve the thermal performance of the heat sink. Present rectangular pin fin consists, innovative form of the perforation (with inclination angles). To investigate the thermal behavior of the present model, changes in each of the geometric consideration (shape, size and number of perforations) and inclination angles were considered. Signum function is used for the modeling the opposite and the mutable approach of the heat transfer area. The Degenerate Hypergeometric Equation (DHE) was used as a new derivative method to find the general solution, then solved by Kummer's series. Two validation ways (previous work and Ansys 16.0-Steady State Thermal) are considered. The present mathematical model has big reliability according to the high agreement of the validation results about (0.31%- 0.60%). Also, the results show a decrease of the fin temperature as a result of the increase the heat transfer area. It was found, use of the perforated fin leads to decrease the thermal resistance and improve the thermal performance of the pin fin by enhancing the heat transfer and increase the effectiveness.

Keywords: Perforated fin, Incline perforation, Natural convection, Heat transfer enhancement, Performance analysis.

Perforeli Kanatlarda Şekil, Boyut Ve Eğim Açısının Isıl Performansa Etkisi

Özet

Bu çalışma elektronik parçaların soğutulmasında kullanılan perforeli kanatların ısıl performansını arttırmak için yapılmıştır. Dörtgen kesitli kanatlar için değişik tarzda eğimli bir perforeli kanat konusunda yeni ve orijinal sonuçlar elde edilmiştir. Mevcut modelin ısıl performans üzerindeki etkileri detaylı olarak araştırılmış ve sunulmuştur. Çalışmada teorik çözüm için Signum Fonksiyonu kullanılmıştır. Dejeneratif Hipergeometrik Denklemi ile birlikte Kummer's Serisi kullanılarak genel çözüm elde edilmiştir. Mevcut sonuçlar ANSYS 16.0 ve sürekli rejim sonuçları ile mukayese edilerek doğrulanmıştır. Sonuçlar arasında bide üç ile altı mertebesinde farklılık görülmüştür. Ayrıca, sonuçlar ısı transfer alanının artmasıyla kanat sıcaklığının azaldığını göstermektedir. Perforasyon etkisi ile ısıl direncin azaldığı ve bu nedenle ısıl performansın yani kanat etkenlik değerinin arttığı gözlenmiştir.

Anahtar Kelimeler: Perforeli kanat, Eğimli perforasyon, Doğal taşınım, Isı transfer artışı, Isıl performans.

1. Introduction

Modern development leads to closely positioned components and high densities of electrical power [1]. That's meaning, should be increase the heat transfer from the heat sink. For this reason, the investigators used the perforation towards straight direction to improve the thermal resistance. Moreover, the changes of the shapes, sizes, numbers and orientation of the perforations were adopted to optimize the thermal performance.

Computational technique is used by the most investigators to solve the governing equations. Five cases with single perforation and three cases with multiple perforations of an annular finned-tube system were evaluated to find the best performance by [2] in extreme climatic conditions, a single perforation location at 120° provided the favorable results. Also, the enhancement of the heat transfer can be reached to the 5.96%.

Circular, rectangular and trapezoidal cross section area of the perforation was studied by [3]

to find the effects of the number and geometry of the hollow fin on the heat transfer through rectangular fins attached to microchannel heat sink, results show the improvement is strongly depends on the numbers of the hollows and negligible influence of the hollow geometry. To show the advantages of the perforation, [4] shows The thermal profile of the perforated fins in a staggered manner performs better than the solid elliptical pin fin according to the Static temperature, Nusselt number and total heat that is calculated.

The effects of the porosity on the performance of the fins were investigated by [5,6] for longitudinal and lateral perforation. Rectangular cross section with different dimensions and multi numbers of the perforation was considered to show the thermal enhancement at various operating conditions. Higher performances for perforated fins are observed. Also the increased effectiveness by increasing porosity ratio.

The Nusselt Number and the friction factor were optimized separately and together for the circular perforated of the rectangular cross section by [7], the results show the higher thermal performance of the pin fin dependent on the lower clearance ratio and lower inter-fin spacing ratio also the efficiency can be increased by 1.1 and 1.9 based on the Reynolds numbers. Likewise, the pin fin efficiency of the circular cross section can be increased by 1.4 and 1.6 by using the circular perforation and the Nusselt number having inversely proportional to the clearance ratio and inter-fin spacing ratio according to [8,9]. A copper material possesses higher thermal conductivity when compared with other material by [10], also a large number of perforated were given the higher heat transfer coefficient.

The larger hollow pin diameter ratio, offered higher augmentation factor for upward orientation, and the situation was reversed for sideward orientation for the circular pin fin using the circular perforation that are studied by [11].

The Reynolds number and size of perforation have a larger impact on the Nusselt number for rectangular fin using the lateral perforations (square and circular) that are presented by [12]. Perforated pin fin in the cylindrical channel was tested by change the

number of a circular perforation, The results show the number of perforations has the significant increase of the convective heat transfer about (30% to 40%) [13].

Other investigations found the temperature distribution of perforated fin by analytical study,[14] reached to the temperature distribution equation of perforated flat plate based on the mathematical model that solved by Fourier series and Flocke's theory. [15] reported the decrease of thermal conduction resistance of pin fin due to triangular perforation, which leads to improved the heat dissipation that calculated by use variation approach, finite element techniques.

Likewise, [16] applied the same technique to find the effects of the orientations of the rectangular perforations under natural convection, the results show the inclined orientation is better for low each of the thickness and thermal conductivity while the parallel orientation is better for higher thickness. Also, [17] concluded to enlarge of perforated size and increase the thermal conductivity leads to augmentation the heat transfer from the rectangular fin.

In [18] the optimization of the thermal resistance was performed on pin-fin heat sinks with a constant Reynolds number. The results show increased the number of the fin leads to decrease the thermal resistance without limit for height (40 mm) while the optimum number of fins can be found at the height (20mm and 30mm).

New approach introduced in this article, by proposing two novelty points, firstly at geometric model, the incline perforation is considered. Secondly, at Analytical process, the new differential technique is used to derive the general form of the temperature distribution regardless of the perforation shape. Also, the Signum function is used for modeling the opposite and the mutable approach of the heat transfer area. After that, the effects of the incline perforated on the thermal performance can be studied.

2. Geometric Model

The incline perforated region of the pin fin is shown in Figure 1. In the general form, an

undefined section of perforation was considered. Inclination started from $(\beta=0)$ at straight perforation. The fin has a rectangular cross section area with one and two perforations. Also, the base fin is located at the x-z plane and y-axis at the fin length. Due to the incline perforation, the heat transfer area is changing with y-direction as well as change with the inclination angle.

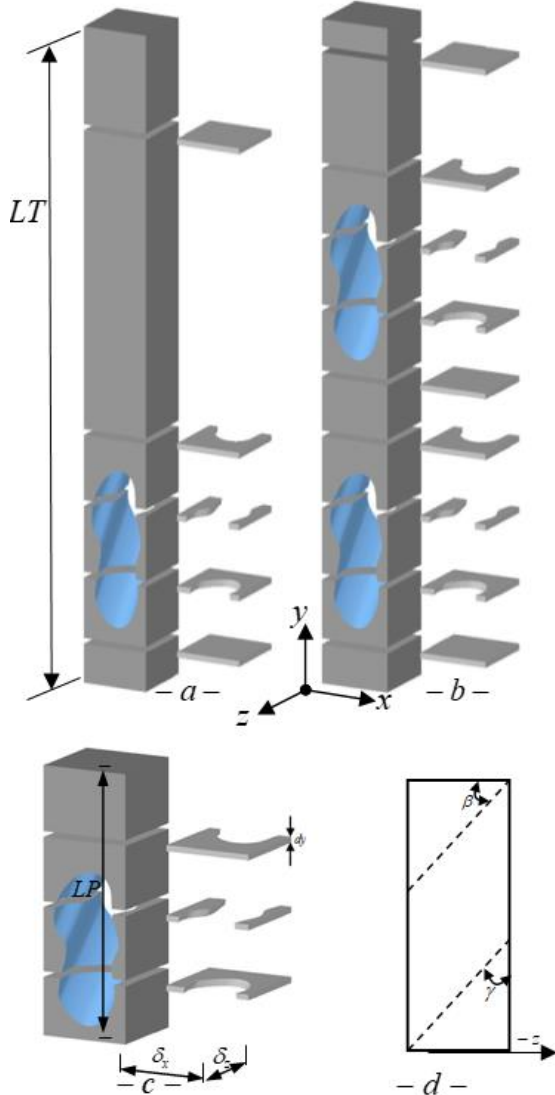


Figure 1. Fin with incline perforated. a- fin one perforation. b- fin with two perforations. c- 3-D model of the perforated region with different layer. d- side view.

3. Energy Analysis and Assumption

Energy balance is applied to the element shown in Figure 2, to obtain the differential equation of energy (1) in the perforated region.

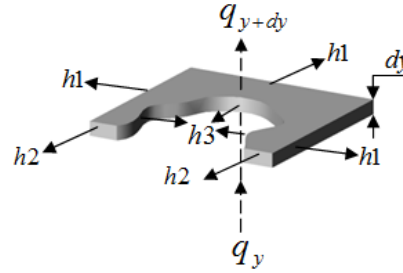


Figure 2. Element description

In this study, heat transfer analysis relies on a set of assumptions:

- 1- Steady heat conduction with no heat generation.
- 2- One-dimensional heat transfer analysis depended on the impairment of the Biot number at z-axis and x-axis.
- 3- Constant conductivity ($k = 222 \text{ W/m.K}$, (A1050)).
- 4- Constant base temperature.
- 5- Insulation tip fin, radiation effects are neglected.
- 6- Uniform ambient temperature and uniform convection heat transfer coefficient.
- 7- Convection coefficient is divided into three types (external non-perforated (h1), external perforated (h2) and internal perforated (h3)).

$$\frac{d}{dy} (A_{cond} \cdot \frac{d\theta}{dy}) dy = [h1P_{conv1} + h2P_{conv2} + h3P_{conv3}] \frac{\theta dy}{k} \quad (1)$$

$$\theta = T(y) - T_{air}$$

Where A_{cond} is the conduction area, P_{conv} is the perimeter of the convection. Various convection heat transfer coefficients were appeared due to incline perforation. Moreover, Convection coefficients depended on the properties of cooling fluid, specifications of the perforated fin and the open perforated ratio (ROP). ROP represents the ratio of actual perforated area to maximum perforation effects. Convection coefficients $h1$, $h2$ and $h3$ were calculated according to the ref. [19 , 20,21], respectively.

4. General Solution

Equation (1) can be represented by use the Degenerate Hypergeometric Equation (DHE)[22,23].

$$g \frac{d^2 u}{dg^2} + (ku1 - g) \frac{du}{dg} - (ku2)u = 0 \quad (2)$$

Where: $u = e^{g/2} G$, $g = \xi^2 \sqrt{p1}$,

$$\theta = G / \sqrt{A_{cond.}}, \xi = y + \frac{p2}{2p1}$$

$ku1, ku2 = \text{constants}$.

The DHE equation (2) was solved by Kummer's series [24,25] to get the general solution of the present model.

$$u(g) = CO_i \phi(ku1, ku2, g) + CO_{i+1} \psi(ku1, ku2, g), i = 1,3,5,\dots \quad (3)$$

Where:

$\phi =$ confluent hypergeometric function of the first kind.

$\psi =$ confluent hypergeometric function of the second kind.

$CO =$ Constant for the general solution.

Boundary conditions, for the constant base temperature:

$$u \Big|_{g=\frac{p2^2}{4p1^{3/2}}} = \theta_b \sqrt{A_b} e^{\frac{p2^2}{8p1^{3/2}}}, \quad \frac{du}{dg} \Big|_{g=(LP+\frac{p2}{2p1})^2 \sqrt{p1}} = 0$$

Which compatible to the boundary conditions at original form.

$$\theta \Big|_{y=0} = \theta_b, \quad \frac{d\theta}{dy} \Big|_{y=LP} = 0$$

Solve of the equation (3) with above boundary conditions, which leads to the temperature distribution equation.

$$\frac{\theta(y)}{\theta_b} = \frac{e^{-\frac{(y+\frac{p2}{2p1})^2 \sqrt{p1}}{2}}}{\sqrt{A_{cond.}}} [\zeta_{10} \phi(ku1, ku2, ((y + \frac{p2}{2p1})^2 \sqrt{p1})) - \zeta_{11} \psi(ku1, ku2, ((y + \frac{p2}{2p1})^2 \sqrt{p1}))] \quad (4)$$

Where: $p1, 2, \dots$ Constant [22]

$$\zeta_{10} = \frac{\zeta_4 \zeta_6 + \zeta_8 \zeta_9}{\zeta_1 \zeta_2 (\zeta_4 \zeta_6 + \zeta_8 \zeta_9) - \zeta_1 \zeta_3 (\zeta_4 \zeta_5 + \zeta_7 \zeta_9)}$$

$$\zeta_{11} = \frac{\zeta_4 \zeta_5 + \zeta_7 \zeta_9}{\zeta_4 \zeta_6 + \zeta_8 \zeta_9} \zeta_{10}$$

$$\zeta_1 = \frac{e^{-\frac{p2^2}{8p1^{3/2}}}}{\sqrt{A_b}}, \quad \zeta_2 = \phi(ku1, ku2; \frac{p2^2}{8p1^{3/2}})$$

$$\zeta_3 = \psi(ku1, ku2; \frac{p2^2}{8p1^{3/2}}), \quad \zeta_4 = \frac{e^{-\frac{(LP+\frac{p2}{2p1})^2 \sqrt{p1}}{2}}}{\sqrt{A_{cond.}}_{LP}}$$

$$\zeta_5 = \phi'[ku1, ku2; ((LP + \frac{p2}{2p1})^2 \sqrt{p1})]$$

$$\zeta_6 = \psi'[ku1, ku2; ((LP + \frac{p2}{2p1})^2 \sqrt{p1})]$$

$$\zeta_7 = \phi(ku1, ku2; ((LP + \frac{p2}{2p1})^2 \sqrt{p1}))$$

$$\zeta_8 = \psi(ku1, ku2; ((LP + \frac{p2}{2p1})^2 \sqrt{p1}))$$

$$\zeta_9 = -\frac{(LP + \frac{p2}{2p1})(\sqrt{p1} \sqrt{A_{cond.}})_{LP} e^{-\frac{(LP+\frac{p2}{2p1})^2 \sqrt{p1}}{2}}}{A_{cond.})_{LP} \frac{A'_{cond.})_{LP} e^{-\frac{(LP+\frac{p2}{2p1})^2 \sqrt{p1}}{2}}}{2\sqrt{A_{cond.}}_{LP}} - \frac{A_{cond.})_{LP}}{A_{cond.})_{LP}}$$

5. Modeling of The Heat Transfer Area

In this study, two shapes of perforation (elliptical and rectangular) were considered. The change of the heat transfer area (Conduction area $A_{cond.}$ and convection perimeter $P_{conv.}$) is depending on the two parameters (y-axis and inclination angle), which leads to many difficulties when calculated the area at any specification. Likewise, the extreme ends for $A_{cond.}$ and $P_{conv.}$ can be represented by a point or

by a line depended on the inclination angle as shown in figure (3).

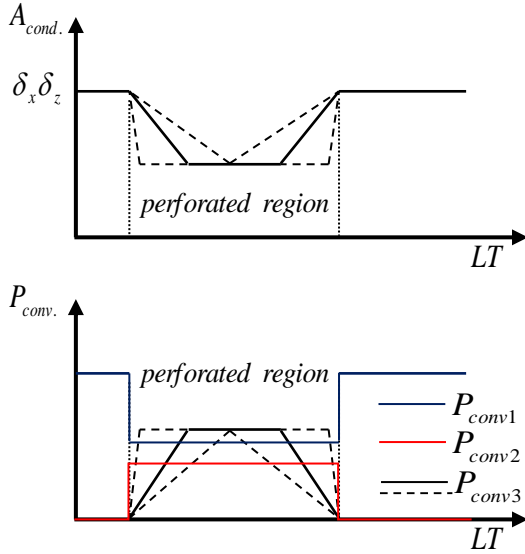


Figure 3. Change of the heat transfer area (conduction area and convection perimeter).

Signum function (sgn) [26] is used to represent the opposite and the mutable approach of variables $A_{cond.}$ and $P_{conv.}$. In case of the elliptical perforation, figures (4 and 5) show the change of the perforated section with the y -axis based on the inclination angle. The equations of heat transfer area are derivative and formulated based on the group of the constants (a, a_1, a_2) as shown in the table (1). Moreover, equations (5– 8) are used to calculate the heat transfer area at any specification. In case of the rectangular perforation, ref.[22 and 23] was adopted.

$$A_{cond.} = \frac{AA}{a} (a_1 - y) sgn(a - y) + (\delta_z \delta_x) - AA \quad (5)$$

$$P_{conv1} = 2\delta_z + a_2 \quad (6)$$

$$P_{conv2} dy = \int_{-b3}^{b3} (\delta_x - 2r \sqrt{1 - \frac{y^2}{b3^2}}) dy \quad (7)$$

$$P_{conv3} = 4 \int_0^{w1} \sqrt{(r^2 \cos^2 \Omega) + (b2^2 \sin^2 \Omega)} d\Omega \quad (8)$$

Where:

$$sgn(a - y) = \tanh[(N(a - y)], \quad N \gg 1$$

$$zp = z + \frac{\delta_z}{2}$$

$$w1 = \tan^{-1} \frac{\delta_z/2}{r \sqrt{1 - \frac{(\delta_z/2)^2}{b2^2}}}, \quad a = \delta_z \tan \beta$$

$$AA = (\pi r b2) - 4r \int_{-b2}^{-\delta_z/2} \sqrt{1 - \frac{zp^2}{b2^2}} dzp$$

$$b2 = \frac{1}{2} (\delta_z + \frac{2r - \delta_z \sin \beta}{\cos \beta} \tan \gamma), \quad b3 = r / \cos \beta$$

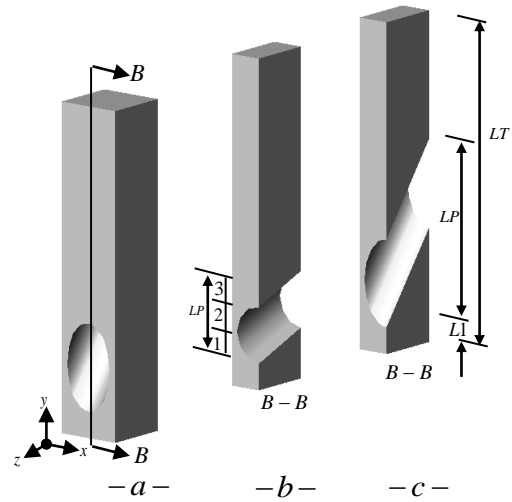


Figure 4. Ellipse perforated with different angle a) 3-D plot b) smaller angle c) bigger angle.

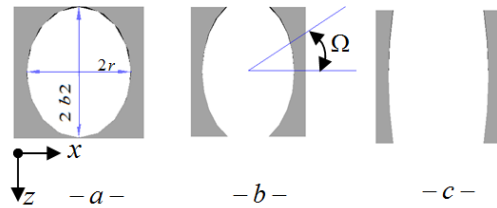


Figure 5. Ellipse section of perforated at a) bigger angle b) smaller than a c) smaller than b.

Table 1. Constant value

Region No.	Constant value	
	a_1	a_2
1	a	δ_x
2	y	0
3	LP-a	δ_x

In each shape of perforation, results of the two models (I and II) are calculated with natural convection, at a certain Rayleigh number ($Ra=10^6$). Models, I and II are described as follows:

Model I, elliptical perforation :
 $\delta_x = \delta_z = 0.01 (m), r = 0.0035(m),$
 $LT = 0.05(m)$

Model II, elliptical perforation :
 $\delta_x = \delta_z = 0.01 (m), r = 0.004(m),$
 $LT = 0.05(m)$

Model I, rectangular perforation:
 $\delta_x = \delta_z = 0.01 (m), bx = by = 0.007(m) ,$
 $LT = 0.05(m)$

Model II, rectangular perforation :
 $\delta_x = \delta_z = 0.01 (m), bx = by = 0.008(m),$
 $LT = 0.05 (m)$

6. Numerical Solutions and Simulation

The language of Matlab (R2014a) was used to calculate the thermal parameters based on the analytical solution. While, thermal analysis have been simulated by using -Ansys 16.0-Steady State Thermal- for all cases that are adopted in this study. Several grids are studied to ensure that the solutions are independent grids as shown in the tables (2 and 3) for the elliptical perforation and tables (4 and 5) for the rectangular perforation. The more accurate grid is required for the perforated region due to curvatures and edges. This problem is solved by changing the advanced size function to be proximity and curvatures, also the face size is calculated according to equation (9).

$$\text{Max. Face size} = \frac{\delta_x \text{ or } \delta_z}{NG}, NG = 20 - 30 \quad (9)$$

The minimum temperature was compared until independent grids were succeeded. All the results are calculated at the base temperature ($90^\circ C$) and air temperature ($25^\circ C$). Two cases (case -1- and case -2-) were adopted to show the grid configurations as shown in figures (6 and 7) for the elliptical perforation and figures (8 and 9) for the rectangular perforation. The descriptions of two cases are shown below:

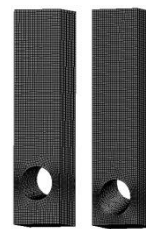
Case-1- model I with one perforation; Case-2- model II with two perforations.

Table 2. Grid independent studies

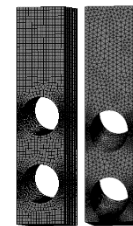
Inclination angle	Grid	Min. Temperature	
Case-1-	$\beta=8$	115901	87.1
		137423	87.69
		148908	87.939
		158390	87.945
	$\beta=22$	129236	86.882
		147208	87.121
		160411	87.649
	172179	87.66	

Table 3. Grid independent studies

Inclination angle	Grid	Min. Temperature	
Case-2-	$\beta=9$	119932	85.86
		142111	86.24
		160854	86.528
		171546	86.53
	$\beta=25$	190234	85.29
		211906	85.78
		219523	86.16
		231248	86.18



— a — — b —
Figure 6. Grid configuration for the case -1- a) $\beta = 8$
 b) $\beta = 22$



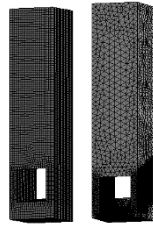
— a — — b —
Figure 7. Grid configuration for the case -2- a) $\beta = 9$
 b) $\beta = 25$.

Table 4. Grid independent studies

Inclination angle	Grid	Min. Temperature	
Case-1-	$\beta=8$	131901	87.11
		150423	87.58
		162908	87.89
		172530	87.907
	$\beta=22$	140236	86.419
		158208	86.92
		171411	87.351
		183371	87.38

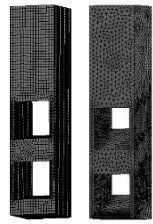
Table 5. Grid independent studies

Inclination angle	Grid	Min. Temperature	
Case-2-	$\beta=9$	83932	83.828
		108111	84.31
		123854	84.749
		134317	84.771
	$\beta=25$	121234	83.53
		137906	84.025
		149523	84.597
		161873	84.612



– a – – b –

Figure 8. Grid configuration for the case -1- a) $\beta = 8$
b) $\beta = 22$



– a – – b –

Figure 9. Grid configuration for the case -2- a) $\beta = 9$
b) $\beta = 25$.

7. Results and Discussion

7.1 Validation of analytical model

In the first method, Kirpikov [14] derived the temperature distribution along the perforated fin is a function of the Biot number. Equation to calculate the Biot number of the present model describe as:

$$Bi = \frac{LT^2[\sum hi A_{conv i}]}{k \int A_{cond} dy} \quad i = 1,2,3 \quad (10)$$

The high similarity between the results are shown below the perforation region, but a spacing was increased between the results in the perforation region. Maximum difference can be reached to (0.52%-0.6%) as shown in Figures (10 and 11) for elliptical and rectangular perforation, respectively.

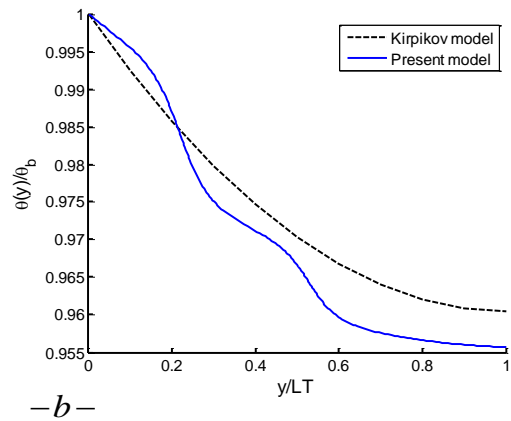
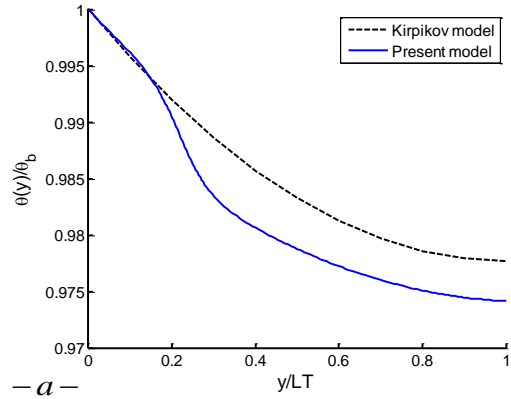


Figure 10. Comparisons between present model and Kirpikov model at $\beta = 0^\circ$. a) Case-1- b) Case-2- .

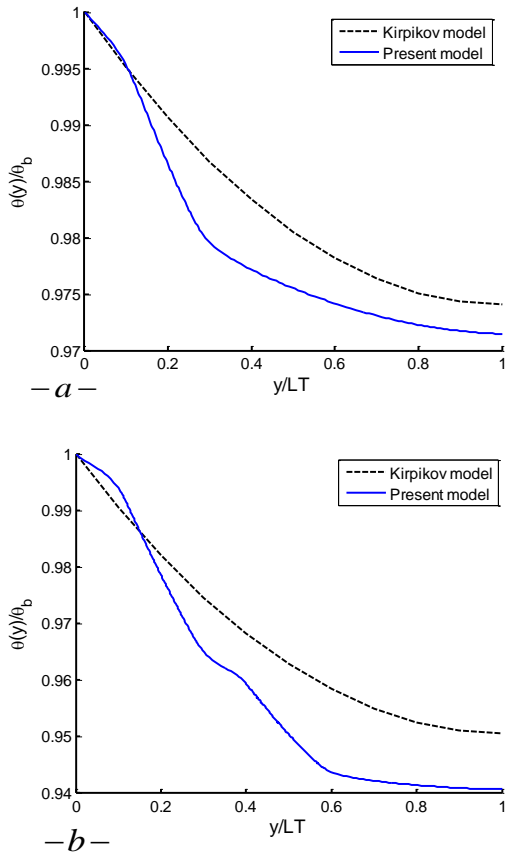


Figure 11. Comparisons between Present model and Kirpikov model at $\beta = 0^\circ$. a) Case-1- b) Case-2-.

Furthermore, above the perforation region the results spacing was decreased.

The reasons of the spacing of results can be explained as follows:

- 1- In Kirpikov model, heat transfer coefficient was not classified into three regions.
- 2- In Kirpikov model, approximate solution (Fourier series) was adopted.
- 3- In Kirpikov model, convection coefficient of inner surface was assumed as a ratio from the external coefficient (not depended on the size and length of the perforation).

In the second way of the validation, two inclination angles are adopted for each case that is considered in the calculation process. The distribution of the fin temperature (θ/θ_b) was calculated along the fin length (y/LT) to show the convergence between the analytical solution (by using the present mathematical techniques) and numerical solution (by using Ansys simulation) as shown in Figures (12 and 13) for

the elliptical perforation and figures (14 and 15) for rectangular perforation.

Increase each of the inclination angle, size and number of perforations which leads to decrease the temperature of the fin as a result of many reasons:

- Increase of the inner convection area.
- Distribute the inner convection area on the longer length in the y-axis.
- Increase of the external perforated area.
- The conduction area that is replaced by the convection area was increased.

The results show, the temperature profile does not have the classic shape as a result to add convection effects through the conduction cross section area. But, in any case the profile of the results is the same for the analytical and numerical models. In addition, agreements of results are complete resemblance below the fin length 0.2 or 0.3 based on the inclination angle. While, above these limits the a maximum difference can be reached to the (0.33%) .

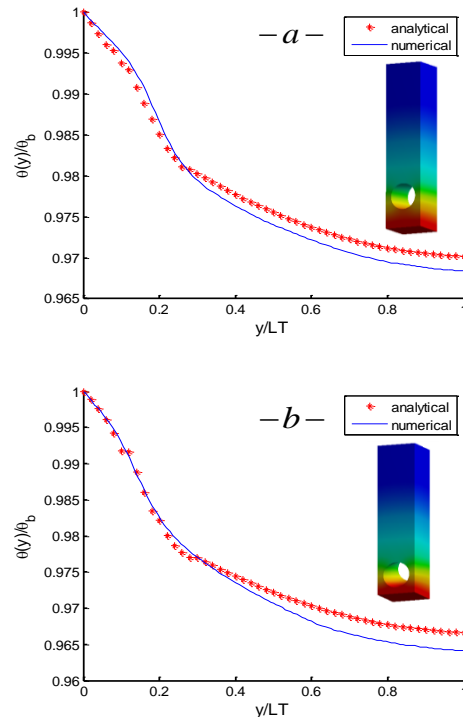


Figure 12. Comparisons between analytical and numerical results for the case-1- a) $\beta = 8^\circ$ b) $\beta = 22^\circ$.

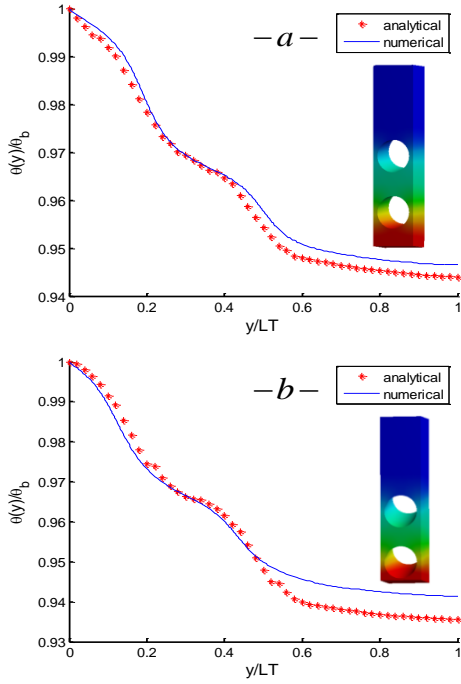


Figure 13. Comparisons between analytical and numerical results for the case-2- a) $\beta = 9^\circ$ b) $\beta = 25^\circ$.

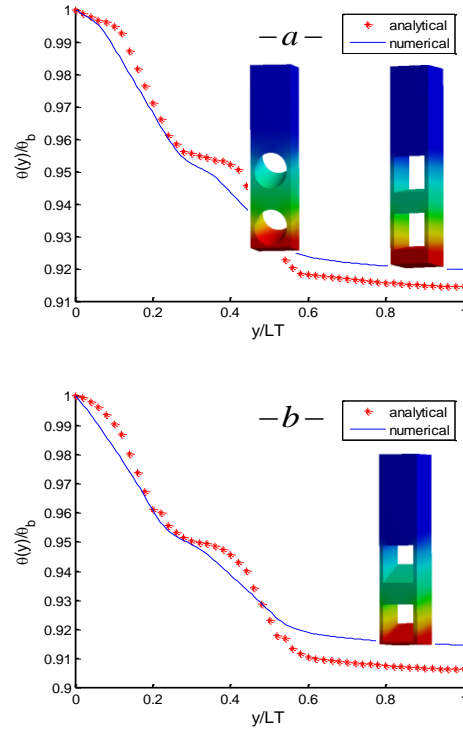


Figure 15. Comparisons between analytical and numerical results for the case-2- a) $\beta = 9^\circ$ b) $\beta = 25^\circ$

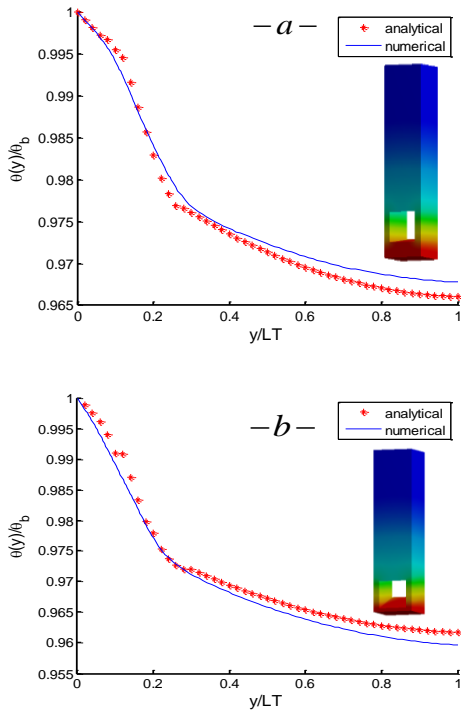


Figure 14. Comparisons between analytical and numerical results for the case-1- a) $\beta = 8^\circ$ b) $\beta = 22^\circ$.

7.2 Effects of inclination (thermal resistance)

The heat transfer area was changed due to the inclined perforation. Which leads to variable thermal resistance (R_{th}) along the fin length. According to the insulated fin tip, equation to calculate the thermal resistance described as:

$$R_{th} = \frac{A_{conv}}{\int \sqrt{h p k A} dA_{conv} \tanh\left(\frac{\int \sqrt{h p / k A} dA_{conv}}{A_{conv}} LT\right)} \quad (11)$$

Where:

$$A_{conv.} = \int_0^{LT} (P_{conv1} + P_{conv2} + P_{conv3}) dy$$

In inclined perforation region, the conduction area was replaced by the convection area, which leads to improve the thermal resistance. Figures (16 & 17) show the result of the thermal resistance with inclination angles for one and two perforations of the elliptical perforation, respectively. While the figures (18

and 19) show the results for one and two perforations of the rectangular perforation, respectively. All results show the decreases of the thermal resistance about (3.9% - 5.2%) with an increase for both the inclination angle and perforation size. Also, using the double perforations leads to improve the thermal resistance about (6.3%) .

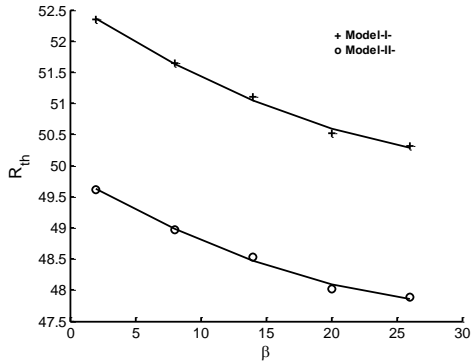


Figure 16. Variation of the R_{th} with inclination angle.

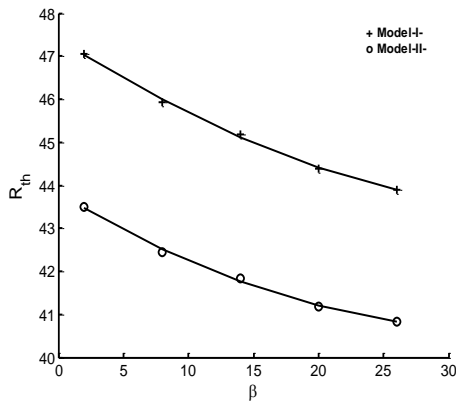


Figure 17. Variation of the R_{th} with inclination angle.

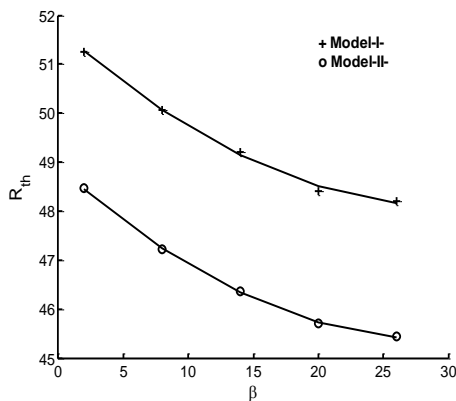


Figure 18. Variation of the R_{th} with inclination angle.

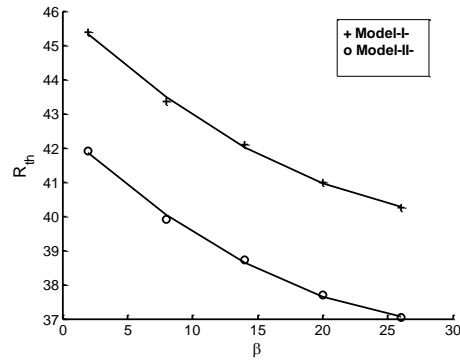


Figure 19. Variation of the R_{th} with inclination angle.

The change of the perforation shape has a less improve about (2%) when compared with the other parameters. But the use of the rectangular perforations leads to better results when compared with an elliptical shape.

7.3 Effects of the inclination (Heat ratio)

The heat transfer ratio q_p / q_s is described as the ratio between the heat transfer of a perforated fin to heat transfer of the solid fin at the same properties and operating conditions.

$$q_p \text{ or } q_s = -k A_b \left. \frac{d\theta}{dy} \right|_{y=0} \quad (12)$$

Heat transfer is possible to increase, according to the minimization of the thermal resistance and decreases of the temperature distributions that is obtained from inclined perforation.

Figures (20 and 21) show the increase of the heat transfer ratio about (1.14-1.48) times of the single and double elliptical perforations, respectively. Similarly, Figures (22 and 23) show the increase of the heat transfer ratio about (1.168-1.65) times of the single and double rectangular perforations, respectively.

Increase the inclination angles, size and number of the perforations leads to improve the heat transfer ratio due to the decrease each of the fin temperature and thermal resistance. Also, the change of the shapes of perforation (rectangular and elliptical) leads to more improvement of the thermal performance.

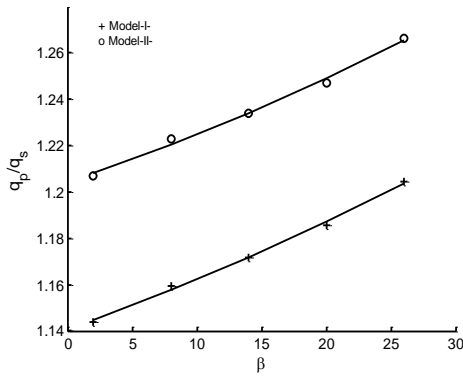


Figure 20. Effects of inclination angles on the heat transfer ratio.

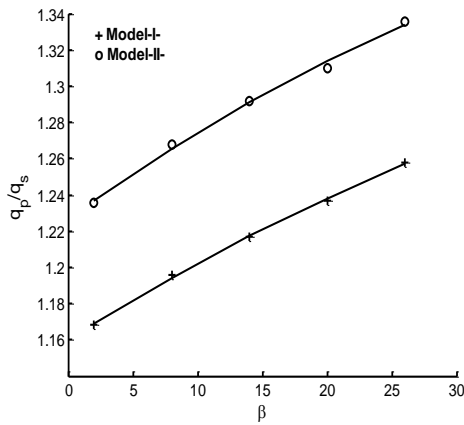


Figure 21. Effects of inclination angles on the heat transfer ratio.

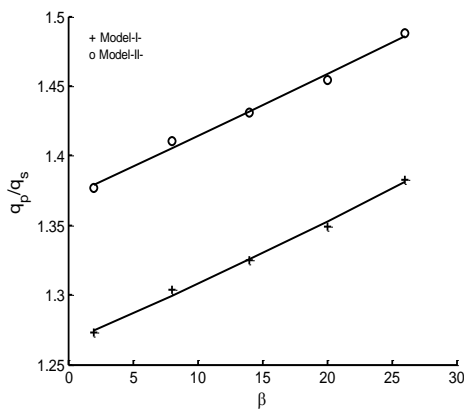


Figure 22. Effects of inclination angles on the heat transfer ratio.

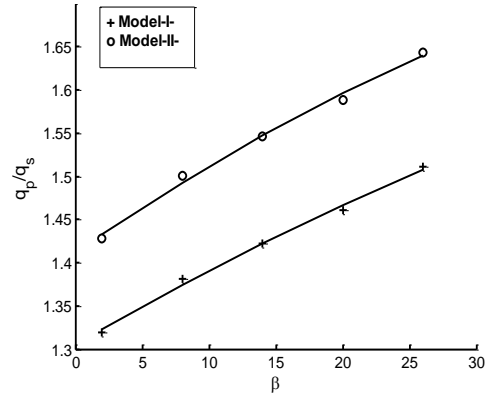


Figure 23. Effects of inclination angles on the heat transfer ratio.

7.4 Effects of the inclination (Effectiveness)

Effectiveness of the inclined perforated fin was increased, according to the decreases of the thermal resistance and increase the heat transfer of the perforated fin when compared with unperforated fin. Figures (24 and 25) show the increase of the effectiveness about (5% - 10%) of the single and double elliptical perforations, respectively. Increased one or all of the parameters (inclination angles and size of perforations) which leads to increase the effectiveness. Also, additional improvement can be achieved when used the double perforations. Likewise, Figures (26 and 27) show the increase of the effectiveness about (8.6% -14%) of the single and double rectangular perforations, respectively. The maximum effectiveness can be reached to the 32.5 of the rectangular perforations and 29.4 of elliptical perforations.

$$\varepsilon = \frac{q_{p \text{ or } s}}{q_{no \text{ fin}}} \quad (13)$$

9. Conclusion

- Many advantages can be achieved with inclined perforation as describe:
 1. Increase of the inner convection area.
 2. Distribute the inner convection area on the longer length in the y-axis.
 3. Increase of the external perforated area.

4. The conduction area that is replaced by the convection area was increased.
- The energy differential equation can be solved by using the DHE and Kummer's series.

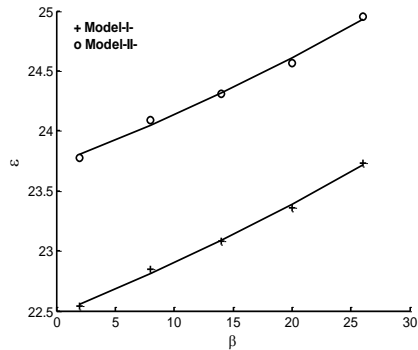


Figure 24. Change the effectiveness with the inclination angles.

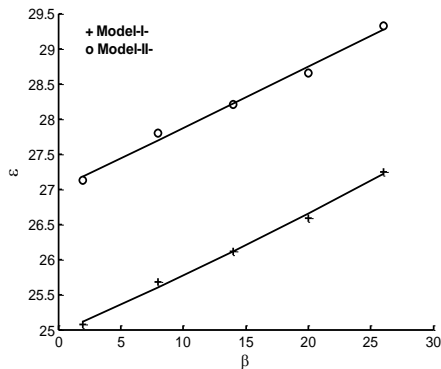


Figure 25. Change the effectiveness with the inclination angles.

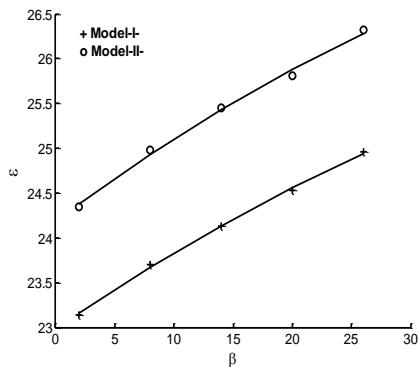


Figure 26. Change the effectiveness with the inclination angles.

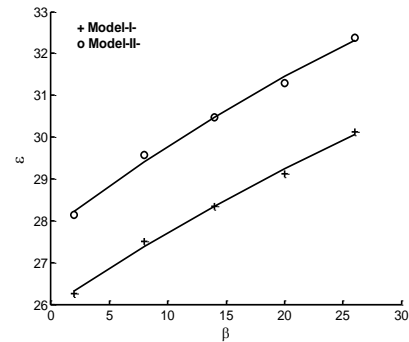


Figure 27. Change the effectiveness with the inclination angles.

- The opposite approach of the variable heat transfer area can be modelled with an especial form of the Signum function.
- The general solution can be taken as the basis to resolve any perforation shape at different specification according to the good agreement of the validation methods and various cases.
- The comparison results show the temperature can be decreased with inclination angle and a maximum drop achieved with inclination angle (25°) of the double perforation.
- Various results suggest that the use of the inclined perforation fin leads to decreased thermal resistance and improve in the thermal performance of the pin fin by enhancing the heat transfer about (65%).
- The change of the perforation shape has a smaller effect on the performance when compared to other parameters that are adopted in this study..

References

1. Saad A. El-Sayed , Mohamed, Abdel-latif, E. Abouda, (2002). Investigation of turbulent heat transfer and fluid flow in longitudinal rectangular-fin arrays of different geometries and shrouded fin array, *Experimental Thermal and Fluid Science* **26** , 879–900.
2. Rupak k. Banerjee , madhura karve,(2012), evaluation of enhanced heat transfer within a four row finned tube array of an air cooled steam condenser, *numerical heat transfer*, **61**: 735–753.
3. H. J. Tony tan, m.z. Abdullah and m. Abdul mujeebu (2013), effects of geometry and number of hollow on the performance of rectangular fins

- in microchannel heat sinks, *J. of Thermal Science and Technology - TIBTD Printed in Turkey*.
4. Monoj Baruah, Anupam Dewan and P. Mahanta (2011). Performance of Elliptical Pin Fin Heat Exchanger with Three Elliptical Perforations, *CFD Letters Vol. 3(2)* [S2180-1363 (11) 3265].
 5. M.R. Shaeri, M. Yaghoubi (2009^a), Thermal enhancement from heat sinks by using perforated fins, *Energy Conversion and Management* 50.
 6. M.R. Shaeri, M. Yaghoubi, K. Jafarpur (2009^b), Heat transfer analysis of lateral perforated fin heat sinks, *Applied Energy* 86 (2009).
 7. Bayram Sahin, Alparslan Demir (2008^a). Performance analysis of a heat exchanger having perforated square fins, *Applied Thermal Engineering* [28 (2008) 621–632]
 8. Bayram Sahin, Alparslan Demir (2008^b). Thermal performance analysis and optimum design parameters of heat exchanger having perforated pin fins, *Energy Conversion and Management* [49(2008) 1684-1695].
 9. Amol B. Dhumne, Hemant S. Farkade (2013), Heat Transfer Analysis of Cylindrical Perforated Fins in Staggered Arrangement, *International Journal of Innovative Technology and Exploring Engineering (IJITEE)*, Volume-2, Issue-5, April.
 10. Saurabh D. Bahadure, Mr. G. D. Gosavi (2014). Enhancement of Natural Convection Heat Transfer from Perforated Fin, *International Journal of Engineering research*, Volume No.3, Issue No.9, pp : 531-535.
 11. E. A. M. Elshafei (2010). Natural Convection Heat Transfer from a Heat Sink with Hollow / Perforated-Circular Pin Fins, *Energy* [35 (2010) 2870e2877].
 12. Kavita H. Dhanawade, Vivek K. Sunnapwar and Hanamant S. Dhanawade (2014), Thermal Analysis of Square and Circular Perforated Fin Arrays by Forced Convection, *International Journal of Current Engineering and Technology*.
 13. Ashok Fule, A .M Salwe, A Zahir Sheikh, Nikhil Wasnik (2014), Convective heat transfer comparison between solid and perforated pin fin, *international journal of mechanisms and robotics research*, Vol. 3, No. 2, April.
 14. Kirpikov.V.A and I.I. Leifman (1972). calculation of the temperature profile of a perforated fin, *instituted of chemical apparatus design, Moscow*. Vol.23, No.2, pp.316-321, August.
 15. Abdullah H. M. AlEsa (2009). One-dimensional finite element heat transfer solution of a fin with triangular perforations of bases parallel and towered its base, *Arch Appl Mech* [79: 741–751].
 16. Abdullah H. Al-Essa, Fayez M.S. Al-Hussien (2004), The effect of orientation of square perforations on the heat transfer enhancement from a fin subjected to natural convection, *Heat and Mass Transfer* 40 / 509–515.
 17. Kumbhar D.G, Dr.N.K sane, Chavan S.T. (2009), Finite Element Analysis and Experimental Study of Convective Heat Transfer Augmentation from Horizontal Rectangular Fin by Triangular Perforations, *international conference on advances in mechanical engineering*, National Institute of Technology, Surat - 395 007, Gujarat, India, *International Conference on Advances in Mechanical Engineering*, [August:376-380].
 18. Mohamed L. Elsayed and Osama Mesalhy (2014), Studying the performance of solid/perforated pin-fin heat sinks using entropy generation minimization, *springer-Heat Mass Transfer*, 01-12.
 19. Incropera, Dewitt, Bergman and Lavine (2007), *Fundamental of heat and mass transfer*, John Wiley & Sons; 6th edition, [p:95-160 and 560-594].
 20. Zan WU, Wei LI, Zhi-jian SUN, Rong-hua HONG (2012), Modeling natural convection heat transfer from perforated plates, *Journal of-Zhejiang University-SCIENCE A* [13(5):353-360].
 21. Raithby GD; Hollands KGT (1998), *Natural convection*. In: Warren M. Rohsenow, James R Hartnett, Young I. Cho, *Handbook of heat transfer*, MCGRAW-HILL 3rd edition, [p:4-1 to 4-80].
 22. Hisham H. JASIM and Mehmet Sait SÖYLEMEZ (2016^a), The Temperature Profile for the Innovative Design of the Perforated Fin, *Int. Journal of Renewable Energy Development* 5(3) 2016: 259-266.
 23. Hisham H. JASIM and Mehmet Sait Söylemez (2016^b), Enhancement Of Natural Convection Heat Transfer Of Pin Fin Having Perforated With Inclination Angle, *J. of Thermal Science and Technology, Isı Bilimi ve Tekniği Dergisi*, 36, 2, 111-118.
 24. Andrei D. Polyanin and Valentin F. Zaitsev (2003), *hand book of Exact solution for ordinary differential equations*, 2nd ed (USA). By CHAPMAN & HALL/CRC, P.213-490.
 25. Hazewinkel. M, (1995), *Encyclopaedia of Mathematics: A-Integral- Coordinates*, Springer science and business media, [p:105-110 and 797-800].
 26. John W. Harris and Horst Stocker (1998), *Hand book of mathematics and computational science*, springer (USA) [p:130-150].

Calculation of Optimum Insulation Thickness and Energy Savings for Different Climatic Regions of Turkey

Ebru Kavak AKPINAR*, İbrahim Halil DEMİR

Firat University, Department of Mechanical Engineering, Elazığ, Turkey

* ebruakpinar@firat.edu.tr

(Geliş/Received: 18.10.2017; Kabul/Accepted: 29.08.2018)

Abstract

In this study, the optimum insulation thickness, energy savings and payback periods were calculated based on life-cycle cost analysis for the cities of Balıkesir, Kayseri, Malatya, Mersin, Muğla, Şanlıurfa and Trabzon. These cities were selected from Turkey's four climate zones. The calculations were carried out for coal as energy source, expanded polystyrene (EPS) and extruded polystyrene (XPS) as insulation materials on two types of walls: (1) sandwich and (2) externally insulated. Results indicated that insulation thicknesses varied between 0.002–0.049 m, with the amount of life-cycle energy saving as 0.629–21.047 \$/m² and a payback period of 0.3–6.5 years depending on the type of fuel, insulation material and wall-type.

Key words: Degree-Day Method, Energy saving, Optimum insulation thickness, XPS, EPS, Coal, Turkey

Türkiye'nin Farklı İklim Bölgeleri İçin Enerji Tasarrufu ve Optimum Yalıtım Kalınlığının Hesaplanması

Özet

Bu çalışmada Balıkesir, Kayseri, Malatya, Mersin, Muğla, Şanlıurfa ve Trabzon illerinin optimum yalıtım kalınlığı, enerji tasarrufu ve geri ödeme süreleri yaşam döngüsü maliyet analizlerine göre hesaplanmıştır. Bu şehirler, Türkiye'nin dört iklim bölgesinden seçilmiştir. Hesaplamalar enerji kaynağı olarak kömür, iki tip duvar üzerinde: (1) sandviç ve (2) dıştan yalıtılmış, yalıtım malzemesi olarak genişletilmiş polistiren (EPS) ve ekstrüde polistiren (XPS) için yapılmıştır. Sonuçlar, yakıt türüne, yalıtım malzemesine ve duvar tipine bağlı olarak yaşam döngüsü enerji tasarrufu 0.629–21.047 \$ / m² ve 0.3-6.5 yıl geri ödeme süresi ile yalıtım kalınlıklarının 0.002-0.049 m arasında değiştiğini gösterdi.

Anahtar kelimeler: Derece-Gün Yöntemi, Enerji tasarrufu, Optimum yalıtım kalınlığı, XPS, EPS, Kömür, Türkiye

1. Introduction

Energy consumption is distributed among four main sectors such as industrial, building (residential/commercial), transportation, and agriculture. The building sector is the largest energy consumer following the industrial sector [1-2].

Thermal insulation is the first of the methods for decreasing the energy consumption. Reduction of the energy consumption to the minimum values for the buildings is compulsory according to national regulations. Most of the studies focus on the determination of optimum thickness of insulation for external walls in buildings based

on cooling degree days (CDD) and heating degree days (HDD) [3-15].

In this study, seven different cities of Turkey (Balıkesir, Kayseri, Malatya, Mersin, Muğla, Şanlıurfa and Trabzon) were selected as to represent the first, second, third, and fourth climatic zones (Fig. 1). The effect of two different wall structures was considered to determine the optimum insulation thickness, energy savings and payback period for EPS and XPS insulation materials, using coal for fuel.



Figure 1. Four different degree-day regions of Turkey according to TS 825 Standard

2. Material and Methods

2.1. Calculation of degree days

According to Turkish Standard Number (TS 825), heat insulation rules for buildings, four different degree-day (*DD*) regions have been defined for Turkey, as shown in Fig. 1. Climatic conditions are the main factors affecting the thermal load requirements of buildings [16-18].

The degree day method is one the simplest methods used in the heating, ventilating and air-conditioning industry to estimate heating and cooling energy requirements [19]. Degrees days are a specialized type of weather data, calculated from the readings of the outside air temperature. Many approaches and techniques to calculating HDDs can be found in the literature [20-22]. In this study, calculations of optimum insulation thickness, payback period and energy savings were performed using $T_b = 25^\circ\text{C}$ base temperature. The HDDs were calculated (Table 2, 2002–2012) based on the daily data of the maximum and minimum air temperatures collected from the 7 main stations of the Turkey climate network (Fig. 1) for the colder eight months (October–May).

The calculation of HDDs was carried out by means of different equations, depending on the relationship between the base temperature T_b and the mean T_m , minimum T_{min} and the maximum T_{max} daily air temperatures. The total number of heating degree-days for the whole heating season can be expressed as [23],

$$(T_m \leq T_b) \quad (1)$$

$$(T_m > T_b) \quad (2)$$

where, T_i is the constantly adopted indoor design air temperature, T_b is the base temperature and T_m is the daily mean outdoor temperature, N is total number of heating days.

The daily mean outdoor temperature is determined by the average of the measured maximum and minimum temperature during the day.

$$T_m = \frac{(T_{m,min} + T_{m,max})}{2} \quad (3)$$

Here, $T_{m,min}$ ve $T_{m,max}$ is the average of the measured lowest and highest temperatures during the day, respectively [23].

In this study, the seven cities from seven different regions in Turkey, Balıkesir, Kayseri, Malatya, Mersin, Izmir, Sanliurfa and Trabzon were selected to determine the optimum insulation thickness. Table 1 shows the climate characteristic and degree days values of each city. Data are mean values of ten years, was taken in 2012 from The State Meteorological Affairs General Directorate (DMI).

2.2. External wall structures in buildings

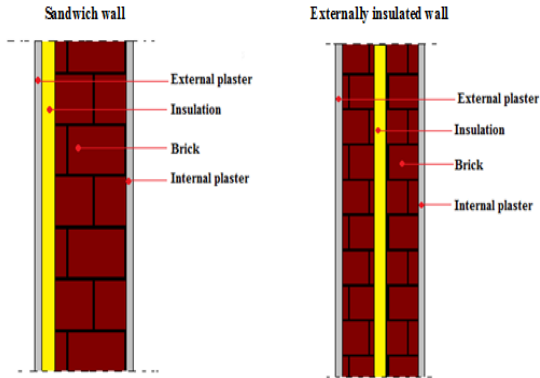
External wall insulation is immensely important in terms of energy saving [2-3]. In Turkey generally, the external walls have a composite structure called sandwich wall or externally insulated wall. The structures of investigated walls (sandwich wall and externally insulated wall) are shown in Fig. 2. The sandwich wall is formed from 2 cm internal plaster, two pieces of 13 cm horizontal hollow brick, insulation material between horizontal hollow brick and 3 cm external plaster. Externally insulated wall is consisted from 2 cm internal plaster, 29 cm horizontal hollow brick, insulation and 3 cm external plaster. In the calculations, as the insulation material, *expanded polystyrene* (EPS) ($k = 0.032 \text{ W/mK}$) and *extruded polystyrene* (XPS) ($k = 0.040 \text{ W/mK}$) were used.

Table 1. Climate zones, heating degree days and certain data for the selected cities

City-Region	Zone	Longitude(°)	Latitude(°)	Elevation (m)	Heating degree days
Balıkesir-Marmara	2	27.52	39.39	147	1914
Trabzon-Black Sea	2	39.43	41.00	30	1724
Kayseri-Central Anatolia	4	35.29	38.43	1068	3113
Muğla-Aegean	1	28.21	37.12	646	1879
Mersin-Mediterranean Sea	1	34.36	36.49	5	852
Şanlıurfa-Southeastern Anatolia	2	38.46	37.08	547	1503
Malatya-East Anatolia	3	38.18	38.21	998	2996

Table 2. The physical properties of the external wall materials

Material	Sandwich wall			Externally insulated wall		
	thickness (m)	k (W/mK)	R (m ² K/W)	thickness (m)	k (W/mK)	R (m ² K/W)
interior plaster (lime based)	0.02	0.87	0.02	0.02	0.87	0.02
horizontal hollow brick	0.13	0.45	0.28	0.26	0.45	0.64
exterior plaster (cement based)	0.03	1.4	0.02	0.03	1.4	0.02
R_i	0.13			0.13		
R_o	0.04			0.04		
R_w(wall layers without the insulation material)	0.77			0.85		

**Figure 2.** Wall models

The heat conduction and resistant values for sandwich and externally insulated wall are given in Table 2. Thermal resistances of the walls are calculated using these coefficients. Thermal resistances of the walls were calculated without taking into account the insulation material. The conductivity and resistant values were determined from TS 825 (Turkish Standard of Thermal Insulation in Buildings) [16].

2.3. Heating load for external walls

The heat loss and the annual heat loss from the unit surface of the external wall are calculated respectively by [3, 6]:

$$q = U \cdot \Delta t \quad (4)$$

$$q_A = 86400 \cdot DD \cdot U \quad (5)$$

The yearly energy requirement is determined by:

$$E_A = \frac{86400 \cdot DD \cdot U}{\eta} \quad (6)$$

Overall heat transfer coefficient for wall is given as,

$$U = \frac{1}{R_i + R_w + R_{ins} + R_o} \quad (7)$$

The thermal resistance of the insulation layer is,

$$R_{ins} = \frac{x}{k} \quad (8)$$

If R_{wt} is the total wall resistance excluding the insulation layer resistance, Eq. (7) can be written as,

$$U = \frac{1}{(R_{wt} + R_{ins})} \quad (9)$$

The annual amount of the energy expended for heating can be obtained as the following,

$$E_A = \frac{86400 \cdot DD}{(R_{wt} + (x/k)) \cdot \eta} \quad (10)$$

The annual energy cost of heating per unit area can be defined as,

$$C_A = \frac{86400 \cdot DD \cdot C_f}{(R_{wt} + (x/k)) \cdot H_u \cdot \eta} \quad (11)$$

The life-cycle cost analysis (*LCCA*) is one of the methods to calculate the optimum insulation thickness. The total heating costs over a period of time of N years is evaluated in the present value using the present worth factor (*PWF*). The present worth factor is calculated based upon the inflation (g) and interest rate (i) as follows [3, 6].

If $i > g$ then

$$r = \frac{i - g}{1 + g} \quad (12)$$

If $i < g$ then

$$r = \frac{g - i}{1 + i} \quad (13)$$

and

$$PWF = \frac{(1+r)^N - 1}{r \cdot (1+r)^N} \quad (14)$$

If $i = g$, then

$$PWF = \frac{1}{1+i} \quad (15)$$

The cost of insulation is given by Eq. (16)

$$C_{ins} = C_i \cdot x \quad (16)$$

The total heating cost of the insulated building is given by

$$C_t = C_A \cdot PWF + C_i \cdot x \quad (17)$$

or

$$C_t = \frac{86400 \cdot DD \cdot C_f \cdot PWF}{(R_{wt} + (x/k)) \cdot H_u \cdot \eta} + C_i \cdot x \quad (18)$$

The optimum insulation thickness is obtained as the following,

$$x_{op} = 293.94 \left(\frac{DD \cdot C_f \cdot PWF \cdot k}{H_u \cdot C_i \cdot \eta} \right) - k \cdot R_{wt} \quad (19)$$

The values of the parameters used in the calculations of the optimum insulation thickness, payback period and life cycle savings for the insulated buildings in selected cities are given in Table 3. The payback period is described as the ratio of the energy cost of the uninsulated building to the energy savings [3, 6, 10].

Table 3. Parameters and values used in the calculation of insulation-thickness

Parameters	Value
Fuel (Coal)	
H_u	25.122x10 ⁶ (J/kg)
η	0.65
Insulation (Expanded polystyrene (EPS))	
k	0.032(W/mK)
Insulation (Extruded polystyrene (XPS))	
k	0.040 (W/mK)
C_i	23.88 \$/m ³
i	16 (%)
g	10 (%)
N	10 year
PWF	1.8

3. Results and Discussion

The optimum insulation thicknesses for the two different wall type were obtained by Eq. (19) and the results for coal fuel and insulation materials (*EPS* and *XPS*) are given in Table 4. Optimum insulation thickness varied between 0.011 and 0.046 for EPS, 0.014 and 0.049 m for

XPS in sandwich wall, whereas the optimum insulation thickness varied between 0.002 and 0.036 m for EPS, 0.006 and 0.039 m for XPS in case of external insulated wall, respectively. The optimum thickness for sandwich wall was higher than that required for external insulated wall. The optimum insulation thickness for *EPS* was less when compared to *XPS*.

Table 4. Optimum insulation-thickness of selected cities for different wall types and insulation materials

City	Sandwich wall		External insulated wall	
	EPS (m)	XPS (m)	EPS (m)	XPS (m)
Balıkesir	0.030	0.033	0.021	0.024
Kayseri	0.046	0.049	0.036	0.039
Malatya	0.045	0.047	0.034	0.038
Mersin	0.011	0.014	0.002	0.006
Muğla	0.030	0.032	0.020	0.023
Şanlıurfa	0.024	0.026	0.014	0.018
Trabzon	0.027	0.030	0.018	0.021

The curves of insulation and fuel costs, and total cost versus the insulation thickness for the selected cities are illustrated for sandwich wall and external insulated wall in Fig.3, respectively. It was seen that the fuel cost decreased with increasing insulation thickness. The total cost decreased until a certain value of the insulation thickness was reached, after which it began to increase again.

On the other hand, the insulation cost increased linearly with insulation thickness. The insulation thickness at the minimum total cost was taken as the optimum insulation thickness.

The payback period is reduced with increasing degree days. The optimum insulation thickness is increased with increasing degree days. Larger insulation thickness is required in colder climates with higher degree days, but less insulation in warmer climates with lower degree

days. Therefore, the optimum insulation thickness for Mersin became lower, since it has more hot days. The optimum insulation thickness for Kayseri became higher, since it has less hot days.

Table 5 displays life cycle energy savings over 10 years and the payback periods for insulated buildings in selected cities for coal. The results according to selected cities showed that life cycle savings varied between 0.629 \$/m² and 21.047 \$/m², and payback periods varied between 0.3 and 6.5 years according to insulation materials (*EPS* and *XPS*) and wall types (*SW* and *EIW*) and the fuel type (coal). Fertelli [14] evaluated the influence of different wall types (stone, brick, concrete and bims) on the optimum insulation thicknesses, energy savings, and payback periods for six different energy types (LPG, electricity, fuel oil, coal, natural gas, and geothermal energy), and four cities from different climate zones (Aydın, Trabzon, Malatya, and Sivas). Insulation thicknesses were determined between 0 – 0.179 m, with the amount of 0 – 235.053 \$/m² of energy saving, and 0 – 11.53 years of payback period, depending on various fuels and wall types. Uçar and Balo [15] calculated the optimum insulation thickness of different wall structures for four different insulation materials and for four climatic zones of Turkey and different fuel types. Their results show that the energy cost savings vary between 4.2 \$/m² and 9.5 \$/m², depending on the city and insulation materials.

Calculation of Optimum Insulation Thickness and Energy Savings for Different Climatic Regions of Turkey

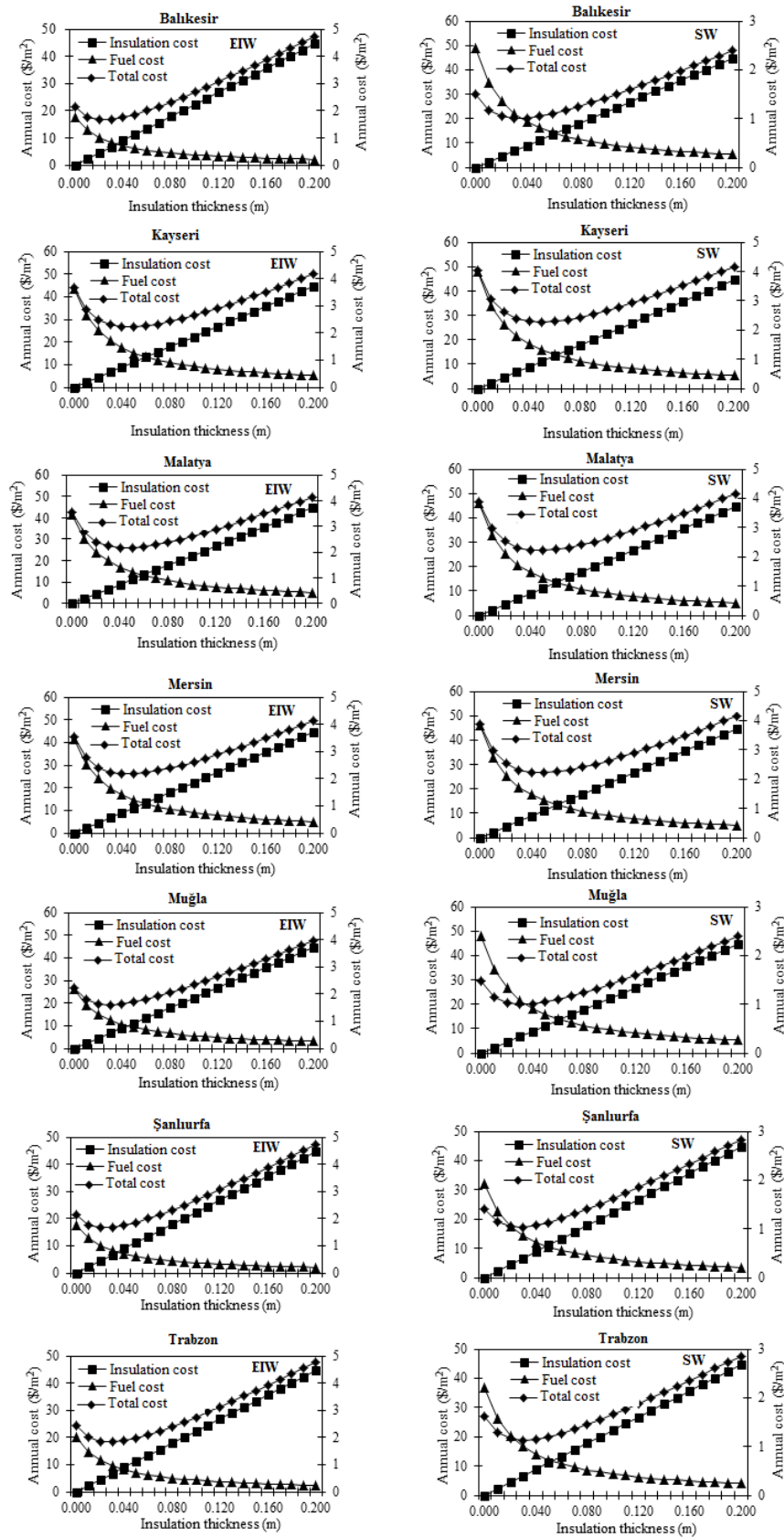


Fig. 3. Effect of insulation thickness on costs for sandwich wall and external insulated wall at selected cities

Table 5. Payback periods and life-cycle energy savings

City	SW			
	EPS (m)		XPS (m)	
	Payback period (years)	Life-cycle energy savings (\$/m ²)	Payback period (years)	Life-cycle energy savings (\$/m ²)
Balıkesir	3.6	10.822	2.9	14.175
Kayseri	5.6	14.430	4.3	21.047
Malatya	5.5	14.117	4.2	20.188
Mersin	1.3	3.978	1.2	6.013
Muğla	3.6	10.822	2.8	13.745
Şanlıurfa	2.9	8.658	2.3	11.167
Trabzon	3.3	9.740	2.6	12.885

City	EIW			
	EPS (m)		XPS (m)	
	Payback period (years)	Life-cycle energy savings (\$/m ²)	Payback period (years)	Life-cycle energy savings (\$/m ²)
Balıkesir	3.7	6.610	2.7	10.332
Kayseri	6.5	11.332	4.4	16.789
Malatya	6.1	10.703	4.6	16.359
Mersin	0.3	0.629	0.7	2.583
Muğla	3.5	6.295	2.6	9.901
Şanlıurfa	2.4	4.407	2.1	7.750
Trabzon	3.1	5.666	2.4	9.040

4. Conclusion

In this study, the optimum insulation thickness of external walls, the energy savings over a lifetime of 10 years, and the payback periods were calculated for two different wall types, coal as energy source, and two different insulation materials in cities from four different climatic zones of Turkey. The calculations were carried out to TS 825. The results showed that the optimum insulation thickness varied between 0.002 and 0.049 m, energy savings varied between 0.629 \$/m² and 21.047 \$/m², and payback periods varied between 0.3 and 6.5 years depending on the cities, the type of wall, the insulation material and the cost of coal fuel. Energy saving was bigger, insulation was more effective, and the payback period was shorter for higher degree-day cities. The highest value of the optimum insulation thickness was reached for Kayseri city by using sandwich wall, XPS as insulation material; whereas the lowest optimum insulation thickness was obtained for Mersin city by using external insulation wall, EPS as insulation material, coal as energy source.

5. References

- Kurt, H. (2011). The Usage of Air Gap in the Composite Wall For Energy Saving and Air Pollution. *Environmental Progress and Sustainable Energy*, **30**, 450–458.
- Bolatturk, A. (2006). Determination of Optimum Insulation Thickness For Building Walls With Respect to Various Fuels And Climate Zones in Turkey. *Applied Thermal Energy*, **26**, 1301–1309.
- Çay, Y, Gürel, A.T. (2013). Determination of Optimum Insulation Thickness, Energy Savings, And Environmental Impact For Different Climatic Regions Of Turkey. *Environmental Progress & Sustainable Energy*, **32** (2), 365-372.
- Kaynaklı, O. (2012). A review of the Economical And Optimum Thermal Insulation Thickness for Building Applications. *Renewable and Sustainable Energy Reviews*, **16**, 415– 425.
- Ekici, B.B., Gulen, A.A., and Aksoy, U.T. (2012). A study on the Optimum Insulation Thicknesses of Various Types of External Walls with Respect To Different Materials, Fuels and Climate Zones in Turkey. *Applied Energy*, **92**, 211–217.
- Comakli, K., Yuksel, B. (2003). Optimum Insulation Thickness of External Walls for Energy Saving. *Applied Thermal Engineering*, **23**(4), 473–479.
- Comakli, K, Yuksel, B. (2004). Environmental impact of Thermal Insulation Thickness in Buildings. *Applied Thermal Engineering*, **24** (2), 933–940.
- Dombayci, O.A. (2007). The environmental impact of Optimum Insulation Thickness for External Walls of Buildings. *Building and Environment*, **42** (11), 3855–3859.
- Durmaz, A., Kadioglu, M., and Sen, Z. (2000). An Application of the Degree-Hours Method to Estimate the Residential Heating Energy Requirement and Fuel Consumption in Istanbul. *Energy*, **25** (12): 1245–1256.
- Hasan, A. (1999). Optimizing Insulation Thickness for Buildings Using Life Cycle Cost. *Applied Energy*, **63**, 115–124.
- Ozkan, D.B., Onan, C. (2011). Optimization of Insulation Thickness for Different Glazing Areas in Buildings for Various Climatic Regions in Turkey. *Applied Energy*, **88** (4), 1331–1342.
- Sundarama, S., Bhaskaranb, A. (2014). Optimum Insulation Thickness of Walls for Energy-Saving in Hot Regions of India. *International Journal of Sustainable Energy*, **33** (1), 213–226.

13. Büyükalaca, O., Bulut, H., Yılmaz, T. (2001). Analysis of Variable-Base Heating And Cooling Degree-Days for Turkey. *Applied Energy*, **69**, 269–283.
14. Fertelli, A. (2013). Determination of Optimum Insulation Thickness for Different Building Walls in Turkey. *Transactions of Famena*, XXXVII-2, ISSN 1333-1124, 103-113.
15. Ucar A., Balo F. (2010). Determination of the Energy Savings and the Optimum Insulation Thickness in the Four Different Insulated Exterior Walls. *Renewable Energy*, **35**, 88-94.
16. TSE (Turkish Standards Institution). (1998). TS 825: Thermal Insulation in Buildings.
17. Dagsoz, A.K. (1995). Degree Day Values in Turkey, National Energy Saving Policy. Heat Insulation in Buildings. Izocam, Istanbul (in Turkish).
18. Sisman, N., Kahyab, E., Aras, N., Aras, H. (2007). Determination of Optimum Insulation Thicknesses of The External Walls And Roof (Ceiling) for Turkey's Different Degree-Day Regions. *Energy Policy*, **35**, 5151–5155.
19. Baskerville, G.L., Emin, P. (1969). Rapid Estimation of Heat Accumulation from Maximum and Minimum Temperatures. *Ecology*; **50**, 514–517.
20. Floyd, R.B., Braddock, R.D. (1984). A Simple Method for Fitting Averaging Diurnal Temperature Curves. *Agricultural and Forest Meteorology*, **32**, 107–119.
21. Yang, S., Logan, J., Coffey D.L. (1995). Mathematical Formulae for Calculating the Based Temperature for Growing Degree Days. *Agricultural and Forest Meteorology*, **74**, 61–74.
22. Matzarakis, A., Balafoutis, C. (2004). Heating Degree-Days Over Greece As an Index of Energy Consumption. *Int. J. Climatol.*, **24**, 1817–1828.
23. Demir, I.H. (2014). Determination of Optimum Insulation Thickness for Building Exterior Walls and Cost Analysis (Bina dış duvarları için optimum yalıtım kalınlığının belirlenmesi ve maliyet analizi). MSc Thesis, Firat University, (in Turkish).

Nomenclature

C_A	annual heating cost (\$/m ² year)
C_f	energy cost of fuel (\$/kg, \$/m ³ , \$/kWh)
C_i	insulation material cost (\$/m ³)
C_{ins}	insulation cost (\$/m ²)
C_t	total heating cost at present value (\$)
CDD	cooling degree days (°C.days)
DD	degree days (°C.days)
E_A	annual heating energy (J/m ² year)
g	inflation rate
H_u	heating value (J/kg, J/m ³ , J/kWh)
HDD	heating degree days (°C.days)
i	interest rate
k	thermal conductivity (W/mK)
$LCCA$	life cycle cost analysis
N	lifetime (years)
PWF	present worth factor
R_i	thermal resistance (inside air) (m ² K/W)
R_{ins}	insulation thermal resistance (m ² K/W)
R_o	thermal resistance (outside air) (m ² K/W)
R_w	total thermal resistance of uninsulated wall plates (m ² K/W)
R_{wt}	total of R_i , R_w , R_o (m ² K/W)
q	heat loss (W/m ²)
U	overall heat transfer coefficient (W/m ² K)
T	temperature (°C)
T_b	base temperature (°C)
T_i	indoor design air temperature (°C)
T_m	daily mean outdoor temperature (°C)
T_{min}	minimum daily air temperature (°C)
T_{max}	maximum daily air temperature (°C)
x	insulation thickness (m)
x_{op}	optimum insulation thickness (m)
η	efficiency of the heating system

Some Population Parameters of Mirror Carp (*Cyprinus carpio* L., 1758) Living in Keban Dam Lake, Elazığ, TURKEY

Metin ÇALTA*, Mustafa DÜŞÜKCAN, Burecu SAYIN
Firat University, Faculty of Fisheries, 23119 Elazığ, Turkey
*mcalta@firat.edu.tr

(Geliş/Received: 28.12.2017; Kabul/Accepted: 20.02.2018)

Abstract

This study was aimed to determine the age and growth of mirror carp (*Cyprinus carpio* L., 1758) population of Keban Dam Lake, Elazığ, Turkey. For this purpose, the fish samples were obtained from the area near the set of Keban Dam Lake by using 20-40 mm mesh size gill nets from November 2016 to December 2016. 120 mirror carps (54 females and 66 males) were examined in the present study. They ranged from 2 to 8 in age, from 21.50 to 37.50 cm in total length and from 172.66 to 789.17 g in body weight. A nonlinear relationship was found between the total length and weight of *C. carpio* ($W=0.0135*TL^{3.0403}$; $r^2=0.9724$). The growth parameters were estimated as 43.09 cm for L_{∞} , 0.176 years⁻¹ for k , -2.423 years for t_0 , 17 years for t_{max} , 2.51 for the growth performance index (Φ) and 1.62 for condition factor (C_f). The age-at-length data fitted to the Von Bertalanffy Growth Function was determined as $L_t=43.09*[1-e^{-0.176(t+2.423)}]$. The absolute, relative and instantaneous growth values of mirror carp from Keban Dam Lake were the highest in the age range of 2-3, followed by the age range of 3-4. However, the values started to decrease after age 4.

Key Words: Mirror carp, *Cyprinus carpio*, growth, age, Keban Dam Lake

Keban Baraj Gölünde Yaşayan Aynalı Sazan (*Cyprinus carpio* L., 1758)'de Bazı Büyüme Parametreleri

Özet

Bu çalışma Elazığ Keban Baraj Gölü'ndeki aynalı sazan (*Cyprinus carpio* L., 1758)'in yaş ve büyümesini belirlemek amacıyla yapıldı. Bu amaçla, balık örnekleri 20-40 mm göz açıklığındaki galsama ağlarını kullanarak Keban Baraj Gölü seti yakınındaki alanlardan Kasım 2016-Aralık 2016 döneminde yakalandı. Çalışmada, toplam 120 adet aynalı sazan (54 dişi ve 66 erkek) incelendi. İncelenen balıkların yaşları 2-8 yıl, toplam boyları 21,5-37,5 cm ve vücut ağırlıkları 172,66-789,17 g arasında değişim gösterdi. *C. carpio*'nun toplam boy-vücut ağırlığı arasında doğrusal olmayan bir ilişki bulundu ($W=0,0135 \times TL^{3.0403}$; $r^2=0.9724$). Büyüme parametreleri olan L_{∞} , k , t_0 , t_{max} , büyüme performans indeksi (Φ) ve kondisyon faktörü (C_f) sırasıyla 43,09 cm; 0,176 yıl⁻¹; -2,423 yıl; 17 yıl, 2,51 ve 1,62 olarak hesaplandı. Von Bertalanffy Büyüme Fonksiyonu $L_t = 43,09 * [1 - e^{-0,176(t+2,423)}]$ olarak belirlendi. Aynalı sazanın Keban Baraj Gölü'ndeki mutlak, oransal ve anlık büyüme değerleri 2-3 yaş aralığında en yüksek olup, bunu 3-4 yaş aralığı takip etmiştir. Ancak değerler 4 yaşından sonra düşmeye başladı.

Anahtar Kelimeler: Aynalı sazan, *Cyprinus carpio*, büyüme, yaş, Keban Baraj Gölü

1. Introduction

Approximately 28 fish species belong to seven families permanently inhabit in the lake [1]. *Cyprinus carpio* is one of the most dominant fish species in Keban Dam Lake. Mirror carp is a type of *C. carpio* species and differs from others with possessing the irregular and patchy scaling [2]. There are several investigations carried out on some population characteristics (i.e., growth properties, reproduction biology, spermatological parameters, age determination and population

dynamics) of the mirror carp in different water reservoirs of Turkey [3-9]. The age and growth studies are very important for fisheries biology. However, no studies have been found on the age and growth of mirror carp population of Keban Dam Lake. Therefore, the present study aimed to determine the age and growth of the mirror carp population of Keban Dam Lake.

2. Materials and Methods

In this study, 120 mirror carp (*C. carpio* L., 1758) were sampled from the location near to the set of Keban Dam Lake (38° 48' 23.67"K and 38° 46' 23.88"D; see Figure 1) that was constructed on the Euphrates River in the Eastern Anatolia region of Turkey in 1974. It has a large reservoir with 675 km² surface area at normal water level [10]. The mirror carp samples were caught by using 20-40 mm mesh size gill nets from November 2016

to December 2016. They were immediately transferred to the laboratory. The total lengths (TL) and body weights (W) of all individuals were measured to the nearest 1 mm and 0.1 g, respectively. Scales were extracted from each fish, kept in 3% KOH solution for nearly 1 h and stored dry in paper envelopes for further observation. The age of fishes was determined by reading of the growth rings formed on scales under a binocular stereoscopic microscope (Leica S8APO) combined to a computer.

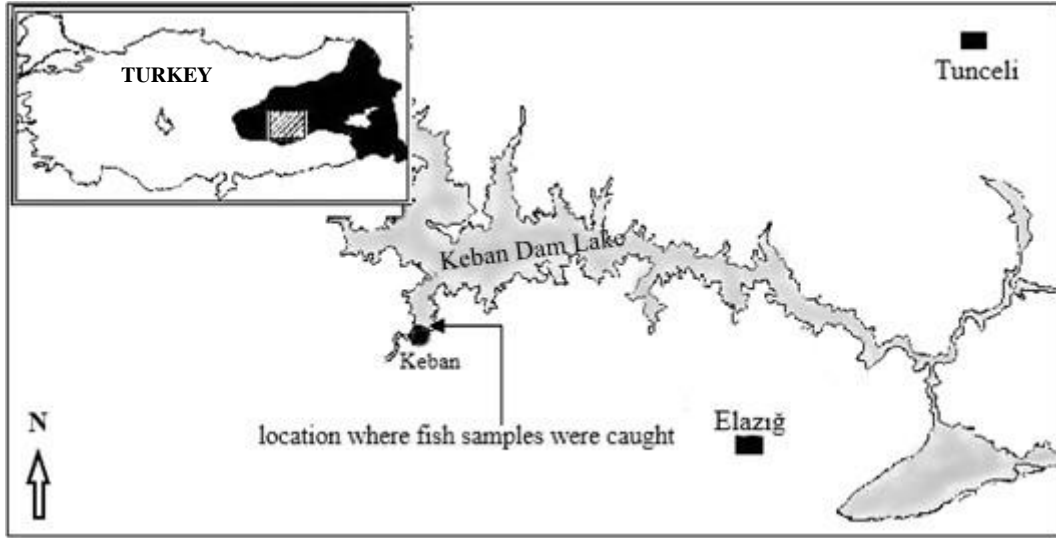


Figure 1. The map of Keban Dam Lake and the location in which the mirror carps were sampled (modified from Tombul and Karadoğan [11])

The length-weight relationship (LWR) was estimated by the equation:

$$W = a * TL^b \quad [2.1.]$$

Where, W is the body weight (g), TL is the total length (cm), a is the intercept and b is the slope [12]. Log-transformation was applied prior to regression, thus the equation was transformed to:

$$\text{Log}W = \text{Log}a + b * \text{Log}TL \quad [2.2.]$$

A log-log plot of TL and W was made in order to remove outliers, and the 95% confidence limits of a and b were calculated with the statistical program (SPSS ver. 22.0, IBM Corporation) in order to confirm the distance between the b value and the isometric value of 3 [13].

The Von Bertalanffy growth function (VBGF) was fitted to individual length and age data for the mirror carp population and expressed with the equation given by Von Bertalanffy [14];

$$L_t = L_\infty * [1 - e^{-k(t-t_0)}] \quad [2.3.]$$

Where, L_t is the length (cm) at age t , L_∞ is the asymptotic length (cm), k is the rate at which the growth curve approaches the asymptotic length (year^{-1}), t_0 is the hypothetical age of the fish at zero length.

The growth performance index (Φ) was estimated in each case according to the formula of Munro and Pauly [15]:

$$\Phi = \text{Log} k + 2 * \text{Log}TL_\infty \quad [2.4.]$$

The longevity was calculated by using equation stated by Taylor [16]:

$$t_{max} = 3/k \quad [2.5.]$$

Where, L_∞ is the asymptotic length (cm), k is the rate at which the growth curve approaches the asymptotic length (year^{-1}), t_{max} is the longevity (maximum age reached by the species).

Fulton's Condition Factor (CF) was calculated using the equation:

$$CF = \frac{\bar{W}}{TL^3} * 100 \quad [2.6.]$$

Where, \bar{W} is mean total weight in g and \bar{TL} is mean total length in cm.

Absolute, relative and instantaneous growth rates were calculated using the formulas given by Ricker [17]:

$$\text{Absolute growth rate} = \frac{TL_2 - TL_1}{t_2 - t_1} \quad [2.7.]$$

$$\text{Relative growth rate} = \frac{TL_2 - TL_1}{TL_1(t_2 - t_1)} * 100 \quad [2.8.]$$

$$\text{Instantaneous growth rate} = \frac{\ln TL_2 - \ln TL_1}{t_2 - t_1} \quad [2.9.]$$

Where TL_1 and TL_2 are the respective total lengths of fish at the age t_1 and t_2 .

3. Results

The results showed that the age composition of the mirror carp varied from 2 to 8 (Table 1). According to the percentage occurrence, the age groups 3 and 4 constituted more than a half of all ages (66.3%). Overall, the sex ratio (females to male) was 1:1.2, which is not significantly different from 1:1 ($\chi^2=0.27$ at $p>0.05$). The number of samples, the total length and body weight of the mirror carps of the different age groups are presented in Table 1. The differences in the mean values of total lengths and body weight between the age groups were statistically significant (ANOVA, $p<0.001$).

Table 1. Age groups, total length (cm) and body weight (g) of the mirror carp caught from Keban Dam Lake (N = sample size; min = minimum; max = maximum; SE = standard error)

Age group	N	Total length (cm)			Body weight (g)		
		min-max	mean \pm SE	95% CI	min-max	mean \pm SE	95% CI
2	14	21.50-24.00	23.08 \pm 0.22	22.59-23.56	172.66-221.46	190.48 \pm 3.67	182.55-198.42
3	40	23.35-28.23	26.26 \pm 0.22	25.82-26.69	200.90-351.10	276.25 \pm 5.90	264.33-288.18
4	36	27.74-31.53	29.30 \pm 0.16	28.98-29.62	270.54-483.18	388.28 \pm 8.12	371.80-404.76
5	10	30.53-31.92	31.25 \pm 0.16	30.89-31.61	450.12-544.76	481.33 \pm 10.26	458.13-504.53
6	12	32.02-33.92	32.90 \pm 0.20	32.46-33.33	544.09-601.40	569.32 \pm 4.85	558.65-580.00
7	4	34.23-34.76	34.54 \pm 0.13	34.12-34.95	609.37-691.69	658.03 \pm 18.51	599.12-716.93
8	4	35.32-37.50	36.15 \pm 0.48	34.61-37.69	699.26-789.17	740.13 \pm 18.67	680.71-799.55
Total	120	21.50-37.50	28.48 \pm 0.32	27.85-29.11	172.66-789.17	374.44 \pm 13.11	348.48-400.39

The normal distribution of total lengths was determined by use of Kolmogorov-Smirnov test ($p>0.05$) (Figure 2). The foremost length group was 28-29 cm (12.5%), followed by 27-28 cm (10%). The total length of fish mostly clustered between 25 and 33 cm (72.5%).

It provided a good fit to the examined age-at-length data, as the coefficient of determination was highly significant ($r^2=0.910$) (Figure 3).

The age-at-length data fitted to the Von Bertalanffy Growth Function was determined as:

$$L_t = 43.088 * [1 - e^{-0.176(t+2.423)}]$$

Growth parameters estimated for the mirror carp caught from Keban Dam Lake between November 2016 and December 2016 were: 43.088 cm for L_∞ , 0.176 years⁻¹ for k, -2.423 years for t_0 , 17 years for t_{max} , 2.51 for growth performance index (Φ) and 1.62 for condition factor (C_f).

Total length-weight relationship and the logarithmic total length-weight relationship of the mirror carp caught from the lake are given in Figure 4 and Figure 5, respectively.

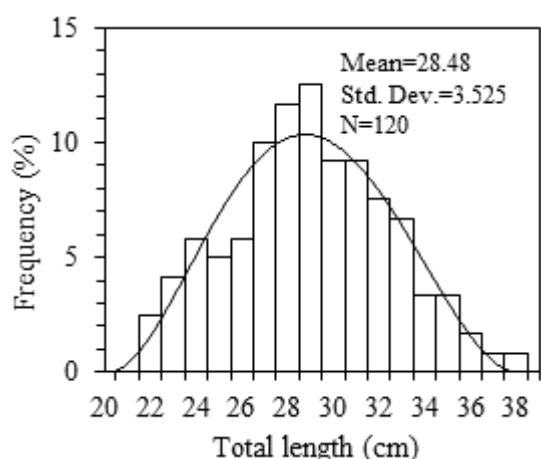


Figure 2. Total length-frequency (%) distribution of the mirror carp caught from Keban Dam Lake

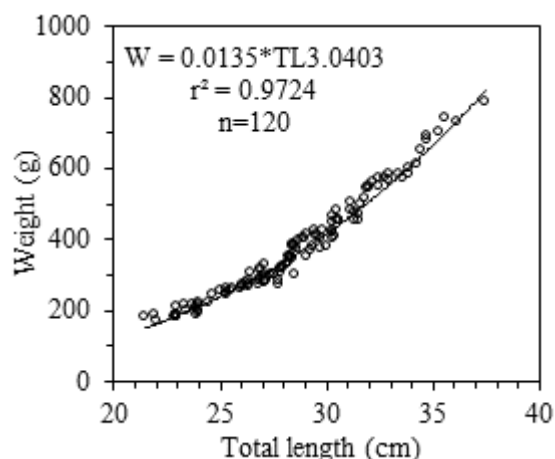


Figure 4. Total length-weight relationship of the mirror carp caught from Keban Dam Lake

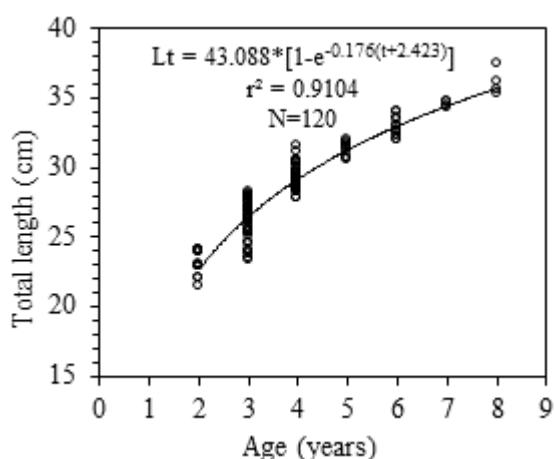


Figure 3. Age-at-total length predicted by Von Bertalanffy growth function of the mirror carp caught from Keban Dam Lake. Circles are experimental values; lines are estimated trend line

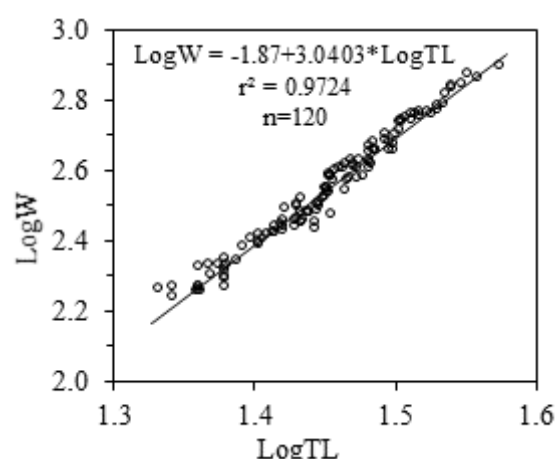


Figure 5. Logarithmic total length-weight relationship of the mirror carp caught from Keban Dam Lake.

Some descriptive statistics and estimated parameters of total length–weight relationships for the mirror carp caught from Keban Dam Lake are given in Table 2.

Table 2. Descriptive statistics and estimated parameters of total length–weight relationships for mirror carp from Keban Dam Lake

N	Total length (cm)		Length-weight relationship parameters					
	min	max	a	95% CL of a	b	SE (b)	95% CL of b	r ²
120	21.50	37.50	0.014	0.011-0.018	3.040	0.047	2.947-3.135	0.972

The absolute, relative and instantaneous growth values of the mirror carp caught from Keban Dam Lake were the highest in age range 2-3, followed by age range 3-4 (Table 3). However, after age 4, the values started to decrease at a significant level.

Table 3. The absolute, relative and instantaneous growth values of the mirror carp caught from Keban Dam Lake.

Age range	Absolut growth (cm)	Relative growth (%)	Instantaneous growth
2-3	3.182	13.789	0.129
3-4	3.046	11.601	0.110
4-5	1.946	6.640	0.064
5-6	1.651	5.284	0.051
6-7	1.634	4.967	0.048
7-8	1.622	4.697	0.046

4. Discussion

In the present study, growth parameters were found to be L_{∞} (cm) = 43.088 cm, $k = 0.176$, $t_0 = -2.423$ and $b = 3.04$. The Brody Growth Coefficient (k) was found in the present study (0.176) is higher than for the carp populations in Gölhisar Lake (0.172) [18], in Hafik Lake (0.140) [19], in Mamasın Lake (0.134) [20], in Tödürge Lake (0.110), [21], in Mogan Lake (0.087) [22]. On the other hand, the L_{∞} value was determined in the present study (43.088) is smaller than for carp populations in the lakes mentioned above. Furthermore, "k" value alone is insufficient to determine the growth performance [15]. Because growth performance was not only related to "k" value, but also to L_{∞} value. Thus, Munro and Pauly, [15] developed an equation that is known as the "Phi Prime Index or growth performance index (Φ)" (equ., 2.5). In the present study, determined Φ value (2.51) was smaller than that of other studies mentioned above.

According to the exponent b value (3.04), the mirror carp (*C. carpio*) population of Keban Dam Lake showed isometric growth ($b \cong 3$). Similar b value has also been found for the common carp (*C. carpio*) population of Gelingüllü Dam Lake (3.023) [5], Kemer Reservoir (3.037) [23] and Sakarya River (2.98) [24]. However, some population of the common carp showed negative allometric growth ($b < 3$) (i.e., Altinkaya Reservoir (2.825) [25], Lake İznik (2.830) [26] and Gölhisar Lake (2.874) [18]). Moreover, positive allometric growth ($b > 3$) was also observed for some populations of common carp (i.e., Almus Dam Lake (3.319) [26], Ömerli Reservoir (3.140) [27]).

The absolute, relative and instantaneous

growth values started to reduce after age range 3-4 (see Table 3). It is well known that the growth is faster in young fish and slow down with reaching the sexual maturity. For mirror carps inhabiting in Keban Dam Lake, sexual maturity age was found as 3 year [6]. This finding supports the our growth values.

In conclusion, the present study is the first study on the some population parameters of mirror carp living in Keban Dam Lake. The findings of this study will be an important reference for the similar studies in the future.

5. References

1. Yıldırım, T., Şen, D., Eroğlu, M., Çoban, M.Z., Demiroğlu, F., Gündüz, F., Arca, S., Demir, T., Gürçay, S., Uslu, A.A. ve Canpolat, İ. (2015). Keban Baraj Gölü balık faunası, Elazığ, Türkiye. *Fırat Üniv. Fen Bil. Der.*, **27**(1), 57-69.
2. AFYD. (2017). Angling for Youth Development. Some coarse species you may encounter; [cited 2017 Oct 18]. Available from <http://www.afyd.co.uk/wp-content/uploads/2013/11/Coarse-Species-for-website.pdf> [cited 2017]
3. Göksu, M.Z.L., Çevik, F., Fındık, Ö. and Sarıhan, E. (2003). Investigation of Fe, Zn and Cd in mirror carp (*Cyprinus carpio* L., 1758) and pike perch (*Stizostedion lucioperca* L., 1758) from Seyhan Dam Lake. *Ege J. Fish. Aqua. Sci.*, **20**, 69-74.
4. Çalta, M. and Ural, M.Ş. (2004). Acute toxicity of the synthetic pyrethroid deltamethrin to young mirror carp, *Cyprinus carpio*. *Fresenius Environ. Bull.* **13**, 1179-1183.
5. Kırankaya, Ş.G., Ekmekçi, F.G. (2004). Gelingüllü Baraj Gölünde yaşayan aynalı sazan (*Cyprinus carpio* L., 1758)'ın büyüme özellikleri. *Tr. J. Vet. Anim. Sci.*, **28**, 1057-1064.
6. Güç, G. (2006). Keban Baraj Gölü (Elazığ)'nde yaşayan aynalı sazan (*Cyprinus carpio* Linnaeus,

- 1758)'in üreme biyolojisi. [Master's Thesis]. Fırat University, Graduate School of Natural and Applied Sciences, 49p.
7. Bozkurt, Y. and Seçer, S. (2006). Evaluation of spermatological parameters of mirror carp (*Cyprinus carpio*) during spawning season. *Ege J. Fish. Aqua. Sci.*, **23**, 195-198.
 8. Temizer, İ.A. ve Şen, D. (2008). Keban Baraj Gölü'nde yaşayan aynalı sazan (*Cyprinus carpio* L., 1758)' da kemiksi yapılardan karşılaştırmalı yaş tayini. *Fırat Üniv. Fen ve Müh. Bil. Der.*, **20**(1), 57-66.
 9. Çolakoğlu, S. ve Akyurt, İ. (2011). Bayramiç Baraj Gölündeki (Çanakkale) aynalı sazan balıklarının (*Cyprinus carpio* L., 1758) populasyon yapısı ve büyüme özellikleri. *İstanbul Univ. J. Fish. Aqua. Sci.*, **26**, 27-46.
 10. DSİ. (2014). Keban Baraj Gölü [cited 2017 Oct 18]. Available from <http://www.dsi.gov.tr/projeler/keban-baraj%C4%B1> [cited 2017 Oct 18]
 11. Tombul, S. ve Karadoğan, S. (1998). Harput'un kuruluş yeri ve şehrin fonksiyonunu yitirmesi üzerinde etkili olan doğal çevre faktörleri, Dünü ve Bugünüyle Harput Sempozyumu, 24-27 Eylül 1998, Elazığ, s. 303-324.
 12. Ricker, W.E. (1973). Linear regressions in fishery research. *J. Fish. Res. Board. Can.* **30**(3), 409-434.
 13. Froese, R. (2006). Cube law, condition factor and weight-length relationships: history, meta-analysis and recommendations. *J. Appl. Ichthyol.*, **22**, 241-253.
 14. Von Bertalanffy, L. (1938). A quantitative theory of organic growth (inquiries on growth laws II). *Human Biol.*, **10**(2), 181-213.
 15. Munro, J.L. and Pauly, D. (1983). A simple method for comparing the growth of fishes and invertebrates. *Fishbyte*, **1**, 5-6.
 16. Taylor, C.C. (1958). Cod growth and temperature. *J. Cons. Int. Explor. Mer.*, **23**, 366-370.
 17. Ricker, W.E. (1979). Growth rates and models. In: Hoar WS, Randall DJ, Brett JR, editors. *Fish Physiology, III, Bioenergetics and Growth*, Academic Press, New York. pp. 677-743.
 18. Alp, A. and Balık, S. (2000). Growth conditions and stock analysis of the carp (*Cyprinus carpio* Linnaeus, 1758) population in Gölhisar Lake. *Turk. J. Zool.*, **24**, 291-304.
 19. Cengizler, İ. and Erdem, Ü. (1989). Hafik Gölündeki sazan (*Cyprinus carpio* L., 1758) populasyonunun bazı yapısal özelliklerinin incelenmesi. *Doğa Tr. Zool. Der.*, **13**, 175-188.
 20. İkiz, R. (1988). Mamasın Baraj Gölü'ndeki sazan (*Cyprinus carpio* L., 1758) populasyonu'nun Gelişmesi ve en küçük av büyüklüğünün saptanması. *Doğa Tu. Zool. Der.*, **12**, 55-67.
 21. Erdem, Ü. (1988). Tötürge Gölü'ndeki sazan (*Cyprinus carpio* L., 1758) populasyonunun bazı biyolojik özelliklerinin incelenmesi. *Doğa Tr. Zool. Der.*, **12**, 32-47.
 22. Düzgüneş, E. (1985). Mogan Gölü'ndeki sazan (*Cyprinus carpio* L., 1758) stoklarının tahmini ve populasyon dinamiği üzerinde bir araştırma. [PhD Thesis]. Ankara University, Graduate School of Natural and Applied Sciences, 91p.
 23. Özcan, G. ve Balık, S. (2007). Kemer Baraj Gölü'ndeki *Cyprinus carpio* L., 1758'nun bazı biyolojik özellikleri. *Türk Sucul Yaşam Dergisi*, **5**, 170-175.
 24. Ölmez, M. (1992). Yukarı Sakarya havzası Sakaryabaşı bölgesi balıklarının populasyon dinamiği üzerinde bir araştırma. [PhD Thesis]. Ankara University, Graduate School of Natural and Applied Sciences, 239p.
 25. Yılmaz, S., Polat, N. ve Yazıcıoğlu, O. (2010). Samsun İli içsularında yaşayan sazan (*Cyprinus carpio* L., 1758)'ın boy-ağırlık ve boy-boy ilişkileri. *Karadeniz Fen Bilimleri Dergisi*, **1**, 39-47.
 26. Karataş, M., Çiçek, E., Başusta, A. and Başusta, N. (2007). Age, growth and mortality of common carp (*Cyprinus carpio* Linnaeus, 1758) population in Almus Dam Lake (Tokat-Turkey). *J. Appl. Biol. Sci.*, **1**, 81-85.
 27. Tarkan, A.S., Gaygusuz, Ö., Acıpınar, H., Gürsoy, Ç. and Özuluğ, M. (2006). Length-weight relationship of fishes from the Marmara region (NW-Turkey). *J. Appl. Ichthyol.*, **22**(4), 271-273.

Occupational Health Risk Analysis and Assessment in Cement Production Processes

Vedat KARAHAN, Cevdet AKOSMAN*

Department of Chemical Engineering Fırat University, 23119, Elazığ, Turkey
*cakosman@firat.edu.tr

(Geliş/Received: 18.01.2018; Kabul/Accepted: 10.07.2018)

Abstract

The purpose of this study is to determine safety risk scores by carrying out risk analysis within plant site according to the occupational health and safety risk management in the cement production processes. To determine occupational and safety risks scores, the plant site studies have been performed by using 5x5 L type risk matrix methodology in the Elazığ-Altınova Cement Plant. The plant site visit covers the sections of raw material processing, storage and transportation, raw material milling, clinker production and cement milling. All possible risks were listed, likelihood and severity of the risks were determined and by using these values and risk scores were calculated. After determining the risks for the workers, the safety risk tables were prepared, and the possible risks were classified as high, moderate and low-risk degrees concerning occupational and safety risk management system. The results of risk assessment revealed that the most dangerous risks were came out in the raw material milling. On the other hand, the highest risk scores were also observed in the raw material milling section. It was found that the crusher, raw material and cement mills and rotary kiln are the most dust, noise, and vibration producing units.

Keywords: Cement Process, Occupational Health and Safety, Risk Definition, Risk Analysis and Assessment, L type risk matrix methodology

Çimento Üretim Proseslerinde İş Sağlığı Risk Analizi ve Değerlendirmesi

Özet

Bu çalışmanın amacı, çimento üretim proseslerinde, iş sağlığı ve güvenliği risk yönetimine göre risk analizi yapılarak güvenlik riski skorlarını belirlemektir. Bu amaçla Elazığ-Altınova Çimento Fabrikasında 5x5 L tipi risk matris metodolojisi kullanılarak saha çalışmaları yapılmıştır. Fabrika ziyareti, hammadde işleme, depolama ve nakliye, hammadde öğütme, klinker üretimi ve çimento öğütme bölümlerini kapsamaktadır. Fabrikada öncelikle olası tüm riskler listelenerek risklerin olasılığı ve şiddeti belirlendi ve bu değerler kullanılarak risk puanları hesaplandı. Risklerin belirlenmesinden sonra güvenlik riski tabloları hazırlanmış ve olası riskler iş ve güvenlik risk yönetimi sistemi açısından yüksek, orta ve düşük risk derecelerine göre sınıflandırılmıştır. Risk değerlendirme sonuçlarına göre en tehlikeli risk bölgesi olarak hammadde öğütme kısmı belirlenmiştir. Öte yandan, en yüksek risk puanı da hammadde öğütme bölümünde elde edilmiştir. Kırıcı, hammadde, çimento öğütme ve döner fırının en toz, gürültü ve titreşim üreten üniteler olduğu görülmüştür.

Anahtar Kelimeler: Çimento Prosesleri, İş Sağlığı ve Güvenliği, Risk Tanımlaması, Risk Analizi ve Değerlendirilmesi, L Tipi Risk Matris Metodolojisi

1. Introduction

The cement sector is one of the important branches of the main industries for the economic development of countries. The supply and treatment of raw materials to produce cement require much energy and labor power. The labors who work for cement plants have exposed some risks such as dust, noise, and vibrations, and they

have to be protected against to this kind of health risks.

Cement is a hydraulic powder material which is created at high temperatures of around 1400 °C. The cement production processes mainly include two steps: (1) the crushing, mixing and roasting of raw materials (silica, calcium carbonate, oxides of alumina and iron), (2) milling of clinker. The

production of cement is undergone a series of processes such as crushing, handling of raw material, grinding clinker, blending, packing and shipping of the final product of cement clinker [1,2]. During all this processes accidents and health problems of the workers cannot be avoided, and workers are exposed to dust, noise and high-temperature effects [3,4].

The workers in a cement factory are exposed to many occupational hazards which contribute to work injuries, dies and allergic problems to cement components [5-9]. Cement can cause ill health in workers through skin and eye contact or inhalation. The risk of injuries and occupational health problems for cement factory workers depends on the duration and level of exposure and individual sensitivity [5]. Noise is also major hazard encounter during the production of cement; especially milling plants used in grind the cement product causes high tension of noise which can simply damage someone hearing levels, maintenance, and cleaning personnel worker are mostly at risk [10,11].

Because of inevitable work-related diseases and accidents, occupational safety regulations are compulsive to prevent such risks through recognition, evaluation, and control of the hazards in an ideal world. Safety management not only saves lives but also is a profit maker for the countries. Therefore, the cement industry is supposed to take correct measurements, evaluation, and control of such risks. Diverse studies for assessing the risks in cement plants have been previously investigated in various studies. Some of these studies concern the reduction of carbon dioxide [12,13], noise pollution risk assessment [11], dust hazard assessment [14], the evaluation of life quality of workers [15,16], occupational health assessment in cement factories [17,18]. Although the main purpose of these studies is to reduce the risks relevant to the workers in cement processes, there is lack of comprehensive determination, analysis, and assessment of occupational health risks for the processes in cement factories. Therefore, preventative and protective measures may need to be implemented to control any risks in the cement factories.

The occupational health and safety cover the determination of risk which is associated with the frequency of failure and consequence effects.

Predicting and evaluation of risk are essential to take appropriate control measures. Evaluation of risk can be performed with qualitative and quantitative methods. Centers and factors of existing danger can be identified by quantitative methods of evaluation and elimination or control of them are provided by taking preventing and control solutions.

This work aims to identify risks and to assess them may occur during cement production. For this reason, a case study is carried out in Elazığ-Altınova Cement Plant.

2. Materials and Methods

In this study, the risk analysis and assessment in cement production have been performed in Elazığ-Altınova according to occupational health and safety management system. The factory under study was first established in Elazığ in 1954, and it started to produce cement by the dry system with a capacity of 85,000 tones/year. In this research, the cement factory has been divided into 5 main sections which are

1. Raw material processing
2. Storage and transportation
3. Raw material milling
4. Clinker production
5. Cement milling

2.1. Description of cement plant under study

Production of cement covers the crushing of raw materials, grinding and mixing of crushed and other raw materials, roasting of the raw material mixture to produce clinker, grinding of clinker along with the additive materials, and packaging.

The first step in cement production processes is the primary crushing of raw materials such as limestone, clay, sand, gypsum, and oxides of alumina and iron. In the crushing section, the crushing of raw materials is made with the help of crusher to reduce size approximately to three inches or smaller [19]. The raw material processing facility includes the crusher, conveyor belts, and the work vehicles. After crushing, the raw materials are transported to storage site by transport vehicles and stored in bunkers and silos.

The raw materials are then first mixed in the appropriate amounts and grounded by using raw material mills in the raw material milling section. The prepared raw material mixture is then fed into the rotary kiln system to produce clinker. The clinker is an intermediate product for manufacturing of cement. The first process is pre-heating in the rotary kiln, and as the temperature increases, physical and chemical changes occur in the pre-calcined materials, and then they melt and merge to form sintered products. Meanwhile, the fuels such as coal and petroleum coke are used to reach temperatures as high as 1450 °C in the rotary kiln [2,20]. The clinker production facility includes the rotating furnace, the preheating cyclones, the clinker cooler, the clinker filters and the work vehicles.

The finishing process for the production of cement is the clinker grinding with gypsum and other constituents. The cement mill is used to crush the clinker into a very fine powder. This fine powder is considered as cement. To control the setting of cement, small amount of gypsum is also added to the cement. Slag and fly ash can also be added to control other properties of the final product. The grinded cement is stored in silos from which it is marketed either in container load or bags. The dry cement production process is very energy intensive.

2.2. Risk analysis and assessment

To determine occupational health risks scores, the plant site studies have been performed by using 5x5 L type risk matrix methodology in the Cement Plant. This method is simple, so it is ideal for analysts who have to do risk analysis alone. However, this method is not sufficient for all processes involving different processes or with very different current schemes, and the success rate of the method changes according to the knowledge of the analyst. This method should be used in such enterprises in order to determine the hazards that require special priority and which require special precautions. A 5x5 L-Type Matrix is especially used in the evaluation of cause-effect relationships. With this method, the result is graded and measured if it is realized with the possibility of realizing an event first.

The plant site visit covers the sections of the raw material process, storage and transportation, raw material milling, clinker production and cement milling. In these sections, all possible risks were listed, likelihood and severity of the risks were determined and by using these values and risk scores were calculated. After determining the risks for the workers, the safety risk tables were prepared, and the possible risks were classified as high, moderate and low-risk degrees concerning occupational and safety risk management system.

Risk analysis examines risks in detail to determine the extent of the risks and the relationships among them. Risk analysis also classifies risks into sets of related risks and ranks them according to importance. Risk analysis evaluates all identified risks to estimate the likelihood of occurrence, consequence of occurrence, and timeframe for necessary mitigation actions. Risk assessment is the qualitative and/or quantitative evaluation of the likelihood and consequence of a risk occurring [21-26].

A Risk Matrix is a graphical representation of the likelihood and consequence scores of a risk (Fig. 1). It is sometimes called a "5x5 Matrix" because it contains five rows and five columns. The rows of a Risk Matrix show likelihood scores, while the columns show the consequence scores.

In the cement factory under study, risk analysis studies have been performed by using 5x5 L type risk assessment decision matrix. Due to its simplicity of this method, the analysts can use this method by themselves. This method is commonly used for the assessment of cause and effect relation. The risk score values of the hazards observed during factory visiting are calculated by the multiplying of likelihood and severity as

$$\text{Risk Score} = \text{Likelihood} \times \text{Severity} \quad (1)$$

The likelihood and severity of risk can be estimated by using Table 1. and Table 2. After estimating of possible risk scores, the assessment of risk is made by taking the Table 3 as a reference. The risk assessment tables are then prepared, and the risks can be classified as high, moderate and low-risk degrees concerning occupational and safety risk management system.

		SEVERITY				
		Critical (5)	Very Serious (4)	Serious (3)	Minor (2)	Negligible (1)
LIKELIHOOD	Frequent (5)	25 Not tolerated	20 High	15 High	10 Moderate	5 Low
	Moderate (4)	20 High	16 High	12 Moderate	8 Moderate	4 Low
	Occasional (3)	15 High	12 Moderate	9 Moderate	6 Low	3 Low
	Remote (2)	10 Moderate	8 Moderate	6 Low	4 Low	2 Low
	Unlikely (1)	5 Low	4 Low	3 Low	2 Low	1 unimportant

Figure 1. 5x5 L type risk decision matrix

Table 1. The probability of a risk

Score	Likelihood	Likelihood of occurrence
1	Unlikely	So unlikely
2	Remote	Unlikely, but possible to occur
3	Occasional	Likely to occur sometime in the life of an item
4	Moderate	Will occur several times in the life of an item
5	Frequent	Likely to occur frequently

Table 2. The severity of a risk for occupational health

Score	Likelihood	Potential Consequence
1	Negligible	Injuries and diseases that do not require medical treatment
2	Minor	Minor injuries that require first-aid only
3	Serious	Severe injuries that require hospitalization or multiple medical treatment
4	Very Serious	Life-threatening injuries or multiple injuries that require hospitalization
5	Critical	Death or multiple injuries that pose threat to life

Table 3. The risk assessment table for occupational health

Risk Score	Risk degree	Actions should be taken to prevent against to risk
25	Not tolerated	The process must not be operated until the risk is reduced to acceptable level. it is necessary to stop single being studied action. The activities must be cancelled if the risk cannot be prevented.
15, 16, 20	Critical	Situation is emergency or required actions must be taken in nearest time. The action can be continue under supervision and control if the risk has not dangerous potential
8, 9, 10, 12	Moderate	The required protective actions must be taken to reduce risk level.
2, 3, 4, 5, 6	Minor (may be tolerated)	Emergency measure is not needed but the ruling measures must continue.
1	Negligible	Taking precaution is not priority

2.3. Definition of risks in the cement plant under study

To achieve comprehensible assessment of risk concerns occupational health, all sources resulting in risks during the cement production process must be defined. Therefore, in all processes in the cement production plant, the possible risks can be encountered as

1. General and routine risk sources for the entire cement production processes
 - Safety
 - Work environment
 - Work and passage areas
 - Work equipment
 - Labelling for safety
 - Protection equipment
 - Manual and automatic load handling
2. Special risks during the cement production processes in plant
 - Raw material processing (crushing)
 - Clinker production (sintering)
 - Grinding and milling processes (raw material, cement, and coal milling)
 - Ladders and scaffolding
 - Forklifts
 - Work vehicles
 - Welding and cutting activities
 - Fuel storage activities
 - Use of hazardous materials
 - Power generating units
3. Environmental risks
 - Dust
 - Noise
 - Heat effects due to high temperatures
 - Fire

3. Results and Discussion

All possible risks in all sections of Cement Plant were listed, likelihood and severity of the risks were identified and by using these values,

the risk scores were calculated. The assessment of possible risks was then done by using the risk assessment tables together with risk decision matrix (Table.1). The total risks of 413 were determined for the Cement Plant, and the classification of these risk scores are given in Table 4. Table 5 reveals that the risk scores were cumulated between “20 and 6” risk scores, and there are no risks both at “25” risk score and under “6” risk score for the entire cement plant. From the Table 5, it was also seen that among these risks, 76 of them were high risks (18.4 %), 333 of them moderate risks (80.6 %), and 4 of them were low risk (1 %). As a result of risk assessment, 128 risk scores of the total risk scores (31.0 %) are determined in the raw material milling section, and these risks are encountered as the most dangerous risks. On the other hand, the highest risk score of “20” (only 1) was also seen in raw material milling section.

Fig. 2 indicates the relative frequency of risk scores in each section of the cement plant. It can be seen from Fig. 2, in the raw material milling section, the highest relative frequency of risk score (the score of “12”) was determined as 0.75, while the lowest relative frequency of risk scores is obtained at “15 and 20 risk” scores. The high and moderate risk sources and their results for all section of Cement Plant are given Table 5 and 6, respectively. From Table 5, It was observed that the workers are exposed to various hazards that result in most serious injuries, death, and breathing problems in the cement factory. The hazards are physical, chemical or accidental due to mechanical and other working conditions.

Table 4. The risk scores estimated at the cement plant

Risk score \ Process	25	20	16	15	12	10	9	8	6	5	4	3	2	1	Total
Raw material processing	-	-	13	1	54	-	33	-	-	-	-	-	-	-	101
Storage and transportation	-	-	13	-	29	-	3	-	-	-	-	-	-	-	42
Raw material milling	-	1	27	-	78	-	18	-	4	-	-	-	-	-	128
Clinker Production	-	-	20	-	63	-	29	-	-	-	-	-	-	-	112
Cement milling and packaging	-	-	2	1	26	-	5	-	1	-	-	-	-	-	35

Among the hazards listed in Table 5, the most observed hazard is the falling of workers from height in the cement factory, this was followed by contact with hot surfaces and materials, exposure to dust, exposure to noise and backfiring of the furnace. The hurling of materials, unauthorized loading, poor ventilation are the other main hazards that cause serious health problems.

The moderate risk score table (Table 6) also reveals that the workers are exposed to similar hazards in high score table that results in most serious injuries, death, breathing problems, gradual hearing impairment, eye problems, and muscular and skeletal disorders in the cement factory. The hazards are physical, chemical or accidental due to mechanical and other working conditions. Among the physical hazards, the most observed hazard is the falling of workers from height in the cement factory, this was followed by contact with hot surfaces and materials, exposure to dust, exposure to noise and backfiring of the furnace. The hurling of

materials, unauthorized loading, poor ventilation are the other main hazards that cause serious health problems.

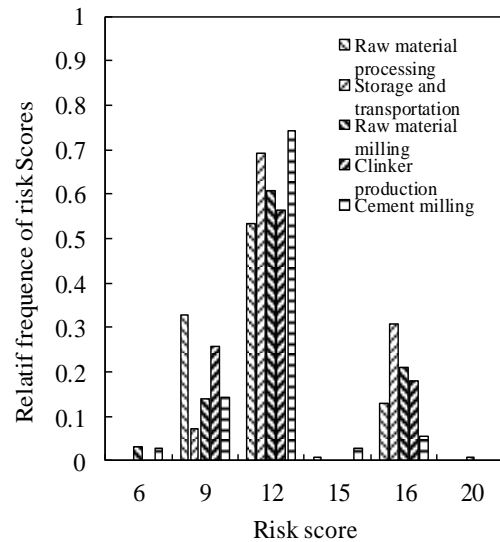


Figure 2. The relative frequency of risk scores

Table 5. Division table for high risk scores

Process	Hazard source/hazard	Risk
Crushing	-Transportation of raw material/ accident on workers, fall from height -The maintenance of the parts of the crusher/accident on workers -Cleaning of hopper and its parts/fall of workers from height, hurling of materials -Evacuation of water from the bottom of crusher/electric shock -Filtering/fall from height	Serious injury/death
Storage and transportation	-Transportation of crushed raw material/accident caused by mobile crane, fall from height -Cleaning of walking passage/ fall from height -Maintenance of the conveyor belts/ fall from height -Cleaning of hopper and its parts/accident on workers, unauthorized loading, working at height -Cleaning of storage area/collapse of roof the storage area, fall from height	Serious injury/death
Raw material milling	-Cleaning and maintenance of mill and its parts/fall of workers from height, work in confined space, unauthorized works, contact with hot surface -Cleaning of hopper and its parts/fall of workers from height, fall of materials, unauthorized loading -Cleaning and maintenance of the conveyor belts/ fall from height, accident -Filtering/fall from height, accident, electric shock, contact with hot surface, poor air conditioning -Cleaning and maintenance of compressor/accident	Serious injury/death/ breathing problems
Clinker production	-Working of rotary kiln/ fall from height, exposure to explosives, exposure to high temperature, contact with hot surface, exposure to hot gases, exposure to dust, backfiring of the furnace -Cleaning and maintenance of elevator/accident -Cleaning and maintenance of rotary kiln and its parts/fall of workers from height, contact to hot surface, face to hot gases, unauthorized works -Cleaning and maintenance of the conveyor belts/ fall from height, accident	Serious injury/death/ breathing problems
Cement milling	-Working of cement mill/face to dust, accident	Serious injury/ breathing problems

Table 6. Division table for moderate risk scores

Process	Hazard source/hazard	Risk
Crushing	<ul style="list-style-type: none"> -Starting up of crusher/accident, exposure to noise, exposure to dust, fall of material pieces -Working with transport vehicles/uncomfortable seats and other devices, long working times, insufficient lighting, poor air conditioning -Transportation of raw material/ accident, fall from height, fall of material pieces, exposure to dust, exposure to noise -The maintenance of the parts of the crusher/accident on workers -Cleaning of hopper and its parts/accident, unplanned loading, fall of workers from height, fall of materials, accident when working with hand tools, exposure to dust, insufficient working area, uncomfortable vehicles, lifting heavy tools with hand, exposure to noise -Cleaning and maintenance of the conveyor belts/ fall from height, accident, exposure to noise, unsuitable air conditioning, slippery ground, exposure to dust -Filtering/accident, fall from height, exposure to dust, accident when working with hand tools, exposure to high pressure 	Serious injury/death/ breathing problems/gradual hearing impairment /eye problems, /muscular and skeletal disorders
Storage and transportation	<ul style="list-style-type: none"> -Working with mobile crane/accidental startup, exposure to vibration, unsuitable working area, accident, poor air conditioning, uncomfortable facilities -Transportation of crushed raw material/accident, exposure to vibration, uncomfortable facilities, exposure to dust -Cleaning of walking passage/accident, unsuitable working area, accident when working hand tools, exposure to dust -Maintenance of the conveyor belts/ accident, absence of protective barrier -Cleaning of hopper and its parts/accident on workers, hurling of material, accident when working with hand tools, exposure to dust, insufficient working area -Cleaning of storage area/exposure to dust, accident on workers, hurling of material, accident when working with hand tools, exposure to dust, insufficient working area 	Serious injury/death/ breathing problems/gradual hearing impairment /eye problems, /muscular and skeletal disorders
Raw material milling	<ul style="list-style-type: none"> -Starting up of mill/accident, exposure to noise, exposure to dust, fall of material pieces -Working with transport vehicles/uncomfortable seats and other devices, long working times, insufficient lighting, poor air conditioning -Cleaning and maintenance of mill and its parts/fall of workers from height, insufficient, working area, unauthorized works, contact with hot surface, slippery ground, accident when working hand tools, exposure to dust, exposure to noise -Cleaning and maintenance of the elevator/accident, unplanned loading, accident when working hand tools, exposure to dust, exposure to noise -Cleaning of hopper and its parts/accident, hurling of materials, accident when working hand tools, exposure to dust, exposure to noise, unsuitable working area -Cleaning and maintenance of the conveyor belts/ fall from height, accident, exposure to noise, unsuitable air conditioning, slippery ground, exposure to dust -Filtering/accident, exposure to dust, contact with hot surface, poor air conditioning, accident when working hand tools, exposure to noise -Cleaning and maintenance of compressor/accident, exposure to noise, poor air conditioning, accident when working hand tools 	Serious injury/death/ breathing problems/gradual hearing impairment /eye problems, /muscular and skeletal disorders
Clinker production	<ul style="list-style-type: none"> -Starting up of rotary kiln/accident, exposure to noise, exposure to dust, fall of material pieces, unsuitable working area, slippery ground -Working with transport vehicles/uncomfortable seats and other devices, long working times, insufficient lighting, poor air conditioning -Cleaning and maintenance of the elevator/accident, unplanned loading, accident when working hand tools, exposure to dust, exposure to noise -Working of rotary kiln/ fall from height, exposure explosives, exposure to high temperature, contact with hot surface, exposure to hot gases, exposure to dust, backfiring of burner, poor ventilation -Cleaning and maintenance of rotary kiln and its parts/fall of workers from height, contact with hot surface, exposure to hot gases, unauthorized works -Filtering/accident, exposure to dust, contact with hot surface, poor air conditioning, accident when working hand tools, exposure to noise -Cleaning and maintenance of the conveyor belts/ fall from height, accident 	Serious injury/death/ breathing problems/gradual hearing impairment /eye problems, /muscular and skeletal disorders
Cement milling	- The similar hazards and cause as in raw material milling	Serious injury/death/ breathing problems/gradual hearing impairment /eye problems, /muscular and skeletal disorders

4. Conclusions

In this study, the occupational health risk analysis and assessment in the Elazığ-Altınova Cement Plant were carried out according to the occupational health and safety risk management in the cement production processes. For this reason, the plant site studies have been performed by using 5x5 L type risk matrix methodology. It was concluded that

- The most dangerous risks were determined in the raw material milling section.
- The highest risk scores were observed in the raw material milling section.
- The crusher, raw material and cement mills and rotary kiln are the most dust, noise, and vibration producing units.
- The workers are exposed to various occupational health hazards that cause various kind of illness in the cement factory workers' health. These are physical, chemical or accidental due to mechanical hazards and other health problems.

The further study can be carried out by using other risk analysis and assessment methods such as X-type matrix, and hazards and operability (HAZOP). These methods can be applied to all of the chemical industries and require team work.

5. References

1. Engin, T. and Ari, V. (2005). Energy auditing and recovery for dry type cement rotary kiln systems e a case study. *Energy Conversion and Management*, **46**, 551-562.
2. Mintus F., Hamel, S. and Krumm, W. (2006). Wet process rotary cement kilns: modelling and simulation. *Clean Technologies and Environmental Policy*, **8**, 112-122.
3. Alvear-Galindo, M. G., Mendez-Ramirez, I., Villegas-Rodriguez, J. A., Chapela-Mendoza, R., Eslava Campos, C. A. and Laurel, A. C. (1999). Risk indicator of dust exposure and health effects in cement plant workers. *Journal of Occupational Environmental Medicine*, **41**, 654-61.
4. Laurell, A. (1999). "Risk indicator of dust exposure and health effects in cement plant workers. *J. Occup. Environ. Med.*, **41**, 654-61.
5. Türkkan, A. (2015). Health effects of cement factories. *Turkish Medical Association Bursa Chamber of Medical Doctors*, Bursa. ISBN: 978-605-5867-90-4.
6. Saucier, K. and Janes, S. (2004). Essential of community based nursing. 1st ed., London: Jonesand Publishers, 271-272.
7. David, K., Kee-Seng C. and Jeyaratnam, J. (2005). Textbook of occupational medicine practice, 2nd ed., Word Scientific Publisher.
8. Herzstein, A., Bunn, B., Fleming, E., Harrengton, M., Jeyoratonam, J. and Abd Gardner, J. (2006). Occupational and environmental medicine, 2nd ed., 183-207, Louse, Mosby.
9. R. Hamdy, "Health Status and Occupation," *J. Occup. Med.*, vol. **45(1)**, pp. 35-9, 2007.
10. El-Sobky, M. K. (2008). Study of accidents among workers Helwan cement factories. MD Thesis, Faculty of Medicine, , Cairo University.
11. Mndeme, F. G. and Mkoma, S. L. 2012. Assessment of work zone noise levels at a cement factory in Tanga. *Ethiopian Journal of Environmental Studies and Management*, **5**, 6-15.
12. Sekhavati1, E., Mohammadzadeh, M., Mohammadfam, I., Zarandi, A. F. (2015). Noise pollution risk assessment in cement factory of Larestan using William Fine Method. *J. Appl. Environ. Biol. Sci.*, **5(8)**, 208-213.
13. Benhelal, E., Zahedi, G., Shamsaei E. and Bahadori, A. (2013). Global strategies and potentials to curb CO₂ emissions in cement industry. *Journal of Cleaner Production*, **51**, 142-161.
14. Ishak, S. and Hashim, H. (2015). Low carbon measures for cement plant. *Journal of Cleaner Production*, **103**, 260-274.
15. Soussia1, T., Guedenon, P., Lawani, R., Gbaguidi, C. D. and Etorh, P. A. (2015). Assessment of cement dust deposit in a cement factory in Cotonou (Benin). *Journal of Environmental Protection*, **6**, 675-682.
16. Huntzinger, D. N. and Eatmon, T. D. (2009). A life-cycle assessment of Portland cement manufacturing: comparing the traditional process with alternative Technologies. *Journal of Cleaner Production*, vol. **17**, 668-675.
17. Demirbağ, B. C., Bayrak, B. Ç., Özkan, G. and Çaylak, E. (2017). Evaluation of the life Quality of workers in a cement factory. *Procedia - Social and Behavioral Sciences*, **237**, 1462-1467.
18. Shafik, S. A. and Abd El-Mohsen, A. S. (2012). Occupational health: Health promotion program to improve health workers in Tourah Cement Factory. *Journal of American Science*, **8**, 486-496.

19. Sana, S., Bhat G. A. and Balkhi, H. M. (2013). Health risks associated with workers in cement factories. *International Journal of Scientific and Research Publications*, **3(5)**, 2250-3153.
20. Mujumdar, K. S. and Ranade, V.V. (2006). Simulation of rotary cement kilns using a one dimensional model. *Chemical Engineering Research and Design*, **84**, 165-177.
21. Wang, S., Lu, J., Li, W., Li, J. and Hu, Z. (2006). Modeling of pulverized coal combustion in cement rotary kiln. *Energy Fuels*, **20**, 2350-2356.
22. Crockford, N. (1986). An Introduction to Risk Management, 2nd ed., Woodhead-Faulkner.
23. Vaughan, E. (1997). Risk Management, John Willey&Sons, , New York.
24. GÜNGÖR, A. (2004). National Health and Safety Management Tool, PhD Thesis, the Institute for Graduate Studies in Science and Engineering, Middle East Technical University, Ankara.
25. Metinsoy, T. (2010). A method of evaluation of relationship between the safety management and overall safety performance in construction industry, PhD Thesis, the Institute for Graduate Studies in Science and Engineering, İstanbul.
26. Ristic, D. (2013). A tool for risk assessment. *Safety Engineering*, **3**, 121-127.

Investigation of Diffusion and Adsorption of Acetone in Building Materials by Dynamic Method

Şakir Yılmaz¹, Cevdet AKOSMAN^{2*}

1. Department of Chemical Engineering Yüzüncüyıl University, 23119, Elazığ, Turkey
2. Department of Chemical Engineering Fırat University, 23119, Elazığ, Turkey

*cakosman@firat.edu.tr

(Geliş/Received: 19.01.2018; Kabul/Accepted: 28.07.2018)

Abstract

In this study, diffusion and adsorption behavior of volatile organic compound of acetone on building materials such as perlite plaster, thermal isolation plate plaster and machine plaster were investigated by using one-sided single pellet moment technique. Experimental studies were conducted in a one-sided single pellet Wicke Kallenbach type diffusion/adsorption cell under isobaric conditions. The amount of acetone in the gas phase was measured by GC technique. The zeroth moment analyses showed that the adsorption of acetone on all gypsum plasters used was found to be reversible. The results indicated that the adsorption degree of acetone on the thermal insulation plaster was the lowest value. The acetone adsorption decreased with increasing temperature while the effective diffusivities of acetone increased with increasing temperature in the gypsum plasters. Moreover, the studies revealed that the adsorption process was physical adsorption process and exothermic.

Keywords: Adsorption, Effective Diffusivity, Acetone, Gypsum Plaster, Dynamic Method

Asetonun Yapı Malzemelerindeki Difüzyon ve Adsorpsiyonunun Dinamik Metotla İncelenmesi

Özet

Bu çalışmada plaster alçı, ısı yalıtım sıvası ve makine sıvası gibi yapı malzemeleri üzerine asetonun difüzyon ve adsorpsiyon davranışı tek taraflı pellet moment tekniği kullanılarak araştırılmıştır. Deneysel çalışmalar, izobarik şartlar altında tek taraflı pelet Wicke Kallenbach tipi difüzyon / adsorpsiyon hücresinde yürütülmüştür. Gaz fazındaki aseton miktarı GC tekniği ile ölçülmüştür. Sıfır moment analizleri, asetonun kullanılan tüm sıva örneklerindeki adsorpsiyonunun tersinir olduğunu ortaya koymuştur. Deneysel sonuçlar, asetonun ısı yalıtım sıvası üzerindeki adsorpsiyon derecesinin en düşük değer olduğunu ortaya koymuştur. Aseton adsorpsiyon katsayısı sıcaklık artışıyla azalırken, asetonun etkin difüzyon katsayısının plaster alçıda sıcaklık artışıyla artmıştır. Deneysel çalışmalar, adsorpsiyon işleminin fiziksel adsorpsiyon ve ekzotermik olduğunu ortaya koymuştur.

Anahtar Kelimeler: Adsorpsiyon, Etkin Difüzyon Katsayısı, Aseton, Plaster Alçı, Dinamik Metot

1. Introduction

Volatile Organic Compounds (VOCs) are one of the main sources of the indoor air contaminants. VOCs including acetone, toluene and methanol in building materials such as adhesives, sealants, paints, solvents, stains, carpets, vinyl flooring, wallboard and engineered woods can act to indoor air quality due to their toxic effect. For this reason, these compounds emitted by building materials are considered as a rising problem for productiveness, comfortable and healthy life [1-4]. Short-term exposure to VOCs which is potentially the most hazardous threat may lead to health problems such

as eye and respiratory irritations, headaches, fatigue, and asthmatic symptoms. Long-term exposure may also lead to cancers [5]. In addition to VOCs that negatively affect indoor air quality, these compounds such as aromatic hydrocarbons and chlorinated hydrocarbons used as dry washing solvents in the chemical industry lead to soil and water pollution [2]. Therefore, the diffusion and adsorption behaviors of VOCs, which recognized as potentially dangerous to humans and living organisms in indoor or outdoor environment, are important to predict the VOC emission.

Gypsum plasters or boards are widely used to cover the interior walls or ceilings of the

residential buildings because of their properties such as aesthetics, easily workable, low density, and insulating behavior. One of the most properties of gypsum plasters is a highly porous material [6]. The diffusion and adsorption of many compounds including moisture and low molecule weight vapors found in indoor environment can cause through this property. The effective diffusivity of the compounds is a key parameter to understand the transport and/or adsorption phenomena in porous media.

In order to calculate the effective diffusivities of diffusing components in porous solids, many experimental methods are available in the literature [6-10]. The single pellet moment technique improved by Dogu and Smith due to put out of action of the interpellet mass transfer and the axial dispersion effects [11,12]. The developed this technique is a very fast and reliable technique for determination of effective diffusivities and adsorption equilibrium constant of tracers in the porous solids.

The objective of this present work is to investigate the diffusion and adsorption behavior of acetone, onto various gypsum plasters (perlite plaster, thermal isolation plate plaster and machine plaster) in the one-sided single pellet at different temperature and isobaric conditions.

2. Materials and Methods

The one-sided single pellet studies were executed by using the pellets prepared from perlite, thermal isolation plate and machine plasters. The gypsum plaster samples were obtained from Arslanlı Corporation which is manufactured in Elazığ-Turkey. The BET surface area and the mean pore diameter of the gypsum plasters used in experimental studies were calculated on a Micromeritics® ASAP 2020.

The true density of the gypsum plaster samples was measured by using helium pycnometer (Quantachrome MVP-1). Some physical properties of the gypsum plasters used in this work are given in Table 1. Acetone (Reidel, 99% purity) are used as VOC in the experiments. The dynamic studies of the adsorption and diffusion of acetone in gypsum plasters were performed in the dynamic diffusion/adsorption apparatus called Wicke-Kallenbach shown in Fig. 1. The pellet holder made of stainless steel with 0.013 m in diameter and 0.003 m in length was used to prepare the gypsum plaster pellets. In order to prepare the gypsum plaster pellets, firstly, the gypsum plasters were mixed with water at weight ratios of 10:2.8 for thermal isolation plate plaster, and 10:6 for perlite and machine plasters. The prepared gypsum plaster pellets were dried to constant weight first at room temperature and in the oven at temperature of 40 °C. Then the plasters were stored in desiccators for further use. The prepared pellets were placed in the diffusion/adsorption cell shown in Fig 1. To prevent gas leakage in the prepared pellets, Teflon O-ring was placed on the upper side of the pellet. Finally, the diffusion/adsorption cell was mounted in GC (SRI 8610) oven with constant temperature controlling unit. TCD was used as detector in GC. The carrier gas passing through the upper face of the pellet was Nitrogen. The experiments performed under isobaric conditions (i.e. 1 atm) were carried out at flow rates ranging from 50-175 ml/min and at different temperatures ranging from 25 to 60 °C. 2 µL pulses of the diffusing and adsorbing tracers were then injected into the carrier gas stream by using a syringe, in order to flow past the upper face of the pellet. The response peaks obtained by GC were analyzed by the moment technique. Then, the experimental data of the moments were computed by the Simpson numerical integration rule.

Table 1. Some physical properties of the gypsum plasters pellets used in this study

Building materials	Solid density, ρ_s , g/cm ³	Apparent density, ρ_p , g/cm ³	Total porosity, $\varepsilon_p = 1 - (\rho_p / \rho_s)$	Mean pore diameter, d , µm	BET surface area, S_g , m ² /g
Perlite plaster	2.34	1.47	0.38	0.014	8.4
Thermal isolation plate plaster	2.65	2.20	0.17	0.021	1.6
Machine plaster	2.36	1.64	0.31	0.021	4.2

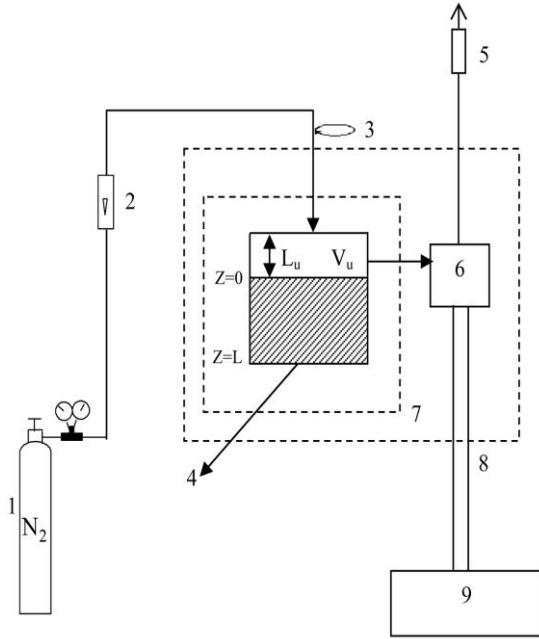


Figure 1. Experimental setup. (1) Carrier gas tube, (2) Rotameter, (3) Sample inlet, (4) Diffusion/adsorption pellet cell, (5) Soap bubble meter, (6) TCD detector, (7) Oven, (8) GC, and (9) Recorder.

2.1. Theory of the one-sided single pellet diffusion/adsorption cell

For adsorption and transport parameters of experimental measurements, theoretical expressions for the distribution of the adsorbing and diffusing tracers in the gypsum plaster pellet and the upper chamber of the diffusion/adsorption cell were used. The species conservation equation for the tracer within the one-sided diffusion/adsorption cell pellet is given by Eq. 1.

$$\varepsilon_p \frac{\partial C_s}{\partial t} = D_e \frac{\partial^2 C_s}{\partial z^2} - N'_s \quad (1)$$

where D_e is the effective diffusivity (m^2/s), ε_p is the pellet porosity, C_s is the tracer concentration in the pores of the pellet ($kmol/m^3$), z is axial coordinate (m), t is time (s) and N'_s is the adsorption rate ($kmol/m^3s$) [12,13].

$$N'_s = \rho_p K_a \frac{\partial C_s}{\partial t} \quad (2)$$

where $\rho_p K_a$ is the overall adsorption constant. Substitution of Eq. 2 into Eq. 1 results in Eq. 3 being obtained as:

$$\varepsilon_p \frac{\partial C_s}{\partial t} = D_e \frac{\partial^2 C_s}{\partial z^2} - \rho_p K_a \frac{\partial C_s}{\partial t} \quad (3)$$

The species conservation equation applied to the upper chamber of the pellet is then given by Eq. 4:

$$-FC_u + D_e \left(\frac{\partial C_s}{\partial z} \right)_{z=0} A = V_u \frac{dC_u}{dt} \quad (4)$$

where F is the carrier gas flow rate (mL/min), C_u is the tracer concentration in the upper chamber ($kmol/m^3$), A is the cross-sectional area of the pellet (m^2) and V_u is the volume of the upper chamber of the diffusion/adsorption cell (m^3).

The initial and boundary conditions of a finite single pellet for Eqs 3 and 4 are explained by Eqs 5 to 8:

$$C_s = 0 \quad (\text{at } t = 0 \text{ for } 0 \leq z \leq L) \quad (5)$$

$$C_s = C_u \quad (\text{at } z = 0 \text{ for all } t) \quad (6)$$

$$\frac{\partial C_s}{\partial z} = 0 \quad (\text{at } z = L \text{ for all } t) \quad (7)$$

$$C_u = C_0 \quad (\text{at } t = 0) \quad (8)$$

The estimation of the adsorption equilibrium constant and effective diffusivity can be performed by solving Eqs 3 and 4. The solutions of these equations have been previously reported in the literature [14,15]. The equations (Eqs 9 to 11) have shown below represent summary of single pellet moment expressions.

$$m_0 = C_0 \tau \quad (9)$$

$$\mu_1 = \frac{m_1}{m_0} = \tau + \frac{AL}{F} (\varepsilon_p + \rho_p K_a) \quad (10)$$

$$\mu_2 = \frac{m_2}{m_0} - \mu_1^2 = \left[\tau + \frac{AL}{F} (\varepsilon_p + \rho_p K_a) \right]^2 + \frac{2}{3} \left(\frac{AL^3}{FD_e} \right) (\varepsilon_p + \rho_p K_a)^2 \quad (11)$$

where m_n is n^{th} moment about the origin, μ_1 is first absolute moment (s), μ_2 is second central moments (s^2), L is pellet length (m) and τ is retention time of tracer at the upper chamber of the diffusion/adsorption cell (s^{-1}).

The top chamber (upper surface of the pellet being covered with an impermeable teflon plate) moment expressions are summarized by Eqs 12 to 14, as follows:

$$m_{0u} = C_0 \tau \quad (12)$$

$$\mu_{1u} = \tau \quad (13)$$

$$\mu_{2u} = \tau^2 \quad (14)$$

where C_0 is initial concentration of tracer in the upper chamber ($kmol/m^3$), μ_{1u} is first absolute moment at the upper chamber of the diffusion/adsorption cell (s) and μ_{2u} is second central moment at the upper chamber of the diffusion/adsorption cell (s^2).

The corrected moment expressions are as shown below:

$$m_{0c} = \frac{m_0}{m_{0u}} = 1 \quad (15)$$

$$\mu_{1c} = \mu_1 - \mu_{1u} = \frac{AL}{F} (\varepsilon_p + \rho_p K_a) \quad (16)$$

$$\frac{\mu_{2c}}{\mu_{1c}^2} = 1 + \frac{2V_u}{AL(\varepsilon_p + \rho_p K_a)} + \left(\frac{2L}{3D_e A} \right) F \quad (17)$$

where μ_{1c} is corrected first absolute moment (s) and μ_{2c} is corrected second central moment (s^2).

The value of the adsorption equilibrium constant, $\rho_p K_a$, can be evaluated from the slope of μ_{1c} vs. $1/F$ data. Also, the calculation of the effective diffusivity, D_e , may be found from slope of the line by plotting (μ_{2c}/μ_{1c}^2) against F .

3. Results and Discussion

The one-sided single pellet moment data were evaluated by using the areas of chromatographic peaks under isobaric conditions, different flow rates and temperatures. Fig. 2 shows a sample of zeroth moment values obtained with

(m_{0u}) and without (m_0) the Teflon plate covering the top surface of the machine plaster pellet at 25 °C. As seen from Fig. 2, both tracers are very close together. Similar results have been obtained in other plaster pellets and other temperature (figure not shown). These results introduce that having reversible adsorption process for the adsorption of acetone onto the gypsum plaster pellets [16,17].

The corrected first absolute moments for acetone onto perlite plaster pellets at temperatures ranging from 25 to 60 °C are given in Fig. 3 as a typical graph. The corrected first absolute moments, μ_{1c} , shown in the graph calculated from the differences μ_1 and μ_{1u} values. According to Fig. 3, the corrected first absolute moment values of perlite plaster pellets for acetone used as a tracer decrease with increasing temperature. The values of the adsorption equilibrium constant, $\rho_p K_a$, of the gypsum plaster pellets used this study found from slope of the line by plotting μ_{1c} against $1/F$. For example, Fig. 4 is represented for all gypsum

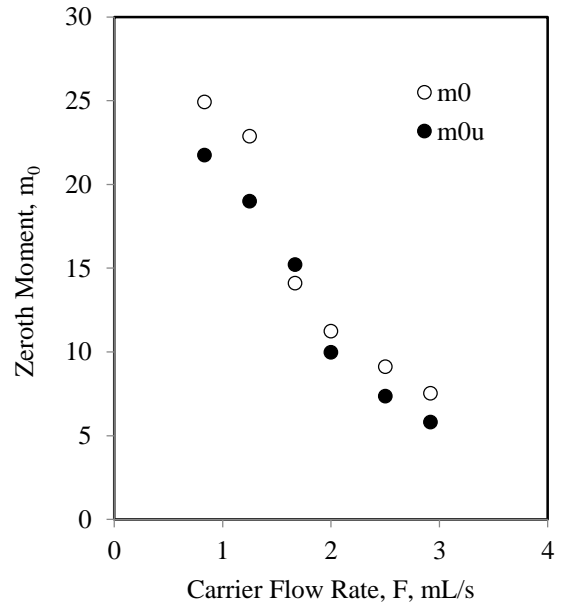


Figure 2. Zeroth moment data for acetone in machine plaster at 25 °C.

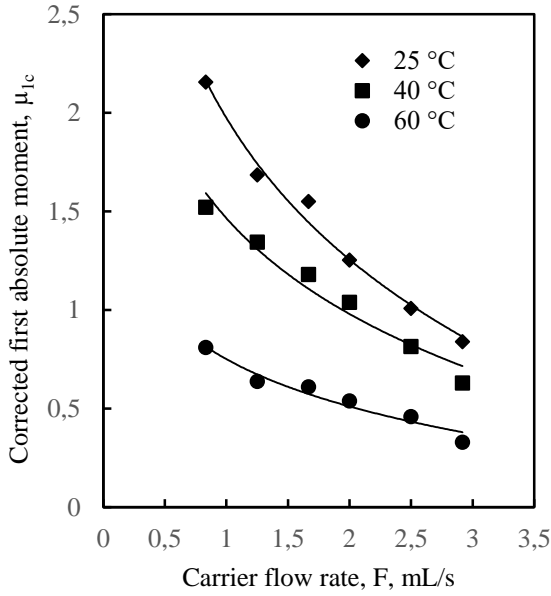


Figure 3. The corrected first absolute moment values of acetone for perlite plaster in the temperature range of 25-60 °C

plaster pellets at 60 °C. The adsorption equilibrium constants of acetone used for the all gypsum plaster pellets was also utilized in the same manner and the results are listed in Table 2. As shown in Table 2, the adsorption equilibrium constant values of acetone in all gypsum pellets are decreased with the increasing temperature. This is a typical characteristic of physical adsorption in the literature [6,10,16]. The values of $\rho_p K_a$ of acetone tracer decreased in the order of thermal isolation plate < perlite < machine plaster. The adsorption of volatile organic compounds in the building material is generally dependent on the type of building material, porosity, specific surface area, and the type of volatile organic compound and vapor pressure.

It can be also said that the adsorption of machine and perlite plaster is higher than thermal isolation plate plaster because the porosity and the surface area of the perlite and machine plaster are higher than thermal isolation plate plaster. Similar results are available in the literature [18-21].

The theoretical temperature dependency of adsorption heat for all the gypsum plaster pellets in which acetone is used can be calculated from the Van't Hoff equation (Eq. 18).

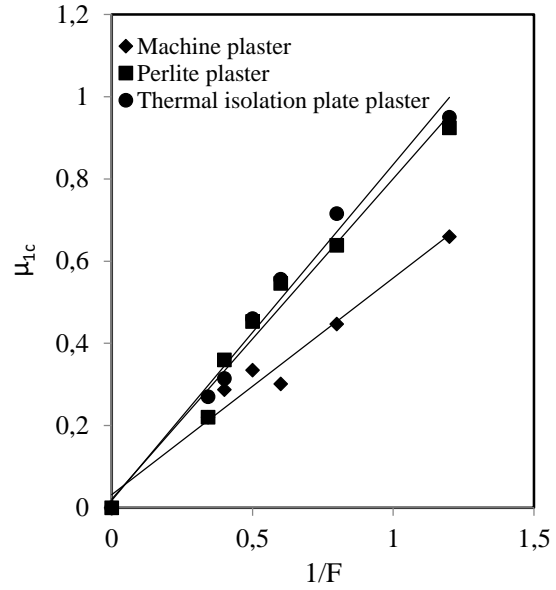


Figure 4. The plot of μ_{1c} against $1/F$ in all gypsum plasters at 60 °C

Table 2. Adsorption equilibrium constants of acetone in the gypsum plaster pellets at different temperatures

Building materials	$\rho_p K_a$		
	25 °C	40 °C	60 °C
Perlite plaster	4.44	3.17	2.36
Machine plaster	4.59	3.25	2.41
Thermal isolation plate plaster	3.87	2.93	2.11

$$\ln(\rho_p K_a) = \Delta S - \frac{\Delta H}{RT} \quad (18)$$

The adsorption heat values (ΔH) and entropy changes (ΔS) of the gypsum plaster pellets can be found from the slope and intercept of the line by plotting $\ln(\rho_p K_a)$ against $1/T$ (Fig. 5). The results calculated by Eq. 18 and obtained from the slope and intercept of the curves shown in Fig. 5 are listed in Table 3a. As can be seen in Table 3, these amounts of acetone onto the gypsum plaster pellets revealed that the adsorption process was physical adsorption process. Moreover, the negative value of ΔH introduced that the adsorption process is exothermic. Furthermore, Gibbs free energy changes (ΔG) of the gypsum plaster pellets can be calculated by Eq. 19.

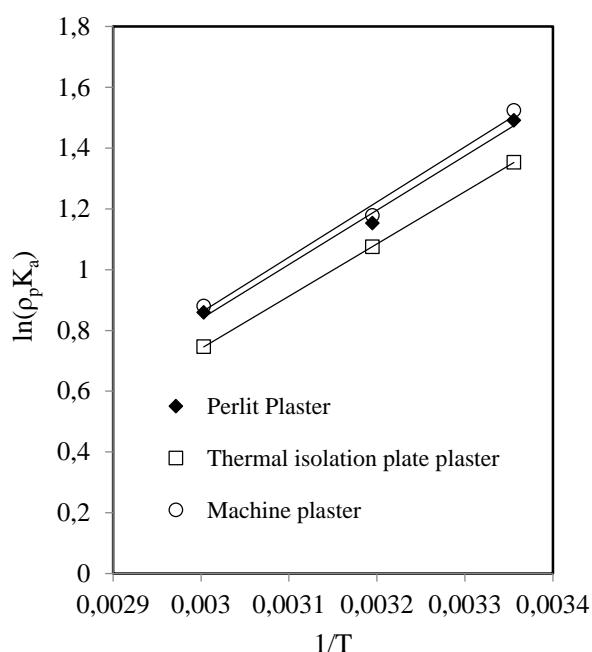


Figure 5. Effect of temperature on adsorption the equilibrium constant of acetone in the gypsum plaster pellets

$$\Delta G = \Delta H - T\Delta S \quad (19)$$

The results calculated by using Eq. 19 for ΔG are given in Table 3b. The negative ΔG value indicated that the adsorption process is spontaneous and feasible. In addition, the negative ΔS value means that the randomness at the solid/solution interface has decreased during adsorption.

The effective diffusivities of acetone in gypsum plaster pellets can be evaluated from the slope of (μ_{2c}/μ_{1c}^2) vs. F data, in Fig. 6 as a sample graph in machine plaster at 60 °C. The obtained effective diffusivity data listed in Table 4. As seen in Table 4, the effective diffusivities of acetone in all gypsum plaster pellets increased with increasing temperature. Also, the effective diffusivities of the thermal isolation plate plaster for acetone were the lowest according to the others. Similar observations were reported in the literature [18-21].

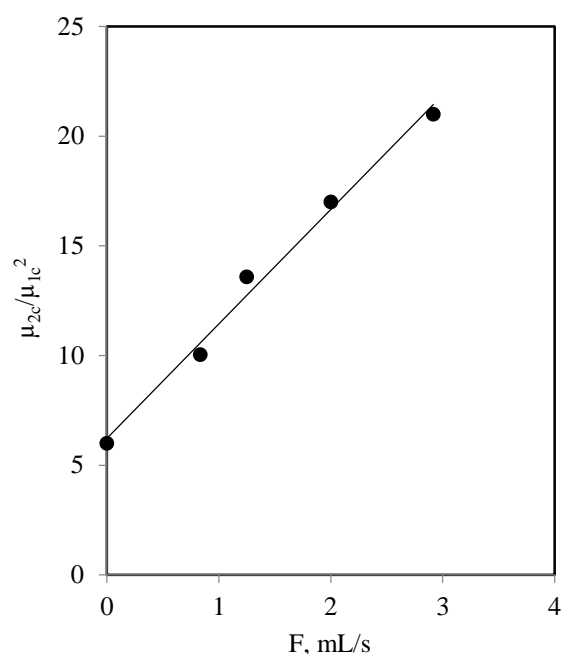


Figure 6. Variation of μ_{2c}/μ_{1c}^2 vs. F in machine pellets at 60 °C for acetone

Table 3. The thermodynamic parameters for acetone in the gypsum plaster pellets a) The values of ΔH and ΔS b) The values of ΔG

Building materials	-ΔH kcal/gmol		-ΔS kcal/gmol	
	25 °C	40 °C	25 °C	40 °C
Perlite plaster	3.544	3.416	8.966	8.778
Thermal isolation plate plaster	3.416	3.605	8.778	9.108
Machine plaster	3.605	3.605	9.108	9.108

Building materials	-ΔG kcal/gmol		
	25 °C	40 °C	60 °C
Perlite plaster	0.872	0.738	0.559
Thermal isolation plate plaster	0.801	0.669	0.494
Machine plaster	0.891	0.755	0.572

Table 4. Effective diffusivities of acetone in the gypsum plaster pellets at different temperatures

Building materials	D _e , cm ² /s		
	25 °C	40 °C	60 °C
Perlite plaster	0.109	0.118	0.183
Thermal isolation plate	0.041	0.067	0.091
Machine plaster	0.056	0.093	0.125

4. Conclusions

In this work, the diffusion and adsorption of acetone in various building materials at different temperatures were investigated by dynamic method. The results indicated that acetone was reversibly adsorbed in gypsum plaster pellets. Physical adsorption was observed when the adsorption heat values were examined. The acetone adsorption decreased with increasing temperature while the effective diffusivities of acetone in the gypsum plasters increased with increasing temperature. Moreover, the reasons such as testing of different volatile organic compounds from acetone, moisture effect on VOC diffusion and adsorption in gypsum plaster samples and binary or multi-component diffusion and adsorption can be recommended for further investigation.

5. References

1. Wang, X., Zhang, Y. and Xiong, J. (2008). Correlation between the solid/air partition coefficient and liquid molar volume for VOCs in building materials. *Atmospheric Environment*, **42**, 7768-7774.
2. T. Urugami, H. Yamada, and T. Miyata. (2001). Removal of dilute volatile organic compounds in water through graft copolymer membranes consisting of poly (alkylmethacrylate) and poly(dimethylsiloxane) by pervaporation and their membrane morphology. *Journal of Membrane Science*, **187**, 255-269.
3. Cox, S.S., Zhao, D. and Little, J.C. (2001). Measuring partition and diffusion coefficients for volatile organic compounds in vinylflooring. *Atmospheric Environment*, **35**, 3823-3830.
4. Huang, H. and Haghghat, F. (2002). Modelling of volatile organic compounds emission from dry building materials. *Building and Environment*, **37**, 1349-1360.
5. Liu, Z., Ye, W. and Little, J.C. (2013). Predicting emissions of volatile and semivolatile organic compounds from building materials: A review. *Building and Environment*, **64**, 7-25.
6. Kalender, M. (2016). Determination of effective diffusivities and convective coefficients of CO₂ in gypsum plasters by dynamic single pellet experiments. *Building and Environment*, **105**, 164-171.
7. Dogan, M. and Dogu, G. (2003). Dynamics of flow and diffusion of adsorbing gases in Al₂O₃ and Pd-Al₂O₃ pellets. *AIChE Journal*, **49**, 3188-3198.
8. Sun, W., Costa, C.A. and Rodrigues, A.E. (1995). Determination of effective diffusivities and convective coefficients of pure gases in single pellets. *Chemical Engineering Journal*, **57**, 285-294.
9. Guangsuo, Y., Jiangua, Y. and Zunhong, Y. (2000). The measurement of effective diffusivity for sulfur-tolerant methanation catalyst. *Chemical Engineering Journal*, **78**, 141-146.
10. Akosman, C. and Zirekgür, N. (2004). Effective diffusivities and convective coefficients for CaO-CaSO₄ and CaO-CaCl₂ pellets. *Chemical Engineering & Technology*, **27**, 50-55.
11. Dogu, G. and Smith, J. (1975). A dynamic method for catalyst diffusivities. *AIChE Journal*, **21**, 58-61.
12. Dogu, G. and Smith, J. (1976). Rate parameters from dynamic experiments with single catalyst pellets. *Chemical Engineering Science*, **31**, 123-135.
13. Doğu, G., Pekediz, A. and Doğu, T. (1989). Dynamic analysis of viscous flow and diffusion in porous solids. *AIChE Journal*, **35**, 1370-1375.
14. Dogu, T., Yasyerli, N., Dogu, G., McCoy, B.J. and Smith, J.M. (1996). One-sided single-pellet technique for adsorption and intraparticle diffusion. *AIChE Journal*, **42**, 516-523.
15. Yasyerli, N., Dogu, G., Dogu, T. and McCoy, B.J. (1999). Pulse-response study for the humidity effect on sorption of ethyl bromide on clays. *AIChE Journal*, **45**, 291-298.
16. Akosman, C. and Kalender, M. (2009). Analysis of diffusion and adsorption of volatile organic compounds in zeolites by a single pellet moment technique. *Clean –Soil, Air, Water*, **37**, 115-121.
17. Doğu, T., Cabbar, C. and Doğu, G. (1993). Single pellet technique for irreversible and reversible adsorption in soil. *Environmental and Energy Engineering*, **39**, 1895-1899.
18. Bodalal, A., Zhang, J.S. and Plett, E.G. (2000). A method for measuring internal diffusion and equilibrium partition coefficients of volatile organic compounds for building materials. *Building and Environment*, **35**, 101-110.
19. Haghghat, F. and Popa, J. (2003). The impact of VOC mixture, film thickness and substrate on adsorption/desorption Characteristics of some building materials. *Building and Environment*, **38**, 959-964.
20. Luo, R. and Niu, J.L. (2006). Determining diffusion and partition coefficients of VOCs in cement using one FLEC. *Building and Environment*, **41**, 1148-1160.

21. Yang, X., Deng, Q. and Zhang, J. (2009). Study on a new correlation between diffusion coefficient and temperature in porous building materials. *Atmospheric Environment*, **43**, 2080-208

***Pseudomonas aeruginosa* Expressing *Vitreoscilla* Hemoglobin Shows Increased Production of L-Lysine α -Oxidase: an Enzyme used in Cancer Therapy**

Hüseyin Kahraman

Inonu University, Faculty of Science and Art, Biology Department, 44280-Malatya/Turkey.
huseyin.kahraman@inonu.edu.tr

(Geliş/Received: 08.03.2018; Kabul/Accepted: 10.09.2018)

Abstract

L-lysine α -oxidase (LO) is one of a few microbial enzymes with therapeutic potential in certain cancers. The enzyme has been determined in several bacteria and fungi. Its production is mainly regulated by carbon sources and oxygen. . Thus, the aim of this study was to determine the nutritional requirements and effect of oxygen concentration on the production of LO in *P. aeruginosa*, and in their recombinants using a highly efficient oxygen uptake system, the *Vitreoscilla* hemoglobin. This study concerns the effect of a higher oxygen uptake provided by a recombinant system, the *Vitreoscilla* hemoglobin, on the production of LO in *Pseudomonas aeruginosa*. The results showed that the recombinant bacterium expressing *Vitreoscilla* hemoglobin gene (*vgb*) had distinct L-lysine activity from the host strain under both carbon catabolite repression and no repression conditions. In a rich medium supplemented with glucose, the recombinant strain showed 20-40 % higher L-lysine activity than the host strain. This difference was even more significant in the medium with no glucose supplement, where the recombinant strain showed almost 2-fold higher enzyme activity throughout the incubation. The results sometime were contradictory in terms of the effect of carbon source (mainly glucose) and oxygen on the production of this enzyme.

Keywords: *Vitreoscilla* hemoglobin, *Pseudomonas aeruginosa*, L-lysine α -oxidase

***Vitreoscilla* Hemoglobini İçeren *Pseudomonas aeruginosa*'da Kanser Tedavisinde Kullanılan Bir Enzim Olan L-Lizin α -Oksidaz Üretimi Arttırılması**

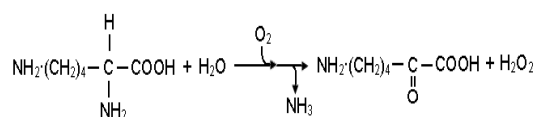
Özet

L-lizin birçok bakteri ve mantarda tespit edilmiştir. Enzimin üretimi esas olarak karbon kaynakları ve oksijen ile düzenlenmektedir. Bu nedenle, bu çalışmanın amacı, *Pseudomonas aeruginosa*'daki LO üretimindeki besin gereksinimlerini ve oksijen konsantrasyonunun etkisini, yüksek verimli bir oksijen alım sistemi olan *Vitreoscilla* hemoglobin kullanan rekombinantlarda α -oksidaz (LO), bazı kanserlerde terapötik potansiyeli olan birkaç mikrobiyolojik enzimden biridir. Enzim belirlemektir. Bu çalışma, bir rekombinant sistem olan *Vitreoscilla* hemoglobini tarafından *P. aeruginosa*'da LO'nin üretimine yüksek oksijen alımının etkisi ile ilgilidir. Sonuçta, *Vitreoscilla* hemoglobin genini (*vgb*) eksprese eden rekombinant bakterinin, hem karbon katabolit baskısı hem de baskı koşulu olmaksızın rekombinat suştan farklı L-lizin aktivitesine sahip olduğunu göstermektedir. Glikozla zenginleştirilmiş zengin bir ortamda, rekombinant suş, yabancıl bakteriden % 20-40 daha fazla L-lizin aktivitesi göstermiştir. Bu fark, rekombinant suşun, üretim boyunca neredeyse 2 kat daha yüksek enzim aktivitesi gösterdiği glikoz takviyesi olmayan ortamda ise daha da anlamlıydı. Sonuç olarak, bu enzimin üretiminde karbon kaynağının (esas olarak glikoz) ve oksijenin etkisi açısından bir çelişkiye görülmektedir.

Anahtar Kelimeler: *Vitreoscilla* hemoglobin, *Pseudomonas aeruginosa*, L-lysine α -oksidaz

1. Introduction

L-Lysine α -oxidase (LO) (1.4.3.14) as one of the potent antitumor enzymes was isolated and purified from *Trichoderma viride* Y-244-2 for the first time in Japan [1]. L-lysine α -oxidase (LO) belongs to the group of oxidases of L-amino acids. The enzyme catalyzes oxidative deamination of L-lysine yielding hydrogen peroxide, ammonia, and the corresponding keto acid, α -keto- ϵ -aminocaproic acid: [2]



LO has a molecular weight of approximately 116,000 and 2 mol of FAD/mol of enzyme; it consists of two subunits of identical molecular weight (about 56,000): 1 mol of FAD is bound/subunit [3-4]. The determination of many biological nitrogen compounds has relied on monitoring the ammonia released from enzymatic reactions [1, 5-6]. This reaction is frequently monitored by means of amperometric detectors. One of the most important applications of this enzyme is its use as the chemotherapeutic agent in certain kinds of cancers where it is used to "starve" cancer cells of an essential amino acid, L-lysine. The chemotoxic effect of the enzymes is a result of such restriction that causes growth inhibition of neoplastic cells. Since the middle of the last century some enzymes have been of special interest for investigators due to the possibility of their application in medicine, particularly in oncology. Essential amino acids, including L-lysine, cannot be synthesized in the body [7-8]. Thus, enzymes capable of cleaving these amino acids are promising for investigation aimed at their application in oncology [3-4, 7]. The study of LO biological property shows that it exhibits a sufficient level of cytotoxicity toward tumor cells. LO shows antileukemic activity and antimetastatic effect *in vivo* at rather low efficient doses [3, 7]. Glucose is an essential nutrient in industrial microbiological systems that produce lysine [9]. The used of organic chemicals such as solvent hexane for the release of periplasmic enzymes. Might be advantageous as they are costs effective, and cause selective permeabilization of the outer cell

wall barriers allowing large-scale preparation of periplasmic enzymes in a relatively pure form. Gram-negative bacteria, *P. aeruginosa*, could regulate the production of LO, an enzyme expressed by an oxygen-regulated gene. Thus, the aim of this study was to determine the nutritional requirements and effect of oxygen concentration on the production of LO in *P. aeruginosa*, and in their recombinant use a highly efficient oxygen uptake system, the *Vitreoscilla* hemoglobin [10]. In this connection, maintaining an adequate supply of oxygen to aerobically growing cell cultures is a central problem in a variety of bioprocesses involving long-scale growth of microorganisms. This may be particularly severe when recombinant cells are involved.

In this paper, different spectrophotometric determination of lysine based on the detection of ammonia is developed.

2. Materials and Methods

2.1. Chemicals

Trichloroacetic acid (TCA), Nessler reagent chemicals (HgI_2 , KI and NaOH), hexane were purchased from Sigma Chemicals Co. All other chemicals used were of analytical grade. Culture medium and stock solution of carbohydrates were autoclaved separately at 120 °C for 25 min.

2.2. Bacterial strains and cultivation

The bacteria used in this study was *P. aeruginosa* (USDA B771) obtained from the USDA culture collection in Peoria, IL. The transposon-mediated *vgb* transferred recombinant strain of *P. aeruginosa*, named PaJC was described previously [11]. The growth media used for LO production were Luria-Bertani (LB) (MILLER 1972), and semi-synthetic (MMY and MM) medium [12] both at pH 7.0. LB contained (L^{-1}) 10 g peptone, 5 g yeast extract and 10 g NaCl. MMY was (L^{-1}) 0.5 g $\text{MgSO}_4 \cdot 7\text{H}_2\text{O}$, 0.01 g $\text{FeSO}_4 \cdot 7\text{H}_2\text{O}$, 0.5 g KCl, 1 g K_2HPO_4 , 0.5 g yeast extract and 1.5 g L-lysine as the nitrogen source. MM was no added yeast extract. Cells were maintained on LB agar plates at 4 °C with transfers at monthly intervals. A 1/100 inoculate of overnight cultures grown in

LB was made in 20 ml LB in 125 ml Erlenmeyer flasks. Inoculate in flasks were grown for 24 h at 37 °C in a 250 rpm water-bath.

2.3. Permeabilization with solvent

Cells cultivated for LO production were harvested by centrifugation (10,000 rpm for 5 min) at 18 °C temperature, washed once with 0.05M potassium phosphate (KPi) buffer (pH 7.6), and resuspended to $A_{600} = 5.0$ in the same buffer containing organic solvent which was the %2 optimal concentration of hexane for LO release. The suspensions were incubated at room temperature for 1 h, briefly vortexing for every 10 min. Tube caps were left open for 5 min in order to evaporate volatile upper phase prior to analysis of LO activity in the cell-free aqueous phase. Cell suspensions were also made in 0.05M KPi with no solvents. In both types of controls, cells were first suspended in KPi for 30 min.

2.4. Enzyme assay

Apart from amperometric methods, optical monitoring of the ammonia released by LO has been proposed. Ammonia participates in further reactions to form spectrophotometric active derivatives. The enzyme activity was measured by the method of Wriston (1970), use the Nesslerization reaction. This method uses the determination of ammonia liberated from LO in the enzyme reaction by the Nessler reaction. Reaction was started by adding 0.5 ml permeabilized cell suspension from aqueous phase into the 1.5 ml 0.01M l-lysine prepared in 0.05M KPi buffer, pH 7.6 and incubated for 1 hour at 37 °C. The reaction was stopped by the addition of 0.15 ml 1.5 M TCA. The reaction mixture was centrifuged at room temperature (10,000 rpm for 5 min) to remove the precipitate and the ammonia released in the supernatant was determined colorimetrically (A_{480}) by adding 0.25 ml Nessler reagent into tubes containing 0.5 ml supernatant and 1.75 ml dH₂O. The content in the tubes was vortexed and incubated at room temperature for 10 min, and the A_{480} values were reads against the blanks that received TCA before the extract addition. One LO unit (U) is defined as the amount of enzyme that liberates 1

μmol of ammonia per min at 37 °C. Specific activity is expressed as units per milligram of protein released. The ammonia concentration produced in the reaction was determined on the basis of a standard curve obtained with ammonium sulfate as the standard. The limit of detection of ammonia by this method was about 10μM [13].

Permeabilization was carried out at roomtemperature on cell suspensions made in 50mM KPi, containing hexane to 2%. Cells were harvested and suspended in respective buffers to equal $A_{600} = 5.0$. Each value is the average of three independent experiments with error bars indicating STDEVs (σ_{n-1}).

2.5. Protein determination

Total protein was determined colorimetrically [14], using bovine serum albumin as the standard.

3. Results

Since LO acts selectively on l-lysine, virtually not affecting the rate of oxidative deamination of other natural amino acids, structural analogs of l-lysine [3].

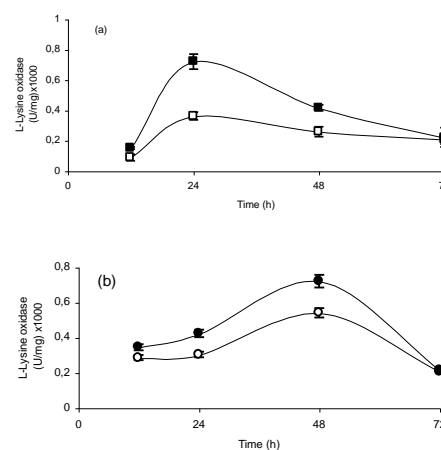


Figure 1. L-lysine α -oxidase activity from *P. aeruginosa* (o) and its *vgb* recombinant (■) grown in LB (a) and LBG (b) medium.

The production of LO, *P. aeruginosa* and *Vitreoscilla* hemoglobin (VHb) expressing recombinant grown under different culture

conditions was investigated. Bacteria were grown in rich or semi-synthetic media with carbon source to determine both the extent of catabolite repression reported for this enzyme. The effect of efficient oxygen uptake system is the VHB, on LO production. Bacteria were grown in different media with or without carbohydrate supplement. Both *P. aeruginosa* and PaJC showed distinct profiles in terms of LO levels. The production of LO by bacteria grown in LB or LB with glucose is summarized in Figure 1. LO production was studied in cells harvested following 72 h cultivation. In *P. aeruginosa*, however, as strain PaJC had a superior LO level to its parental strain. The oxygen uptake rates of PaJC were higher than the non-*vgb*-bearing strains [15]. When compared with their parental strains, much higher oxygen uptake rate of PaJC [11] might contribute to this difference, as LO is an enzyme repressed under high oxygen. *P. aeruginosa* and its recombinants grown in LB medium with 1% glucose showed a different pattern of enzyme activity to that of cells grown in LB with no glucose. In general, the bacteria in MMY and MM medium showed lower enzyme activity than their counterpart in LB medium. *P. aeruginosa* and its *vgb*⁺ strain (PaJC) grown in these medium with 1% glucose had more than 1.5-fold higher LO activity than in LB medium. The effect of glucose on LO activity in *P. aeruginosa* and its recombinant PaJC grown in MMY and MM was opposite to that no glucose MMY and MM medium. At 1% and %0.1 concentrations, however, glucose had opposite results on enzyme production in *P. aeruginosa* and PaJC (Figure 2 and Figure.3).

In general the level of LO in bacteria grown in glucose-supplemented MMY medium was significantly lower than in glucose-supplemented MM medium. The presence of VHB, however, had a differential effect in these two bacteria grown in glucose medium.

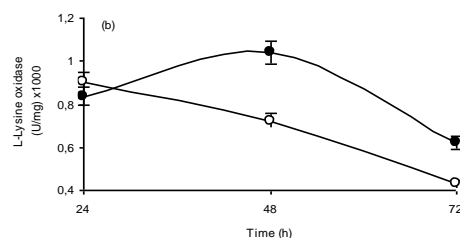
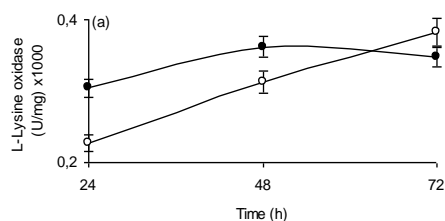
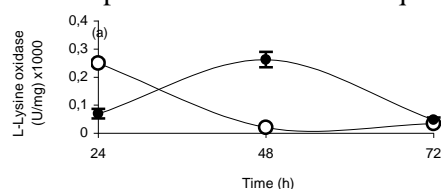


Figure 2. L-lysine α -oxidase release from *P. aeruginosa* (o) and its recombinant (■) KPi/hexane aqueous phase system in MMY a) 1% and b) 0.1% glucose medium.

A comparison of KPi/hexane aqueous phase



system on LO release (determined as specific activity) from *P. aeruginosa* is given in Figure. 2-3. Cells were suspended in 50mM KPi/hexane at pH 7.6 to $A_{600} = 5.0$ for permeabilization extract preparation.

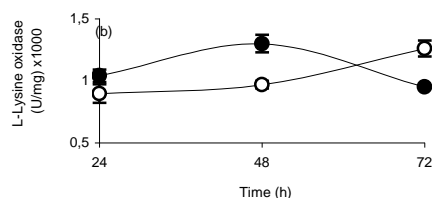


Figure 3. L-lysine α -oxidase release from *P. aeruginosa* (o) and its recombinant (■) KPi/hexane aqueous phase system in MM a) 1% and b) 0.1% glucose medium.

Although similar in medium pH when they were grown in LB and LB with 1% glucose, *P. aeruginosa* and PaJC showed approximate pH values. They were grown in MMY and MMY with 1% glucose, *P. aeruginosa* and PaJC showed distinct pH values. The average medium pH in LB or LB with 1% glucose was 8.60 ± 0.04 for *P. aeruginosa* and its recombinants 8.11 ± 0.04 for PaJC strain. The pH values in semi-synthetic MMY medium supplemented with 0.1% and 1% glucose may also reduce.

4. Discussion

LO is not produced in cultures under anoxia. We showed that the presence of highly efficient oxygen uptake system, Vhb, affects differently the production of LO in three distinctly related medium. The system used here is based on the membrane permeabilization of cells by an aqueous salt/organic solvent phase system; KPi/hexane. The aqueous phase was analyzed for enzyme activity and total protein content after separation of organic phase, which required a simple evaporation of highly water immiscible hexane. The membrane permeabilization system (50mM KPi/ 2 % hexane) used here was highly effective on specific release of LO from bacteria. Furthermore, at concentrations ≥ 0.5 M, KPi heavily interfered with the absorbance (A_{480}) reading as it caused a heavy turbidity by reacting with Nessler reaction reagents. The hydrophobicity characteristics of solvents are commonly indicated as $\log P$, where P is the partition coefficient of the solvent between 1-octanol and water. In general, solvents with low $\log P$ values are regarded as poorer enzyme releasers than solvents with high $\log P$ values ($P > 2.0$). Although hexane with the highest $\log P$ value ($\log P = 3.5$) was the most efficient solvent for LO release. Among the solvents with $\log P$ values > 2.0 , hexane is the smallest molecule which makes it penetrate more efficiently into the outer cell membrane, resulting disorganization of the outer membrane enough to cause the secretion of LO. Due to low affinity for water, hexane can be removed from aqueous phase by a simple evaporation causing almost no contamination or denaturation. Furthermore, contrary to mostly toxic effect of surfactants and other membrane destabilizes on cells, hexane is non-toxic and can be used as suitable medium for microbial processes, such as in whole-cell catalysis. To determine both the expression level and the reaction rate a constant of the enzyme from these sources, the enzyme has to be purified is our next goal.

5. References

1. Saurina, J., Herna'ndez-Cassou, S., Alegret, S., and Fa'bregas, E. (1999). Determination of lysine in pharmaceutical samples containing endogenous ammonium ions by using a lysine oxidase biosensor based on an all-solid-state potentiometric ammonium electrode. *Biosens. Bioelect.*, 14: 67-75.
2. Saurina J., Herna'ndez-Cassou S., Alegret S., and Fa'bregas E. (1999). Amperometric determination of lysine using a lysine oxidase biosensor based on rigid-conducting composites. *Biosens. Bioelect.*, 14: 211-220.
3. Treshalina, H.M., Lukasheva, E.V., Sedakova, L.A., Firsova, G.A., Guerassimova, G.K., Gogichaeva, N.V., and Berezov, T.T. (2000). anticancer enzyme L-lysine α -oxidase. *Appl. Biochem. Biotechnol.*, 88: 267-273.
4. Kusakabe, H., Kodama, K., Kuninaka, A., Yoshino, H., Misono, H., and Soda, K. (1980). A new antitumor enzyme, L-lysine α -oxidase from *Trichoderma viride*, Purification and enzymological properties. *J. Biol. Chem.*, 255: 976-981.
5. Galaris, D., and Evangelou, A. (2002). The role of oxidative stress in mechanisms of metal-induced carcinogenesis. *Crit. Rev. Oncol. Hematol.*, 42: 93-103.
6. Li, W., Nugent, M. A., Zhao, Y., Chau, A. N., Li, S. J., Chou, I., Liu, G., and Kagan, H. M. (2003). Lysyl oxidase oxidizes basic fibroblast growth factor and inactivates its mitogenic potential. *J. Cell. Biochem.*, 88: 152-164.
7. Lukasheva, E.V., and Berezov, T.T. (2002). L-Lysine- α -Oxidase: Physicochemical and biological properties. *Biochem.*, 67: 1152-1158.
8. Murthy, S. N., and Janardanasarma, M. K. (1999). Identification of L-amino acid/ L-lysine α -amino oxidase in mouse brain. *Molec. Cell. Biochem.*, 197: 13-23.
9. Almuaid, A. M., and Townshend, A. (1997). Flow injection amperometric and chemiluminescence individual and simultaneous determination of lysine and glucose with immobilized lysine oxidase and glucose oxidase. *Anal. Chim. Acta*, 338: 149-154.
10. Geckil, H., Gencer, S., and Uckun, M. (2004). *Vitreoscilla* hemoglobin expressing *Enterobacter* differently to carbon catabolite and oxygen repression for production of L-asparaginase, an enzyme used in cancer therapy. *Enzy. Microb. Technol.*, 35: 182-189.
11. Chung, J. W., Webster, D. A., Pagilla, K. R., and Stark, B. C. (2001). Chromosomal integration of the *Vitreoscilla* hemoglobin gene in *Burkholderia* and *Pseudomonas* for the purpose of producing stable engineered strains with enhanced bioremediating ability. *J. Indust. Microbiol. Biotechnol.*, 27: 27-33.
12. Mukherjee, J., Majumdar, S., and Scheper, T. (2000). Studies on nutritional and oxygen requirements for production of L-asparaginase by *Enterobacter aerogenes*. *Appl. Microbiol. Biotech.*, 53: 180-184.

13. Saurina, J., Herna'ndez-Cassou, S., Fa'bregas, E., and Alegret, S. (1998). Potentiometric biosensor for lysine analysis based on a chemically immobilized lysine oxidase membrane. *Analy. Chim. Acta*, 371: 49-56.
14. Lowry, O. H., Rosebrough, N. J., Farr, A. L., and Randall, R. J. (1951). Protein measurement with the folin phenol reagent. *J. Biol. Chem.*, 193: 265-275.
15. Geckil, H., Gencer, S., Kahraman, H., and Erenler, S.O. (2003). Genetic engineering of *Enterobacter aerogenes* with *Vitreoscilla* hemoglobin gene: cell growth, survival and antioxidant enzyme status under oxidative stress. *Res. Microbiol.*, 154: 425-431.

Data Mining Techniques Based Students Achievements Analysis

Dönüş Şengür¹, Songül Karabatak²

¹Milli Eğitim Bakanlığı, Şht.P. Bnb.Zafer KILIÇ Anadolu İmam Hatip Lisesi, Elazığ

²Fırat Üniversitesi, Enformatik Bölümü, Elazığ

*kdksengur@gmail.com

(Geliş/Received: 13.07.2018;Kabul/Accepted: 07.08.2018)

Abstract

In this work, data mining techniques are used to determine the students' achievements in Mathematic class. In other words, we use the data mining techniques to determine if there is any link between the student achievement and various student related data such as student grades, demographic, social information and school related data. Data mining techniques, Decision Tree (DT), Discriminant Analysis (DA), Support Vector Machines (SVM), k-nearest neighbor (K-NN) and ensemble learner are used in prediction purposes. A publicly available dataset is considered in experimental works. Experimental works, on computer environment are carried out to validate the data mining techniques. All data mining methodologies are simulated on MATLAB environment with 5-fold cross-validation technique. The classification performance is measured by accuracy and root mean square error (RMSE) criterions. Three experimental setups and for each setup, three scenarios are considered during experimentation. The obtained results are encouraging and the comparison with some of the existing achievements shows the superiority of our work.

Keywords: Data Mining Techniques, Student's Achievements, Classification, Regression.

Veri Madenciliği Teknikleri ile Öğrencilerin Başarım Analizi

Özet

Bu çalışmada, öğrencilerin matematik dersindeki başarımlarının belirlenmesi için veri madenciliği teknikleri kullanılmıştır. Diğer bir ifade ile öğrenci başarısı ile öğrenci notları, demografik, sosyal bilgiler ve okulla ilgili veriler gibi çeşitli öğrenci verileri arasında herhangi bir bağlantı olup olmadığını belirlemek için veri madenciliği teknikleri kullanılmıştır. Karar Ağaçları (KA), Diskriminant Analiz (DA), Destek Vektör Makineler (DVM), k-en yakın komşular (k-EYK) ve birleştirilmiş öğrenciler yöntemleri tahmin amacıyla kullanılmıştır. Deneysel çalışmalarda halka açık bir veri seti kullanılmıştır. Veri madenciliği tekniklerinin doğruluklarını belirlemek için bilgisayar ortamında çeşitli deneysel çalışmalar gerçekleştirilmiştir. Tüm veri madenciliği yöntemleri MATLAB ortamında 5 kat çapraz doğrulama tekniği ile simüle edilmiştir. Sınıflandırma performansı, doğruluk ve ortalama karesel hatasının karekökü (OKHK) kriterleri ile ölçülmüştür. Üç farklı deneysel çalışma ve her bir deney için ise üç farklı senaryo test edilmiştir. Elde edilen sonuçlar cesaret vericidir ve literatürde mevcut olan bazı sonuçlar ile karşılaştırmalar gerçekleştirilen çalışmanın üstünlükleri gösterilmiştir.

Anahtar Kelimeler: Veri Madenciliği Teknikleri, Öğrenci Başarımı, Sınıflama, Regresyon

1. Introduction

Recently, educational data mining (EDM) has become an emerging topic, which attracts a great amount of the researchers [1-10]. Prediction and/or modelling of various quantities related with education can help to develop better educational environments for students. Especially, student's performance prediction based on various quantities such as student

grades, demographic, social and school related features, has been quite hot in the last decade with numerous publications. For example; Cortez et al. used several data mining techniques to predict the student achievement in secondary education [1]. Authors used four supervised data mining techniques namely, decision trees (DT), random forests (RF), neural networks (NN) and support vector machines (SVM) and demographic, social and school related features

to predict the achievements of the students. Ma et al. used data mining technique to performance evaluation of the students of Singapore [2]. Association rules (AR) method was used to select weak tertiary students for remedial classes. Demographic and school performance quantities were used as input to the AR method. Minaei-Bidgoli et al. modelled the student grades by data mining techniques [3]. The work was applied on 227 students from Michigan State University and three different data mining approaches were considered. Authors indicated that an ensemble classifier yielded the best result. Sengur et al. used various data mining techniques for prediction of the graduate scores of the university students [4]. The first and second years lecture scores were used to predict the graduate points of the students from education faculty. Authors used DT, NN and k-NN classifiers. Kotsiantis et al. used various data mining methods in order to predict the performance of computer science students from a university distance learning program [5]. Demographic and performance attributes were considered as inputs to the classifiers. Authors mentioned that the best accuracy was obtained with Naive Bayes (NB) method. Pardos et al. used regression methods for prediction of the math test scores of students [6]. Authors collected data from an online tutoring system. The authors indicated that the Bayesian Networks produced the best results. Turhan et al. used data mining techniques for modelling of the school administrator's conflict handling styles [7]. Authors proposed neutrosophic weighted SVM technique and showed its efficiency on educational dataset. Kabakchieva et al. used data mining algorithms for prediction of student performance [8]. Author considered four data mining techniques such as rule learner, DT, NN, and a K-NN. Author also mentioned that the best accuracy was obtained with NN classifier. Devasia et al. also used various data mining techniques for student's performance prediction [9]. Authors used a web based system that uses the data mining techniques for feature extraction. 700 students were used in the experiments and 19 attributes were saved. It was mentioned that NB method yielded better results than DT, NN and regression based methods. Vyas et al. used CART method for student's performance

prediction [10]. More specifically, authors used DT approach on student's current performance and some measurable past attributes to detect good and bad performers.

In this paper, various data mining techniques are used for student's performance prediction. The dataset, which was presented in [1], is also used in our work. The dataset attributes, which was collected by using school reports and questionnaires, include student grades, demographic, social and school related features. There are totally 33 attributes where G3 was used as target attribute. Two datasets were provided regarding the performance in two classes: Mathematics and Portuguese language. In [1], the two datasets were modeled under binary/five-level classification and regression tasks that we also follow in our work. Different from in [1], only 10 attributes (famrel, freetime, goout, Dalc, Walc, health, absences, G1, G2 and G3) are considered in our work. In other words, the attributes that have numerical data are considered for modelling. Data mining techniques, DT, discriminant analysis (DA), SVM, K-NN and ensemble learner are used in prediction purposes. Various experimental works, on computer environment are carried out to validate the proposed idea. All data mining methodologies are simulated on MATLAB environment with 5-fold cross-validation technique. The classification performance is measured by accuracy and root mean square error (RMSE) criteria.

The experimental results show that for all of the three modelling tasks (binary/five-level classification and regression), the selected attributes obtain better accuracy and RMSE scores than the result presented in [1] for Mathematics class.

2. Materials and Methods

2.1. Dataset

The dataset, which is used in this work, was produced by Cortez et al [1]. The students who were in two public schools from Portugal during the 2005- 2006 school year were considered for data collection. Questionnaires, paper sheets, three period grades and number of school absences information were used to construct the

attributes of the data set. In addition, demographic, social and school related information were also used in dataset construction. Thus, the dataset contains totally 33 attributes where G3 (final grade) is assigned as target attribute. Two classes namely Mathematics with 395 examples and the Portuguese language with 649 records were collected. In our work, we only use 10 of 33 attributes namely; quality of family relationships (famrel), free-time after school (free-time), going out with friends (gout), workday alcohol consumption (Dalc), weekend alcohol consumption (Walc), current health status (health), number of school absences (absences), first period grade (G1), second period grade (G2) and final grade (G3).

2.2. Data mining techniques

Data mining, which covers a dozens of techniques, aims to extract important knowledge from a given of dataset. This can be done by either supervised or unsupervised way. In supervised classification, a set of labelled dataset is used to figure out some rules that link the input dataset to labels. Thus, the obtained rules can be further used for some unknown dataset to determine their class labels. Data classification and regression can be seen in supervised data mining. DT, discriminant analysis, SVM, k-NN and ensemble learner methods are used in our work. DT is a popular, non-parametric supervised learning method that efficiently classifies datasets [11]. The goal of DT is to create a model that predicts the class label of a test sample by learning simple decision rules inferred from the input data set. Discriminant analysis produces a series of equations based on input feature space that are used to classify a test sample [12]. SVM is another important and efficient supervised classification algorithm [13]. SVM models a decision boundary between classes of training data as a separating hyperplane. In k-NN classification procedure, all training samples are used to classify the test sample according to a pre-defined distance function and the number of nearest neighbor's k [14]. An ensemble learner is known to be constructed from a serious of individual classifiers [15]. In other words, an ensemble

learner determines a test sample class label by combining the decisions of the individual classifiers in some ways.

3. Experimental Works and Results

The aim of this work is to predict the student's performance based on several key factors to determine what affects their educational success/failure. To this end a dataset is used that covers Mathematics class. The data mining techniques are used to model the relationship between factors and final grades. Three different scenarios are considered as it was done in [1]. In the first scenario, the binary classification is considered. In the binary classification, the class labels are pass ($G3 \geq 10$) or fail. In the second scenario, the classification is handled with five levels which start with good to insufficient. In the third one, the regression operation is considered with numeric output that ranges between 0 and 20. In addition, three experimental setups (A, B and C) are considered as suggested in [1]. In A, G3 attribute is used as target and the rest attributes are used as input. In B, G3 is also used as target and except G2, all attributes are used for input. C is similar to B where except G1, all attributes are used as input.

The MATLAB software is used in modelling of the data mining techniques. More specifically, the classification learner application is preferred which enables the user to explore supervised machine learning using various classifiers. In the evaluation of the employed data mining techniques, 5-fold cross validation test is used and the mean accuracy values are recorded. For regression analysis, the regression learner application is used and the RMSE value is calculated for performance evaluation. The DTs, which are used in the prediction, are coarse tree, medium tree and fine tree, respectively. DTs have several positive properties such as easy to interpret, fast for fitting and low memory usage. But they can get low predictive accuracies based on the application. In coarse tree structure, the maximum number of splits is assigned as 4. Similarly, the maximum numbers of splits for medium and fine trees are 20 and 100, respectively. Discriminant analysis is a fast, accurate, easy to interpret and effective classification algorithm where linear and

quadratic discriminants analysis are two main forms of it. While linear discriminant creates linear boundaries between predicted classes, quadratic discriminant constructs non-linear boundaries between predicted classes. SVM algorithm seeks the best hyperplane where the separation of data points of one class from others is guaranteed. The classification learner application presents three different SVM algorithms such as linear, quadratic and cubic, respectively. As k-NN classifiers generally have high predictive accuracy in low dimensions. This can be seen as an advantage of the k-NN classifiers, high memory usage, and not easy to interpret properties make them disadvantageous. Three different k-NN techniques are presented in classification learner application such as fine k-NN, cubic k-NN and weighted k-NN, respectively. In fine k-NN technique, the number of neighbor k is chosen as 1. In addition, for medium and coarse k-NN techniques, the numbers of neighbors are selected as 10 and 100, respectively. In cubic k-NN approach, the cubic distance metrics is used and the numbers of the neighbors are set to 10. In weighted k-NN, the number of neighbor is also set to 10 and a weighted distance function is used for class separation. As ensemble learner covers a dozen of classifiers, they are generally announced as slow approaches. Two different ensemble learner techniques are used in classification learner application such as boosted trees and bagged trees, respectively. In boosted trees technique, the AdaBoost ensemble method is used. In addition, for bagged trees, the random forest approach is adopted.

Table 1 shows the obtained results for binary classification setup. The results for A, B and C scenarios are given in the last three columns of Table 1. For scenario A, the best accuracy score 91.6% is obtained with Quadratic discriminant analysis. The second-best accuracy score 91.4% is produced by linear SVM technique. Linear discriminant analysis produces 90.6% accuracy score that is the best third result for scenario A. DT, DA, SVM and ensemble learners methods obtain better results than k-NN methods. The worst accuracy 81.0% is produced by fine k-NN method and cubic and weighted k-NN methods produce the 83.8% accuracy value.

Boosted and bagged trees methods produce 90.1% and 89.1% scores, respectively.

Table 1. Binary classification results for Mathematics class. The bold case shows the highest accuracy.

Data Mining Technique	Classifier Type	Accuracy (%)		
		A	B	C
DT	Fine Tree	90.1	82.5	88.4
	Medium Tree	89.9	82.0	88.4
	Coarse Tree	90.4	83.0	91.4
Discriminant analysis	Linear Discriminant	90.6	85.3	88.6
	Quadratic Discriminant	91.6	81.0	87.6
SVM	Linear SVM	91.4	86.1	89.6
	Quadratic SVM	86.6	80.8	86.6
	Cubic SVM	86.1	78.2	84.8
k-NN	Fine k-NN	81.0	72.9	78.0
	Cubic k-NN	83.8	79.0	81.5
	Weighted k-NN	83.8	77.0	82.8
Ensemble learners	Boosted Trees	90.1	82.5	87.8
	Bagged Trees	89.1	83.0	90.6

For the scenario B, the best accuracy is obtained by linear SVM method. The accuracy of linear SVM is 86.1%. The second-best accuracy 85.3% for scenario B is produced by linear discriminant analysis. The fine, medium and coarse tree methods produce 82.5%, 82.0% and 83.0% accuracy scores, respectively. The boosted and bagged trees obtain 82.5% and 83.0% scores, respectively. The worst accuracy scores are produced by k-NN methods. While the fine k-NN method produces 72.9% accuracy score, cubic and weighted k-NN methods obtain 79.0% and 77.0% scores. Cubic SVM technique is also produced one the worst result where the accuracy is 78.2%. For scenario C, the best accuracy 91.4% is obtained with coarse tree method. Other DT methods (fine and medium tree) produce 88.4% accuracy scores. The bagged trees method produces the second-best accuracy score where the calculated accuracy is 90.6% and linear SVM technique obtain the third best achievement. With 78.0% accuracy score, the fine k-NN approach yields the worst accuracy score for scenario C.

Table 2. Five-level classification results for Mathematics class. The bold case shows the highest accuracy.

Data Mining Technique	Classifier Type	Accuracy (%)		
		A	B	C
DT	Fine Tree	73.2	53.2	72.4
	Medium Tree	76.5	53.9	74.2
	Coarse Tree	70.4	56.7	71.4
Discriminant analysis	Linear Discriminant	71.4	58.0	71.6
	Quadratic Discriminant	73.4	57.2	71.9
	Linear SVM	74.9	58.2	76.5
SVM	Quadratic SVM	73.4	55.4	71.9
	Cubic SVM	68.6	50.4	65.8
	Fine k-NN	57.2	45.1	50.1
k-NN	Cubic k-NN	55.4	47.8	49.1
	Weighted k-NN	57.5	48.6	53.4
Ensemble learners	Boosted Trees	78.7	61.5	74.7
	Bagged Trees	73.4	53.7	73.4

The prediction achievements for five-level classification setup are given in Table 2. As seen in Table 2, for scenario A, the best achievement is carried out with boosted trees method, where the produced accuracy is 78.7%. With 76.5% accuracy score, the medium tree method obtains the second-best accuracy for scenario A. Quadratic discriminant, quadratic SVM and bagged trees methods produce the 73.4% third-best accuracy score for scenario A. With 55.4% accuracy score, the cubic k-NN obtains the worst achievement. Boosted trees method is also produced the best accuracy score for scenario B. 61.5% accuracy score is recorded by the boosted trees method. Linear SVM method produces the 58.2% accuracy score for scenario B which is the second-best accuracy. In addition, the linear discriminant method produces the 58.0% accuracy score which is the third-best achievement. The worst result 45.1% is produced by fine k-NN method. Linear SVM method obtains 76.5% accuracy score, which is the best achievement for scenario C of five-level classification setup. Boosted trees method produce the 74.7% accuracy value, that is the second-best achievement and medium tree obtains the 74.2% accuracy score which the best-

third achievement. Cubic k-NN produces the worst result where its achievement is 49.1%.

Table 3. Regression results for Mathematics class. The bold case shows the highest accuracy.

Data Mining Technique	Classifier Type	RMSE		
		A	B	C
DT	Fine Tree	1.90	2.49	2.03
	Medium Tree	1.75	2.62	1.86
	Coarse Tree	2.16	2.82	2.11
Linear Regression	Linear	2.10	2.75	1.93
	Robust linear	2.04	2.98	2.04
SVM	Linear SVM	2.00	2.86	2.01
	Quadratic SVM	2.00	2.86	2.01
	Cubic SVM	2.08	3.01	2.03
Ensemble learners	Boosted Trees	1.72	2.42	1.76
	Bagged Trees	1.85	2.62	1.93

The regression results are shown in Table 3 for all A, B and C scenarios. For regression experiments, the DT, linear regression, SVM and ensemble learners techniques are considered and the obtained results were evaluated based on RMSE scores. The lower RMSE score shows the better achievement. As seen in the Table 3, boosted trees method achieves the lowest RMSE scores for all A, B and C scenarios where the RMSE values are 1.72, 2.42 and 1.76, respectively. Medium tree method achieves the second lowest RMSE values where the obtained RMSE values are 1.75, 2.62 and 1.86, respectively and the bagged trees method produces the third lowest RMSE score for A, B and C scenarios, respectively. The bagged trees achievements are 1.85, 2.62 and 1.93, respectively.

We further compare the obtained achievements with the results in [1]. The comparisons are given in Table 4. The first row of Table 4 shows the achievements in [1] and the second row shows our achievements. As seen in Table 4, for only scenario A of the binary classification setup, the Cortez et al.'s achievement is better than ours and in the rest setups and scenarios, our achievements are better than Cortez et al.'s achievements.

Table 4. Comparisons of the results for Mathematics class. The bold case shows the best scores.

Method	Binary classification			Five-level classification			Regression		
	Accuracy (%)			Accuracy (%)			RMSE		
	A	B	C	A	B	C	A	B	C
Cortez et al. [1]	91.9	83.8	70.6	78.5	60.5	33.5	1.75	2.46	3.90
Our Work	91.6	86.1	91.4	78.7	61.5	76.5	1.72	2.42	1.76

4. Conclusions

The main aim of this work is to determine the key variables, which affect the student's educational achievement (success/failure). To this end, the data mining techniques are used. Some of the attributes from the dataset which was produced in [1] is used in our experimental works. The used attributes are famrel, freetime, goout, Dalc, Walc, health, absences, G1, G2 and G3, respectively. As it was stressed in [1], three different experimental setup and for each experimental setup, 3 various scenarios are considered in our works and the obtained results are evaluated accordingly. 13 data mining techniques are run for binary and five-level classification setups and 10 data mining techniques are used for regression setup. DT, DA, SVM and ensemble learner methods generally outperform and k-NN methods generally tend to produce the worst results. We also compare our achievements with the results in [1]. The comparisons show that our achievements are generally better than the achievements in [1].

5. References

1. Cortez, P., and Silva, A. (2008). Using data mining to predict secondary school student performance. In the *Proceedings of 5th Annual Future Business Technology Conference*, Porto, Portugal, 5-12.
2. Ma, Y., Liu, B., Wong, C., Yu, P., and Lee, S. (2000). Targeting the right students using data mining. In *Proc. of 6th ACM SIGKDD International Conference on Knowledge Discovery and Data Mining*. Boston, USA, 457-464.
3. Minaei-Bidgoli, B., Kashy, D., Kortemeyer, G., and Punch, W. (2003). Predicting student Performance: An application of Data Mining Methods with an educational web-based system.

In *Proc. of IEEE Frontiers in Education*. Colorado, USA, 13-18

4. Şengür, D., and Tekin, A. (2013). Öğrencilerin mezuniyet notlarının veri madenciliği metotları ile tahmini. *Bilişim Teknolojileri Dergisi*, **6**(3): 7-16.
5. Kotsiantis S., Pierrakeas, C., and Pintelas P. (2004). Predicting students' performance in distance learning using machine learning techniques. *Applied Artificial Intelligence (AAI)*, **18**(5): 411-426.
6. Pardos Z., Heffernan N., Anderson B., and Heffernan C. (2006). Using fine-grained skill models to fit student performance with bayesian networks. In *Proc. of 8th Int. Conf. on Intelligent Tutoring Systems*. Taiwan.
7. Turhan, M., Şengür, D., Karabatak, S., Guo, Y., and Smarandache, F. (2018). Neutrosophic weighted support vector machines for the determination of school administrators who attended an action learning course based on their conflict-handling styles. *Symmetry*, **10**(5): 176.
8. Kabakchieva, D. (2012). Student performance prediction by using data mining classification algorithms. *IJCSMR*, **1**(4): 686-690.
9. Devasia, T., Vinushree, T. P., and Hegde, V. (2016, March). Prediction of students performance using educational data mining. In *Data Mining and Advanced Computing (SAPIENCE), International Conference on* (pp. 91-95). IEEE.
10. Vyas, M. S., & Gulwani, R. (2017, April). Predicting student's performance using cart approach in data science. In *Electronics, Communication and Aerospace Technology (ICECA), 2017 International conference of* (Vol. 1, pp. 58-61). IEEE.
11. Safavian, S. R., and Landgrebe, D. (1991). A survey of decision tree classifier methodology, *IEEE Transactions on Systems Man and Cybernetics*, **21**: 660-674.
12. Sengur, A. (2008). An expert system based on linear discriminant analysis and adaptive neuro-fuzzy inference system to diagnosis heart valve diseases. *Expert Systems with Applications*, **35**: 214-222.
13. Hastie T., Tibshirani R., and Friedman J. (2001). "The Elements of Statistical Learning: Data Mining, Inference, and Prediction". Springer-Verlag, NY, USA.

14. Fix, E., and Hodges, J. L. (1951). Discriminatory Analysis, Nonparametric Discrimination: Consistency Properties; Technique Report No. 4; U.S. Air Force School of Aviation Medicine, Randolph Field Texas: Universal City, TX, USA, pp. 238–247.
15. Sengur, A. (2012). Support vector machine ensembles for intelligent diagnosis of valvular heart disease. *Journal of Medical Systems*, **36**: 2649-2655.

Prediction Of The Action Identification Levels Of Teachers Based On Organizational Commitment And Job Satisfaction By Using K-Nearest Neighbors Method

Dönüş Şengür^{1,*}, Muhammed Turhan²

¹Ministry of Education, Şht.P. Bnb.Zafer KILIÇ Anadolu İmam Hatip Lisesi, Elazig, Turkey

²Department of Education, University of Firat, 23119 Elazig, Turkey

*kdksengur@gmail.com

(Geliş/Received: 01.08.2018; Kabul/Accepted: 29.08.2018)

Abstract

In this paper, the data mining techniques, which are quite hot in educational environment, are used to predict the action identification levels of the teachers. To this end, the organizational commitment and the job satisfaction levels are used as input to the data mining techniques. The well-known k-nearest neighbors (k-NN) approaches are considered due to their simple and non-parametric nature. Six different k-NN methods namely; fine, medium, coarse, cosine, cubic and weighted k-NN are considered and the obtained results are evaluated based on the prediction accuracy score. A dataset, which covers both organizational commitment and the job satisfaction levels of the teachers, is collected from 126 teachers. Extensive experimental studies are carried out with 5-fold cross validation test in MATLAB environment and the obtained results are recorded accordingly. The obtained results show that the proposed scheme is quite successful in prediction of the action identification levels. Especially, for some of the action identification levels, the obtained accuracy scores are 88.1%, 89.7% and 93.6%, respectively which show the success of the proposed idea.

Keywords: Data mining, k-nearest neighbors, organization commitment, job satisfaction, action identification levels.

Öğretmenlerin Örgütsel Bağlılık Ve İş Doyumuna Dayalı Eylem Kimlikleme Düzeylerinin K-En Yakın Komşular Yöntemi Kullanılarak Tahmin Edilmesi

Özet

Bu çalışmada, eğitim alanında oldukça sık kullanılan veri madenciliği teknikleri, öğretmenlerin eylem kimlikleme düzeylerinin tahmininde kullanılmıştır. Bu amaçla, örgütsel bağlılık ve iş doyumunu düzeyleri veri madenciliği tekniklerine girdi olarak verilmiştir. Basit ve parametrik olmayan yapıları nedeniyle iyi bilinen k-en yakın komşular (k-EYK) yaklaşımlarının kullanılması düşünülmüştür. İsimleri sırasıyla; ince, orta, kaba, kosinüs, kübik ve ağırlıklandırılmış k-EYK olan altı farklı k-EYK yöntemleri kullanılmıştır ve elde edilen sonuçlar tahmin edilen doğruluk değerlerine göre değerlendirilmiştir. Öğretmenlerin hem örgütsel bağlılık hem de iş doyumunu düzeylerini kapsayan bir veri seti, 126 öğretmenden oluşturulmuştur. Kapsamlı deneysel çalışmalar MATLAB programında 5-katlı çapraz geçerlilik testi ile gerçekleştirilmiştir ve elde edilen sonuçlar buna göre kaydedilmiştir. Elde edilen sonuçlar, önerilen yöntemin eylem kimlikleme düzeylerinin belirlenmesinde oldukça başarılı olduğunu göstermektedir. Özellikle bazı eylem kimlikleme düzeylerinde, elde edilen doğruluk değerleri sırasıyla; %88,1, %89,7 ve %93,6'dır ki, bu önerilen fikrin ne kadar başarılı olduğunu bir göstergesidir.

Anahtar Kelimeler: Veri madenciliği, k-en yakın komşular, örgütsel bağlılık, iş doyumunu, eylem kimlikleme düzeyleri.

1. Introduction

Organizational commitment is defined as to desire to remain in the organization declared by the employee [1], loyalty and tight commitment [2], belief in the organization's purpose and

retention level [3]. It is difficult for an administrator to be successful in an organization where the employees' organizational commitment is low. In the definition made by Meyer and Allen [4], organizational commitment was defined as the continuation of the work in a

stable manner, the ownership and integration of the values of the workplace. The organizational commitment, as seen in these definitions, is to show the worker the positive and satisfying attitudes displayed at the workplace and the desire to stay with satisfaction [5].

Job satisfaction is related to general attitudes towards work. Persons with high levels of satisfaction usually exhibit a positive attitude, while insatiable people often show negative attitudes toward life [6]. Job satisfaction is also a part of life satisfaction; it can be said that individuals who are satisfied with their job are happier in their lives [7]. Briefly, the job satisfaction makes the employee feel happy about the work [8].

Researches show that organizational commitment and job satisfaction are related to employees' emotions, attitudes and behaviours in the workplace. According to research findings; job satisfaction is positively associated with performance [9], job involvement [10] and motivation [11] while negative associated with turnover intention [12], stress [13] and burnout [14]. Likewise, organizational commitment is positively associated with positive attitudes and behaviours [15-17] and negatively associated with negative attitudes and behaviours [18-20]. Strong relationships between organizational commitment and job satisfaction and positive and negative job attitudes and behaviours suggest that commitment and satisfaction levels are closely related to the manner in which employees perceive the behaviours they exhibit at work.

The theory of action identification argues that any action can be mentally represented or identified in many different ways [21-23]. The theory provides information on how people conceptualize their actions and how they affect action and the emergence of new behaviours [24]. The aim of the theory is to explain the nature and functioning of the bridge between thought and behaviour. At the hierarchical levels, the upper and lower level identities are different from each other in terms of their scope and structure. High-level identities that abstract long-term strategic plans, while responding to the "why" question; low-level identities that explain direct actions and bodily movements respond to "how" [22, 23].

The way that actions are identified is also very important in terms of teaching profession. It can be said that a teacher who feels happy in his/her work will be more committed to school and will endeavour to do his/her job properly [25]. For this reason, it is very important to determine how teachers identify the actions that they perform. However, it is difficult to directly measure the way of teachers identify their actions. Researchers hypothesize that teachers' levels of action identification can be predicted using variables such as job satisfaction and organizational commitment.

Data mining is a convenient way to extract important knowledge from a given raw data for various purposes [26]. Educational domain is one of the leading areas where lots of studies have been conducted with data mining approaches [27]. Prediction and/or modelling of various quantities related with education can help to develop better educational environments for students, teachers and administrators. Various quantities such as grades, demographic, social and school related features have been used in data mining applications. The studies, which have been carried out so far, are generally related with student's performance prediction [28]. As the related literature is examined, it is seen that the general trend of educational data mining has been on students' performance prediction. Different from the previous studies, in this study, the action identification levels of teachers are predicted based on their organizational commitment and job satisfaction levels. The k-nearest neighbors (k-NN) method which is known to be the easy implemented, effective, and non-parametric classification approach is considered [29]. Six different k-NN approaches are used in the experimental studies on a dataset that was collected from 126 teachers. The dataset contains 14 quantities that are acquired from organizational commitment and job satisfaction questionnaires. There are also 11 action identification items that are used independently. Various experimental studies are conducted to validate the proposed approach and the obtained results show k-NN approach is quite efficient in determining the action identification levels of the teachers based on their organization commitment and job satisfaction levels.

The organization of the paper is as following. Next section briefly introduces the details about data collection and k-NN approach. In Section 3, the experimental setup and the obtained results are given. Finally, we conclude the paper in Section 4.

2. Materials and Methods

This section briefly reviews the dataset collection and the k-NN theory. The reader may refer to [29] for more details about the k-NN approach.

2.1. Dataset collection

In order to determine the relationship between teachers' level of action identification and organizational commitment, a data was collected from 127 teachers working in the province of Elazığ in the academic year 2014-2015 by using the method of disproportionate stratified sampling. 64 (50.4%) of the 127 participants were male and 63 (49.6 %) of the 127 participants were female. 98 (77.2%) of the participants were married, and 29 (22.8%) of them were single; 23 (18.1%) were class and 104 (81.9%) were branch teachers. The ages of participants were ranged from 23 to 62 and the average age was 36.3.

The Action Identification Form developed by Turhan and Sengur [30] and Organizational Commitment Scale developed by Meyer and Allen [31] and adapted to Turkish by Wasti [32] were used to collect the data. The Organizational Commitment Scale was a 5-Likert type and the scale in which validity and reliability studies were performed by Basol and Yalcin [33], was used as a short form with 9 items selected by paying attention to the scope validity. In addition, the internal consistency coefficient of the scale for this study was calculated as 0.784.

2.2. k-Nearest neighbors approach

Data mining, which covers a dozens of classification and regression techniques, aims to extract valuable knowledge from a given raw dataset. This can be done by either supervised or unsupervised. In supervised classification, a set of labelled dataset is used for mining some rules

that connect the input dataset to labels. As it was mentioned earlier, k-NN is one of the simplest, easy-implemented, non-parametric and supervised data classification techniques. k-NN uses a distance function to calculate the similarities between test samples and the training samples. The labels of the test samples are then determined by majority voting procedure. Each test sample label is determined by the labels of its k nearest training samples which have high similarity with that test sample. k-NN approach uses Euclidean, Mahalanobis, Hamming and Minkowski distances for distance function.

3. Experimental Studies and Results

In this study, a dataset, which was collected from 126 teachers, is used to validate the proposed idea. The dataset contains 14 items where 9 of them come from the organizational commitment questionnaires and the rest of the items are from the job satisfaction questionnaires. As it was mentioned earlier, the organizational commitment and job satisfaction of teachers are used to determine their action identification levels. There are also 11 action identification items that are used independently. The action identification levels are given in the appendix.

k-NN method generally has high predictive accuracy in low dimensions. This situation can be seen as an advantage of the k-NN method. High memory usage, and not easy to interpret properties make k-NN method disadvantageous. In this study, six different k-NN methods are used that are in the classification learner application of the MATLAB. These approaches are fine, medium, coarse, cosine, cubic and weighted k-NN, respectively. In fine k-NN approach, the number of neighbor k is chosen as 1.

In addition, for medium and coarse k-NN approaches, the numbers of neighbors are selected as 10 and 100, respectively. In cosine and cubic k-NN approaches, the cosine and cubic distance metrics are used and the numbers of the neighbors are set to 10. In weighted k-NN, the number of neighbors is also set to 10 and a weighted distance function is used for class separation.

The obtained results are evaluated with mean accuracy score where 5-fold cross validation test is applied. Accuracy is defined as the ratio of the correct predictions to the total number of evaluated cases. As there are 11 action identification levels, the experiments are conducted for each action identification level and the results are given in Tables 1 to 11.

Table 1. The prediction results for the first action identification level. The bold case shows the best accuracy.

Method	Classifier Type	Accuracy (%)
k-NN	Fine k-NN	65.9
	Medium k-NN	77.8
	Coarse k-NN	77.0
	Cosine k-NN	73.8
	Cubic k-NN	76.2
	Weighted k-NN	73.8

Table 1 shows the obtained results for the first action identification level. As seen in Table 1, medium k-NN approach produces the best accuracy score where it is 77.8%. The second best accuracy 77.0% is yielded by coarse k-NN technique. Fine k-NN approach produces the worst accuracy where its score is 65.9%.

Table 2. The prediction results for the second action identification level. The bold case shows the best accuracy.

Method	Classifier Type	Accuracy (%)
k-NN	Fine k-NN	80.2
	Medium k-NN	88.9
	Coarse k-NN	88.9
	Cosine k-NN	88.1
	Cubic k-NN	88.9
	Weighted k-NN	88.1

The prediction performances for the second action identification level are given in Table 2. As seen in Table 2, medium, coarse and cubic k-NN approaches obtain the 88.9% accuracy scores which are the highest among all k-NN techniques. 80.2% accuracy score is produced by fine k-NN which is the worst one and cosine and weighted k-NN techniques obtain the 88.1% accuracy scores.

Table 3. The prediction results for the third action identification level. The bold case shows the best accuracy.

Method	Classifier Type	Accuracy (%)
k-NN	Fine k-NN	59.5
	Medium k-NN	73.0
	Coarse k-NN	74.6
	Cosine k-NN	68.8
	Cubic k-NN	72.2
	Weighted k-NN	69.8

Coarse k-NN approach produces the 74.6% accuracy score which the best one for the third action identification level as shown in Table 3. The second best accuracy 72.2% is produced by cubic k-NN method. Fine k-NN produces the 59.5% accuracy score which is again the worst one. Cosine and weighted k-NN techniques produce almost similar accuracy score where the recorded accuracy scores are 68.8% and 69.8%, respectively.

Table 4. The prediction results for the fourth action identification level. The bold case shows the best accuracy.

Method	Classifier Type	Accuracy (%)
k-NN	Fine k-NN	79.4
	Medium k-NN	89.7
	Coarse k-NN	89.7
	Cosine k-NN	89.7
	Cubic k-NN	89.7
	Weighted k-NN	89.7

Except fine k-NN approach, all k-NN methods produce 89.7% accuracy score for the fourth action identification level as tabulated in Table 4. The fine k-NN yields 79.4% accuracy score.

Table 5. The prediction results for the fifth action identification level. The bold case shows the best accuracy.

Method	Classifier Type	Accuracy (%)
k-NN	Fine k-NN	62.7
	Medium k-NN	71.4
	Coarse k-NN	71.4
	Cosine k-NN	73.8
	Cubic k-NN	71.4
	Weighted k-NN	74.6

The prediction scores for the fifth action identification level are given in Table 5. As seen in Table 5, the weighted k-NN method obtains 74.6% accuracy score which is the best and fine k-NN approach produces 62.7% accuracy score which the worst one. Medium, coarse and cubic k-NN methods produce 71.4% accuracy scores and cosine k-NN yields the 73.8% accuracy value.

Table 6. The prediction results for the sixth action identification level. The bold case shows the best accuracy.

Method	Classifier Type	Accuracy (%)
k-NN	Fine k-NN	88.9
	Medium k-NN	93.7
	Coarse k-NN	93.7
	Cosine k-NN	93.7
	Cubic k-NN	93.7
	Weighted k-NN	92.9

Table 6 shows the obtained results for the sixth action identification level. As seen in Table 6, medium, coarse, cosine and cubic k-NN methods obtain the 93.7% accuracy scores. This value is the highest prediction score in all action identification levels. Weighted and fine k-NN methods produce 92.9% and 88.9% scores, respectively.

Table 7. The prediction results for the seventh action identification level. The bold case shows the best accuracy.

Method	Classifier Type	Accuracy (%)
k-NN	Fine k-NN	69.8
	Medium k-NN	79.4
	Coarse k-NN	81.0
	Cosine k-NN	81.0
	Cubic k-NN	79.4
	Weighted k-NN	79.4

The obtained results for the seventh action identification level are given in Table 7. Coarse and cosine k-NN approaches obtain the 81.0% accuracy scores which are the best one for this level. Medium, cubic and weighted k-NN methods produce 79.4% accuracy, respectively. The worst accuracy is also produced by fine k-NN method.

Table 8. The prediction results for the eighth action identification level. The bold case shows the best accuracy.

Method	Classifier Type	Accuracy (%)
k-NN	Fine k-NN	58.7
	Medium k-NN	66.7
	Coarse k-NN	65.9
	Cosine k-NN	62.7
	Cubic k-NN	64.3
	Weighted k-NN	62.7

The prediction results for the eighth action identification level are shown in Table 8. As can be seen, the medium k-NN approach produces 66.7% accuracy score which is the highest one. Coarse k-NN method produces 65.9% score which is the second best one. Cosine and weighted k-NN methods achievements are identical where 62.7% accuracy scores are recorded. The worst accuracy 58.7% is also obtained by fine k-NN.

Table 9. The prediction results for the ninth action identification level. The bold case shows the best accuracy.

Method	Classifier Type	Accuracy (%)
k-NN	Fine k-NN	58.7
	Medium k-NN	66.7
	Coarse k-NN	65.9
	Cosine k-NN	62.7
	Cubic k-NN	64.3
	Weighted k-NN	62.7

Medium k-NN approach produces 66.7% achievement score which is the best accuracy for the ninth action identification level as seen in Table 9. Coarse and cubic k-NN techniques produce the second and third best achievements, respectively. Cosine and weighted k-NN techniques yield the 62.7% accuracy scores. The worst accuracy 58.7% is obtained by fine k-NN method.

Table 10. The prediction results for the tenth action identification level. The bold case shows the best accuracy.

Method	Classifier Type	Accuracy (%)
k-NN	Fine k-NN	58.7
	Medium k-NN	51.6
	Coarse k-NN	31.7
	Cosine k-NN	49.2
	Cubic k-NN	44.4
	Weighted k-NN	55.6

As seen in Table 10, the fine k-NN approach produces the 58.7% best accuracy score for the tenth action identification level. This is quite surprising because for all other action identification levels, the fine k-NN approach produce the worst results. Coarse k-NN method produces the worst accuracy 31.7% for the tenth action identification level.

Table 11. The prediction results for the eleventh action identification level. The bold case shows the best accuracy.

Method	Classifier Type	Accuracy (%)
k-NN	Fine k-NN	73.8
	Medium k-NN	84.1
	Coarse k-NN	84.1
	Cosine k-NN	84.1
	Cubic k-NN	84.1
	Weighted k-NN	83.3

Finally the obtained results for the eleventh action identification level are tabulated in Table 11. Medium, coarse, cosine and cubic k-NN classifiers produce the same best achievements where their scores are 84.1%. Weighted and fine k-NN methods obtain the 83.3% and 73.8% scores, respectively.

4. Conclusions

In this paper, the action identification levels of the teachers are predicted based on their Organizational commitment and job satisfaction levels. The prediction is carried out with the popular k-NN methods. The dataset is collected from 126 teachers where 14 quantities and 11 action identification levels are used in the experimental works. In the experimental works 14 quantities are used as inputs and each action identification level is used as output. Thus, the

experiments are repeated 11 times. From obtained results, it is seen that the best prediction is carried out for sixth action identification level and the worst accuracies are recorded for tenth action identification level. Generally speaking, the fine k-NN approach produces the worst accuracy scores and medium k-NN method generally produces the best accuracy scores. The obtained results also show that the data mining can be used as a convenient tool for action identification level determination.

5. References

1. Manion, J. (2005). *From Management to Leadership: practical strategies for health care leaders*. San Francisco: Jossey-Bass.
2. Daft, R. L., & Marcic, D. (2009). *Understanding management (6th ed.)*. Mason, OH: South-Western College.
3. Mathis, R. L., & Jackson, J. H. (2008). *Human Resource Management (12th edition)*. Mason, OH: Thomson South-Western.
4. Meyer, J. P. ve Allen, N.J (1991). "A Three-Component Conceptualization Of Organizational Commitment", *Human Resource Management Review*, **1 (1)**, S. 61.
5. Swailes, S. (2002). "Organizational Commitment: A Critique Of The Construct And Measures", *International Journal Of Management Reviews*, **4(2)**, S. 159.
6. Kondalkar, V.G. (2007). *Organizational Behavior*, New Age International Publishers, New Delhi.
7. Sinha, J. B. P. (2008). *Culture and organizational behavior*. New Delhi: Sage Publications.
8. Gibson, J. L., Ivancevich J. M. ve Donnelly J. H. (1997). *Organizations: Behavior, Structure, Processes*, Irwin Mcgraw-Hill, New Jersey.
9. Platis, C., Reklitis, P., & Zimeras, S. (2015). Relation between job satisfaction and job performance in healthcare services. *Procedia-Social and Behavioral Sciences*, 175, 480-487.
10. Zincirli, M. (2017). *Üniversitelerdeki Örgüt Yapısının Akademisyen Davranışları Üzerindeki Etkisi*. Fırat Üniversitesi Eğitim Bilimleri Enstitüsü Yayınlanmamış Doktora Tezi. Elazığ.
11. Roos, W., & Van Eeden, R. (2008). The relationship between employee motivation, job satisfaction and corporate culture. *SA Journal of Industrial Psychology*, **34(1)**, 54-63.
12. Shaw, J.D. (1999) Job Satisfaction and Turnover Intentions: The Moderating Role of Positive Affect, *The Journal of Social Psychology*, 139:2, 242-244

13. Chaplain, R.P. (1995) Stress and Job Satisfaction: a study of English primary school teachers, *Educational Psychology*, 15:4, 473-489
14. Tarcan, G.Y., Tarcan, M. & Top, M. (2017). An analysis of relationship between burnout and job satisfaction among emergency health professionals, *Total Quality Management & Business Excellence*, 28:11-12, 1339-1356
15. Meyer, J. P., Paunonen, S. V., Gellatly, I. R., Goffin, R. D., & Jackson, D. N. (1989). Organizational commitment and job performance: It's the nature of the commitment that counts. *Journal of applied Psychology*, 74(1), 152.
16. Saks, A. M. (2006). Antecedents and consequences of employee engagement. *Journal of managerial psychology*, 21(7), 600-619.
17. Spence L., H. K., Finegan, J., & Shamian, J. (2002). The impact of workplace empowerment, organizational trust on staff nurses' work satisfaction and organizational commitment. In *Advances in Health Care Management* (pp. 59-85). Emerald Group Publishing Limited.
18. Blau, G. J., & Boal, K. B. (1987). Conceptualizing how job involvement and organizational commitment affect turnover and absenteeism. *Academy of management review*, 12(2), 288-300.
19. Leiter, M. P., & Maslach, C. (1988). The impact of interpersonal environment on burnout and organizational commitment. *Journal of organizational behavior*, 9(4), 297-308.
20. Leong, C. S., Furnham, A., & Cooper, C. L. (1996). The moderating effect of organizational commitment on the occupational stress outcome relationship. *Human relations*, 49(10), 1345-1363.
21. Vallacher, R. R. and Wegner, D. M. (1987). What do people think they're doing? Action identification and human behavior. *Psychological Review*, 94, 3-15.
22. Vallacher, R. R., ve Wegner, D. M. (1989). Levels of personal agency: Individual variation in action identification. *Journal of Personality and Social Psychology*, 57(4), 660-671.
23. Wegner, D. M., Vallacher, R. R., Macomber, G., Wood, R., ve Arps, K. (1984). The emergence of action. *Journal of Personality and Social Psychology*, 46(2), 269-279.
24. Hunt, G. W., ve Hoyer, W. D. (1993). Action Identification Theory: an Examination of Consumers' Behavioral Representations, in *NA - Advances in Consumer Research Volume 20*, eds. Leigh
25. Turhan, M., ve Şengür, D. (2015). Öğretmenlerin eylem kimlikleme tarzları ile örgütsel vatandaşlık davranışları arasındaki ilişki. 10. Ulusal Eğitim Yönetimi Kongresi'nde sunulmuş bildiri (s. 296-297). Gaziantep: Pegem Akademi.
26. Luan, J. (2002). Data mining applications in higher education, John Wiley and Sons, New York.
27. Şengür, D. (2013). Öğrencilerin Akademik Başarılarının Veri Madenciliği Metotları ile Tahmini, Fırat Üniversitesi, Eğitim Bilimleri Enstitüsü, Bilgisayar ve Öğretim Teknolojileri Eğitimi, Yüksek Lisans Tezi.
28. Cortez, P., and Alice M. G. S (2008). "Using data mining to predict secondary school student performance.", pp. 5-12.
29. Duda RO, Hart PE., (2001), Pattern classification and scene analysis. New York: John Wiley and Sons.
30. Turhan, M., Karabatak, S., & Şengür, D. (2018). Öğretmenlerin Eylem Kimlikleme Biçimleri İle Tükenmişlik Düzeyleri Arasındaki İlişki. *Turkish Studies*, 13(4), 793-808.
31. Meyer, J.P., & Allen, N.J. (1997). Commitment in the workplace. theory, research and application. London: Sage Publications.
32. Wasti, S. A. (2000). Meyer ve Allen üç boyutlu örgütsel bağlılık ölçeğinin geçerlilik ve güvenilirlik analizi. 8. Ulusal Yönetim ve Organizasyon Kongresi Bildirileri, 401-410.
33. Başol, G., & Yalçın, B. (2009). Eğitim örgütlerinde Meyer ve Allen Üç Boyutlu Örgütsel Bağlılık Ölçeğinin geçerlik ve güvenilirlik çalışması, 5th International Balkan Educational and Science Congress Full Text Book, 2, 497-507, Trakya University, Edirne, Turkey.

Appendix

The action identification levels	
1. To read and sign written orders	<input type="checkbox"/> To be informed about developments and decisions about our profession <input type="checkbox"/> Signing the part of me that I left on the signature circle.
2. Performing the guard duty	<input type="checkbox"/> Providing school security and contributing to making the school a healthy environment from every angle <input type="checkbox"/> Waiting on guard
3. The teachers' board, which is held during the year, participates in the meetings of the group teachers' board.	<input type="checkbox"/> To discuss professional issues in the courts and to make decisions. <input type="checkbox"/> Sitting at the meeting place
4. Participation in parents' meetings	<input type="checkbox"/> Cooperating with the parents for the student <input type="checkbox"/> Being in school during the meeting
5. To attend official ceremonies (October 29, November 10, etc.)	<input type="checkbox"/> Work to ensure that students are aware of national days. <input type="checkbox"/> Waiting at the ceremony and performing the procedure.
6. Using tools in the classroom and laboratory courses	<input type="checkbox"/> To support the lesson with materials to make the course more productive. <input type="checkbox"/> To perform the specified events on the annual plan.
7. Teacher's job as branch guide teacher (classroom teacher)	<input type="checkbox"/> Cooperating with other teachers, parents and school guidance teachers for students <input type="checkbox"/> Perform formal actions for the class
8. vocational studies conducted throughout the year (such as preparation of seminar topics given at the end of the year)	<input type="checkbox"/> To contribute to education-teaching activities <input type="checkbox"/> To fulfill administrative obligations on paper
9. Duties given in social activities (Social club and community service studies)	<input type="checkbox"/> To overcome the awareness of taking part in the work that will benefit the student, gathering. <input type="checkbox"/> Prepare the documents required by the school administration for social activities
10. Evaluating the students with point	<input type="checkbox"/> Digitize the situation so that the learner can evaluate himself / herself and the learner <input type="checkbox"/> Scoring as specified in the curriculum
11. Teaching	<input type="checkbox"/> Building the future of students <input type="checkbox"/> telling the students the lessons in the curriculum

Length-Weight Relationship of Common Carp (*Cyprinus carpio* L., 1758) from Taqtaq Region of Little Zab River, Northern Iraq

Rzgar Farooq RASHID, Metin ÇALTA^{1*}, Asiye BAŞUSTA¹

¹ Fırat University, Faculty of Fisheries, 23119 Elazığ, Turkey

*: mcalta@firat.edu.tr

(Geliş/Received: 12.04.2018; Kabul/Accepted: 29.08.2018)

Abstract

In this study, total length-weight relationship (LWR) of common carp (*Cyprinus carpio* L., 1758) from Taqtaq Region of Little Zab River, Northern Iraq were determined. For this purpose, totally 100 carps (56 female and 44 male) were used. Total lengths and weights of them were measured. The total length and weight ranges were 40-52 cm and 1300-2620 g, respectively. The logarithmic and linear equations for total length-weight relationships (LWRs) were found as $\text{Log}W = -1.007+2.574\text{Log}TL$ ($r^2=0.939$) for combined sexes, $\text{Log}W = -0.971+2.553\text{Log}TL$ ($r^2=0.925$) for females and $\text{Log}W = -1.61+2.607\text{Log}TL$ ($r^2=0.958$) for males. The “b” values calculated for combined sexes (2.574), for females (2.553) and for males (2.607) were smaller than 3. According to “b” values, common carp population living in the Taqtaq Region of the Little Zab River of Northern Iraq shows a negative allometric growth.

Keywords: *Cyprinus carpio*, common carp, Little Zab river.

Kuzey Iraktaki Küçük Zap Suyunun Tagtag Bölgesinden Elde Edilen Sazan Balığı (*Cyprinus carpio* L., 1758) Boy-Ağırlık İlişkisi

Özet

Bu çalışmada, Kuzey Iraktaki Küçük Zap Nehrinin Tagtag bölgesinden elde edilen sazan (*Cyprinus carpio* L., 1758)'in toplam boy-ağırlık ilişkisi (LWR) incelendi. Bu amaçla, toplam olarak 100 adet sazan (56 dişi ve 44 erkek) kullanıldı. Balıkların toplam boy ve ağırlıkları ölçüldü. Toplam boyları 40-52 cm, ağırlıkları ise 1300-2620 g arasındadır. Toplam boy-ağırlık ilişkisinin logaritmik doğrusal denklemleri tüm bireyleri için $\text{Log}W = -1.007+2.574\text{Log}TL$ ($r^2=0.939$), dişiler için $\text{Log}W = -0.971+2.553\text{Log}TL$ ($r^2=0.925$) ve erkekler için ise $\text{Log}W = -1.61+2.607\text{Log}TL$ ($r^2=0.958$) olarak bulundu. Tüm bireyler (), dişiler () ve erkekler () için hesaplanan “b” değerleri 3’den daha küçük bulundu. “b” değerlerine göre, Kuzey Iraktaki Küçük Zap Nehrinin Tagtag bölgesinde yaşayan sazan popülasyonunun negatif allometrik bir büyüme gösterdiği görülmektedir.

Anahtar Kelimeler: *Cyprinus carpio*, sazan balığı, Küçük Zap suyu.

1. Introduction

Common carp, *Cyprinus carpio*, is one of the most widely cultured freshwater fish species in the World [1]. It appears in ponds, lakes and slow moving rivers [2]. Although it likes warm water, it also tolerates cold, several pollutants and low dissolved oxygen concentration in water. Common carp has been successfully introduced into most fresh waters throughout the world because of fast growing and adapting to poor environmental conditions [3, 4]. It is an important animal protein source for human around the world due to be available round the year. In Turkey,

common carp is a popular cultured freshwater fish after rainbow trout.

Length-weight relationships (LWRs) allow estimation of fish weight from length or vice versa [5, 6]. LWRs are important for fisheries biology and population dynamics where many stock assessment models require the use of length-weight parameters [7]. LWR equations are also useful to assess the fitness, healthy status and life history parameters like reproduction in fishes [7]. Although LWRs are of fundamental importance in fisheries science, recent data from Northern Iraq freshwater fishes are generally lacking. The present study describes the LWRs of the most abundant fish species, common carp, living in

Taqtaq Region of Little Zab River, Northern Iraq. The data is believed to be the first published reference on LWRs for this river.

2. Materials and Methods

A total of 100 common carp samples were caught from Taqtaq Region of Little Zab River, Northern Iraq (Fig. 1) between March 2017 and April 2017. The sampling was made by gill nets with various mesh sizes. Total length (TL) and weight (W) were measured to the nearest 1cm and 1g respectively. Length-weight relationships (LWRs) were calculated using the linear regression analysis, $\text{Log}W = \text{Log} a + b \text{Log} TL$, where W is body weight (g), TL is the total length (cm), a is

the intercept of the regression curve (coefficient related to body form) and b is the regression coefficient (exponent indicating isometric growth) [8]. The 95% confidence interval (CI) was also determined for parameters “a” and “b” [7].

Student t-test was used to find the significant differences in length and weight between females and males and to demonstrate the significant differences of the obtained “b” values from the expected isometric value (i.e. $b = 3$). Chi-square test was used to find the significant differences of sex ratio from expected rate 1/1. All statistical analyses were performed by using SPSS software version 22.



Figure 1. Map of the Little Zab River, Northern Iraq from where common carps were sampled.

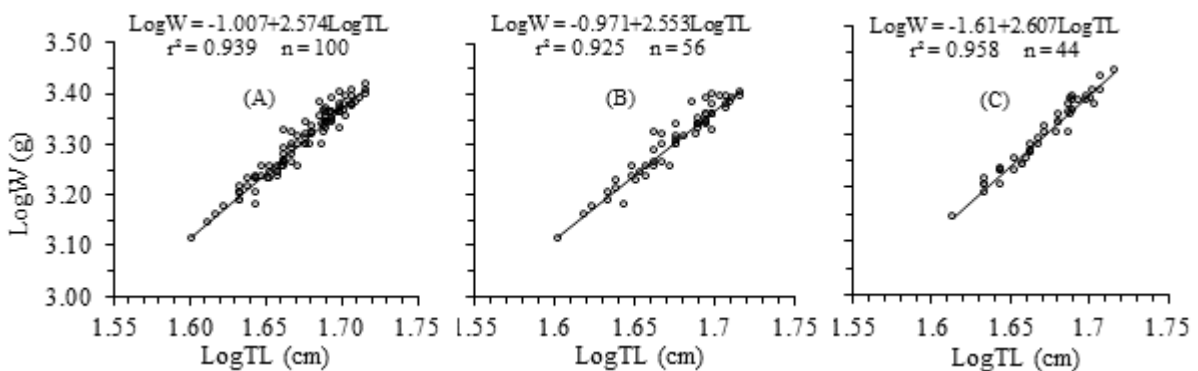
3. Results and Discussion

In the present study, total 100 mirror carps (56 females and 44 males) were examined. Overall sex ratio (female/male) was 1/0.79, which is not significantly different from expected rate 1/1 ($X^2=0.23$ at $P>0.05$). Minimum, maximum, mean, standard deviation and standard error of total length and body weight for combined sex, female and male are presented in Table 1. The differences between females and males in term of total length and body weight were not significant statistically (student t-test, $P>0.05$).

The data were transformed in logarithm and linear relationship obtained with a high degree of determinant coefficient (Fig. 2). The determinant coefficients (r^2) were highly significant for combined sexes (0.939), females (0.925) and males (0.958). The value of regression coefficient ‘b’ from pooled data showed an negative allometric growth of the common carp in the Little Zab River as the values were smaller than 3 (Table 2).

Table 1. Total lengths (TL, cm) and body weights (W, g) of *C. carpio* population from Taqtaq Region of Little Zab River, Northern Iraq.

	Combined Sex		Female		Male	
	TL (cm)	W (g)	TL (cm)	W (g)	TL (cm)	W (g)
Min.	40	1300	40	1300	41	1400
Max.	52	2620	54	2540	52	2620
Mean	47.38	2041.3	47.59	2065.0	47.11	2011.1
SD	2.78	310.2	2.87	318.9	2.66	299.6
SE	0.28	31.02	0.38	42.6	0.40	45.2
N	100	100	56	56	44	44

**Figure 2.** Length-weight relationships (LWRs) in combined sex (A), female (B) and male (C) of *C. carpio* from Taqtaq Region of Little Zab River, Northern Iraq.**Table 2.** Descriptive statistics and estimated parameters of total length–weight relationships for *C. carpio* from Taqtaq Region of Little Zab River, Northern Iraq

N	Total length (cm)		Length-weight relationship parameters					
	Min	Max	<i>a</i>	95% CL of <i>a</i>	<i>b</i>	SE (<i>b</i>)	95% CL of <i>b</i>	<i>r</i> ²
100	40	52	0.098	0.063-0.173	2.574	0.066	2.428-2.691	0.939

The results of the present study indicate that common carp stocks from Taqtaq Region of Little Zab River, Northern Iraq showed negative allometric growth ($b = 2.574$ which is smaller than 3). Similar results have been found for the common carp population of Altinkaya Reservoir (2.825) [9], Lake İznik (2.830) [10], Lake Tödürge (2.306) [11], Gölhisar Lake (2.874) [12] and Bafra Fish Lake (2.822) [13]. However, some population of the common carp showed isometric growth ($b \cong 3$) (i.e. Gelingüllü Dam Lake (3.023) [14], Kemer Dam Lake (3.037) [15], Bayramiç Reservoir (3.010) [16] and Sakarya River (2.98) [17]. Moreover, positive allometric growth ($b > 3$) was also observed for some

populations of common carp (i.e., Almus Dam Lake (3.319) [18], Ömerli Reservoir (3.140) [19]).

These variations could be attributed to differences in age, maturity and sex. Geographic location and associated environmental conditions, such as seasonality, stomach fullness, disease and parasite loads, can also affect the value of b [20].

5. References

1. FIGIS (2011). Fisheries Global Information System (FAO-FIGIS)-FIGIS Institutional Websites. In: FAO Fisheries and Aquaculture

- Department [online]. Rome. (available at: www.fao.org/fishery/figis/en).
2. Vostradovisky, J. (1973). Freshwater fishes. The Hamblyn Publishing Group Limited, London.
 3. Welcomme, R.L. (1988). International introductions of inland aquatic species. *FAO Fish.Tech. Pap.* **285**, 237-278.
 4. Seegers, L., De Vos, L. and Okayo, D.O. (2003). Annotated checklist of the freshwater fishes of Kenya from Lake Victoria. *J.E. Afr. Nat. Hist.* **92**, 11-47.
 5. Xiong, W., Tao, J., Zhang, D.C., Liu, C.L., He, D.K. and Chen, Y.F. (2015). Length-weight relationships for four small fish species caught in wetlands of central Yangtze River, *China. J. Appl. Ichthyol.* **31**, 219-220.
 6. Zhu, T.B., Yang, D.G., Liu, Y. and Li, F. (2015). Length-weight relationships of six fish species from the Zengqu River and the Ouqu River, Southwest China. *J. Appl. Ichthyol.* **31**, 1153-1154.
 7. Froese, R. (2006). Cube law, condition factor and weight-length relationships: history, meta-analysis and recommendations. *J. Appl. Ichthyol.*, **22**, 241-253.
 8. Froese, R. (1998). Length-weight relationships for 18 less-studied fish species. *J. Appl. Ichthyol.* **14**, 117-21.
 9. Bircan, R., Erdem, M. (1994). Altınkaya Baraj Gölü'ndeki sazan balığının (*Cyprinus carpio* L., 1758) gelişmesine ilişkin bir araştırma. XII. Ulusal Biyoloji Kongresi, 6-8 Temmuz, Edirne: 12-20.
 10. Tarkan, A.S., Gaygusuz, Ö., Acıpınar, H., Gürsoy, Ç., Özuluğ, M. (2006). Length-weight relationship of fishes from the Marmara region (NW-Turkey). *J. Appl. Ichthyol.*, **22**(4), 271-273.
 11. Erdem, Ü. (1988). Tötürge Gölü'ndeki sazan (*Cyprinus carpio* L., 1758) populasyonunun bazı biyolojik özelliklerinin incelenmesi. *Doğa Tr. Zool. Der.*, **12**: 32-47.
 12. Alp, A., Balık, S. (2000). Growth conditions and stock analysis of the carp (*Cyprinus carpio* Linnaeus, 1758) population in Gölhisar Lake. *Turk. J. Zool.*, **24**: 291-304.
 13. Yılmaz, S., Yazıcıoğlu, O., Polat, N. (2012). Bafra Balık Gölleri (Samsun, Türkiye)'ndeki sazan (*Cyprinus carpio* L., 1758) 'ın yaş ve büyüme özellikleri. *Karadeniz Fen Bilimleri Dergisi* **2**: 1-12.
 14. Kırankaya, Ş.G., Ekmekçi, F.G. (2004). Gelingüllü Baraj Gölünde yaşayan aynalı sazan (*Cyprinus carpio* L., 1758)'ın büyüme özellikleri. *Tr. J. Vet. Anim. Sci.*, **28**: 1057-1064.
 15. Özcan, G., Balık, S. (2007). Kemer Baraj Gölü'ndeki *Cyprinus carpio* L., 1758'nun bazı biyolojik özellikleri. *Türk Sucul Yaşam Dergisi*, **5**: 170-175.
 16. Çolakoğlu, S., Akyurt, İ. (2011). Bayramiç Baraj Gölündeki (Çanakkale) aynalı sazan balıklarının (*Cyprinus carpio* L., 1758) populasyon yapısı ve büyüme özellikleri. *İstanbul Univ. J. Fish. Aqua. Sci.*, **26**: 27-46.
 17. Ölmez, M. (1992). Yukarı Sakarya havzası Sakaryabaşı bölgesi balıklarının populasyon dinamiği üzerinde bir araştırma. [PhD Thesis]. Ankara University, Graduate School of Natural and Applied Sciences, 239p.
 18. Karataş, M., Çiçek, E., Başusta, A., Başusta, N. (2007). Age, growth and mortality of common carp (*Cyprinus carpio* Linnaeus, 1758) population in Almus Dam Lake (Tokat-Turkey). *J. Appl. Biol. Sci.*, **1**: 81-85.
 19. Vilizzi, L., Tarkan, A.S., Ekmekçi, F.G. (2013). Stock characteristics and management of insights for common carp (*Cyprinus carpio*) in Anatolia: a review of weight-length relationships and condition factors. *Turkish Journal of Fisheries and Aquatic Sciences* **13**:759-775.
 20. Bagenal, T.B., Tesh, F.W. (1978). Age and Growth. In: T.B. Bagenal, (Ed.) *Methods for Assessment of Fish Population in Fresh Waters*. IBP Handbook No: 3, Blackwell Scientific Publications, Oxford: 101-136.

TURKISH JOURNAL OF SCIENCE & TECHNOLOGY (TJST)

INSTRUCTIONS FOR AUTHORS

Turkish Journal of Science & Technology is an international journal covering all aspects relating to science, engineering and technology.

The following types of article will be considered:

1. Research Articles: Original research in various fields of science, engineering and technology will be evaluated as research articles. Papers must include an English abstract and if possible a Turkish abstract.

2. Research Notes: These include articles such as preliminary notes on a study, manuscripts.

3. Reviews: Reviews of recent developments, improvements, discoveries and ideas in various fields of selected subjects will be requested by the editor or advisory board.

4. Letters to the Editor: These include opinions, comments relating to the publishing policy of Turkish J. of Sci. & Tech., news and suggestions. Letters are not to exceed a single page.

All manuscripts will be subject to multiple **peer review** before publication. Submitted manuscripts must not be under consideration for publication elsewhere or have already been published. The editor reserves the right to decide that a paper may be treated as a Research Note.

Manuscripts should be sent to below address:

Firat University, Fen Bilimleri Enstitüsü,
Turkish Journal of Sci. & Tech. Editörlüğü,
23119 Elazığ- TURKEY

There are **no page charges**.

SUBMISSION OF MANUSCRIPTS

1. Manuscripts must be submitted in typewritten on one side of the page in a legible font, double-spaced with ample margins. All manuscripts must be accompanied by the **Copyright Release Form**, which can be found following the Instructions. This form must be completed and signed by all the authors before processing of the manuscript can begin. If the manuscript is submitted by e-mail a high quality scan of the Copyright Release Form is acceptable.

Manuscripts must be written in **English**. Contributors who are not native English speakers are strongly advised to ensure that a colleague fluent in the English language, if none of the authors is so, has reviewed their manuscript. Concise English without jargon should be used. Repetitive use of long sentences and passive tense should be avoided. All abbreviations and acronyms should be defined at first mention. To facilitate reader comprehension, abbreviations should be used sparingly. After the manuscript has been accepted for publication, i.e. after referee-recommended revisions are complete, the authors will not be permitted to make any additions. Before publication, the **galley proof** is always sent to the authors for correction. Mistakes or omissions that occur due to some negligence on our part during the final printing will be rectified in an errata section of a later issue. However, this does not include those errors left uncorrected by the authors in the galley proofs.

All due care will be taken with material submitted, but the Advisory Board and the publisher cannot be held responsible for any loss or damage.

2. Manuscripts should have the following **format**: title, name(s) of author(s), key words (3-6), abstract, text, references.

3. The abstract must be brief and informative and must not exceed 200 words. It should include all new names, combinations and rank transfers.

4. The text may be divided into reasonable subdivisions by the authors with numbered (1, 2,...), but the aim of the article, results and discussion must be included. An Introduction and Materials and Methods section may also be included if appropriate.

Within the main text, **author citations** should follow:

Brummitt and Powell, [1]For three or more authors use 'et. al.' for example Özcan et. al. [1]

References in the text should be numbered in square brackets as [1]. Multiple references should be arranged chronologically.

5. In the reference list, references should be numbered in the order of appearance in the text and should appear in the following style:

Journal articles: (i) Surname(s) and initial(s) of author(s), (ii) Year of publication (in parentheses), (iii) Title of article (in lower case), (iv) Title of journal (in italics), (v) Volume number, (vi) Page numbers.

For example, Emiroglu, M. E., and Baylar, A. (2003). Study of the Influence of Air Holes along Length of Convergent-Divergent Passage of a Venturi Device on Aeration. *Journal of Hydraulic Research*, **41** (5), 513-520.

Chapters in books: (i) Surname(s) and initial(s) of author(s), (ii) Year of publication (in parentheses), (iii) Title of chapter (in lower case), (iv) Name of editor (if applicable), (v) Title of book (in upper case and italics), (vi) Page numbers,

(vii) Place of publication, (viii) Name of publisher.

For example, Endler JA (1982). Pleistocene forest refuges: Fact or fancy? In: Prance GT (ed.) Biological Diversification in the Tropics, pp. 641-657. New York: Plenum Press.

Books: (i) Surname(s) and initial(s) of author(s), (ii) Year of publication (in parentheses), (iii) Title of book (in upper case and italics), (iv) Place of publication, (v) Name of publisher.

For example, Mabberley DJ (1987). The Plant-Book. A Portable Dictionary of the Higher Plants. Cambridge: Cambridge University Press.

Ahmed, A. (1974). Aeration by Plunging Liquid Jet. Ph.D. thesis, Loughborough University of Technology, Leicestershire, UK. References to web sites, computer programs, and unpublished theses or reports are unacceptable.

6. All scientific names cited in the running text, irrespective of rank, **must be italicised**. In headings, scientific names must be in bold and not italicised. **Authors of genera and lower taxa** must be cited at the first mention of the taxa in both the abstract and the text.

7. Figures and Tables

All illustrations (photographs, line drawings, graphs, maps, etc.), not including tables, must be labelled "Figure".

The **correct position** of each table and figure must be clearly **indicated** in the paper

All tables and figures must have a number (Table 1, Figure 1) and a caption or legend. All tables and figures must be numbered consecutively. All captions and legends must also appear on a separate sheet, double-spaced and labelled according to the relevant table or figure.

Tables and figures, including caption, title, and column heads, **must not exceed** 16 x 20 cm and should be no smaller than 8 cm in width. Tables must be clearly typed, each on a separate sheet, and double-spaced. Tables may be continued on another sheet if necessary, but the dimensions stated above still apply.

Figures must be the originals. Reduced photocopies are not acceptable. **Photographs** must be clear, black and white, and on glossy paper. **Three sets of photographs** must be submitted.

Before submitting your manuscript, ensure that all the following requirements have been met:

- The **Copyright Release** Form, appearing on the following page, has been completed and **signed by all the authors**
- Spell check and grammar check have been performed
- **Paper** is submitted in **triplicate** (one original, two copies)
- **Entire paper** is **double-spaced** including abstract, tables, captions/legends, and references (NOT 1.5)
- Margins are c. 3 cm each side
- Font size is 12 pt or 3 mm
- There are **no word breaks** at the ends of lines
- **Decimals** are shown by a **decimal point** (e.g., 10.24) and **not by a comma** (e.g., NOT 10,24)
- The percent sign appears after the number (e.g., 53%) and not before (e.g., NOT %53)
- **Names of authors** are written in full (not abbreviated)
- English address is given
- Turkish address (if applicable) is given
- English title is given
- Turkish title is given (if possible)
- English abstract is given
- Turkish abstract is given (if possible)
- English key words are given
- Turkish key words are given (if possible)
- **Authors of genera and lower taxa** are cited at first appearance in both the abstract and the text
- **Unpublished references** (theses, project reports, etc.) are not referred to or cited
- Three sets of **photographs** are enclosed
- **Original figures** are enclosed
- **Figures** are prepared according to the instructions
- Figures are max 16 x 20 cm; min 8 x 20 cm wide
- Figures are referred to consecutively in the paper
- **Tables** are max 16 x 20 cm; min 8 x 20 cm wide
- Tables are referred to consecutively in the paper
- Table and figure legends/captions are typed on a separate sheet
- **References** are listed in alphabetical order in the style shown in the instructions
- All pages are numbered

Further details can be found on our web site. <http://www.firat.edu.tr>

COPYRIGHT RELEASE FORM

TURKISH JOURNAL OF SCIENCE AND TECHNOLOGY (TJST) Published by Firat University

Firat University, Fen Bilimleri Enstitüsü Müdürlüğü
Turkish Journal of Science & Technology Editörlüğü
Elazığ-TURKEY,
Manuscript title:

Full names of all authors (in order to appear on manuscript):

Name, address etc. of corresponding author:

ID Number: Telephone:

E-mail: Mobile phone:

The author(s) warrant(s) that:

- a) the manuscript submitted is his/her/their own original work;
- b) all authors participated in the work in a substantive way and are prepared to take public responsibility for the work;
- c) all authors have seen and approved the manuscript as submitted;
- d) the manuscript has not been published and is not being submitted or considered for publication elsewhere;
- e) the text, illustrations, and any other materials included in the manuscript do not infringe upon any existing copyright or other rights of anyone. Notwithstanding the above, the Contributor(s) or, if applicable the Contributor's Employer, retain(s) all proprietary rights other than copyright, such as

a) patent rights;

b) to use, free of charge, all parts of this article for the author's future works in books, lectures, classroom teaching or oral presentations;

c) the right to reproduce the article for their own purposes provided the copies are not offered for sale.

However, reproduction, posting, transmission or other distribution or use of the article or any material contained therein, in any medium as permitted hereunder, requires a citation to the Journal and appropriate credit to Firat University as publisher, suitable in form and content as follows:

Title of article, author(s), journal title and volume/issue, Copyright© year.

All materials related to manuscripts, accepted or rejected, including photographs, original figures etc., will be kept by Turkish Journal of Science and Technology editority for one year following the editor's decision. These materials will then be destroyed. I/We indemnify Firat University and the Editors of the Journals, and hold them harmless from any loss, expense or damage occasioned by a claim or suit by a third party for copyright infringement, or any suit arising out of any breach of the foregoing warranties as a result of publication of my/our article. I/We also warrant that the article contains no libelous or unlawful statements and does not contain material or instructions that might cause harm or injury.

This copyright form must be signed by all authors. Separate copies of the form (completed in full) may be submitted by authors located at different institutions; however, all signatures must be original.

ID number: ID number:

Full name (block letters) Full name (block letters)

Signature Date Signature Date

ID number: ID number:

Full name (block letters) Full name (block letters)

Signature Date Signature Date

ID number: ID number:

Turkish authors must supply their ID card number; foreign authors must supply their passport number (if possible)